The enzyme HPGD is critical for regulatory T cell function in adipose tissue

Dissertation
zur
Erlangung des Doktorgrades (Dr. rer. nat.)
der
Mathematisch-Naturwissenschaftlichen Fakultät
der
Rheinischen Friedrich-Wilhelms-Universität Bonn

vorgelegt von

Lisa Maria Schmidleithner
aus Wien, Österreich

Bonn, Mai 2019

Angefertigt mit Genehmigung der Mathematisch-Naturwissenschaftlichen Fakultät der Rheinischen Friedrich-Wilhelms-Universität Bonn

1. Gutachter: PD Dr. med. Marc D. Beyer

2. Gutachter: Prof. Dr. med. Joachim L. Schultze

Tag der Promotion: 18.12.2019

Erscheinungsjahr: 2020

Summary

Regulatory T cells (T_{reg} cells) are essential for maintaining immune homeostasis. However, how T_{reg} cells exert their function in tissue specific environments is often unknown. We have found hydroxyprostaglandin dehydrogenase (Hpgd), the major Prostaglandin E_2 (PGE_2) metabolizing enzyme, to be significantly upregulated in T_{reg} cells compared to conventional T cells (T_{conv}). In the murine system, this upregulation is especially pronounced in the visceral adipose tissue (VAT), a prostaglandin-rich environment.

Furthermore, we could show that through the metabolism of PGE_2 into 15-keto-PGE_2 Hpgd enhances the suppressive capabilities of T_{reg} cells in an, at least partially, Pparγ-dependent manner. *In vivo*, we found that Hpgd-deficient T_{reg} cells were less efficient in preventing the onset of both DSS-induced and adoptive transfer colitis, further indicating that Hpgd plays a role in the suppressive capacity of T_{reg} cells. However, analysis of the transcriptome of these Hpgd-deficient T_{reg} cells did not differ significantly from Hpgd-competent T_{reg} cells, indicating that the observed changes are due to the extrinsic effect caused by the loss of the enzymatic function of Hpgd.

When analyzing the VAT of aged animals with Hpgd-deficient T_{reg} cells, we could detect an influx of non-functional T_{reg} cells as well as an accumulation of pro-inflammatory macrophages and an increase in adipocyte size. Furthermore, while we could neither detect a change in body or organ weight of these animals, nor a change in motility, food and water intake, or respiration, we could observe impaired metabolic signaling. Aged animals with Hpgd-deficient T_{reg} cells respond less to insulin and glucose challenge and show a reduction in insulin signaling.

When subjecting animals with Hpgd-deficient T_{reg} cells to a high fat diet (HFD), we could not detect a difference in weight gain when compared to wildtype littermate control animals. Even though we could detect a slight decrease in insulin responsiveness in animals on a HFD with Hpgd-deficient T_{reg} cells, no difference in the VAT-resident immune cell population or in any other metabolic parameters could be observed.

Additionally, in peripheral blood from human type II diabetes (T2D) patients we observed a dysregulation of the T_{reg} cell population as well as a decrease in HPGD expression in these cells compared to healthy, age-matched controls. Taken together, these data indicate

that both in humans and in the murine system, HPGD expression in T_{reg} cells might be involved in metabolic regulation.

Finally, we analyzed the role of the T_{reg} cell specific transcription factor mesenchyme homeobox 1 (MEOX1) for HPGD expression. We found that MEOX1 is highly upregulated in human T_{reg} cells, especially after stimulation with interleukin (IL) 2. Furthermore, we could show that while MEOX1 expression, like HPGD, is regulated by FOXP3, a loss of MEOX1 does not affect HPGD expression, thus disproving our hypothesis that HPGD may be regulated by the transcription factor MEOX1.

Taken together, we could describe that HPGD is an important mediator of T_{reg} cell suppression, independently of MEOX1. We found that a T_{reg} cell specific deletion of Hpgd in the mouse leads to a dysregulation of the metabolism, and that HPGD levels are significantly decreased in T_{reg} cells isolated from the peripheral blood of T2D patients compared to T_{reg} cells isolated from healthy subjects.

Abbreviations

Table 1: List of abbreviations

Abbreviation	Definition
Angptl4	Angiopoietin-like protein 4
Ap2	Adipocyte protein 2
APC	Antigen presenting cells
AUC	Area under the curve
BAD	BCL2 Associated Agonist Of Cell Death
BAT	Brown adipose tissue
BM	Bone marrow
BMDCs	Bone-marrow derived dendritic cells
BMDMs	Bone-marrow derived macrophages
cAMP	Cyclic adenosine monophosphate
CCR4	C-C motif chemokine receptor 4
CD	Cluster of differentiation
CO_2	Carbon dioxide
COX	Cyclooxygenase
CTLA-4	Cytotoxic T-lymphocyte antigen 4
CTLs	Cytotoxic T Lymphocytes
DCs	Dendritic Cells
FL	Floxed
FOXP3	Forkhead-box-protein P3
GITR	Glucocorticoid-induced TNFR family related gene
GSK	Glycogen Synthase Kinase
HFD	High fat diet
HOMA-IR	Homeostatic Model Assessment for Insulin Resistance
HOX	Homeobox
HPGD	15-hydroxyprostaglandin dehydrogenase
HRP	horseradish peroxidase
IFN-γ	Interferon gamma
IL	Interleukin
INSR1	Insulin receptor 1
IPEX	Immunodysregulation Polyendocrinopathy Enteropathy X-linked

IR	Insulin receptor
IRS	Insulin receptor substrate
KLRG1	Killer-cell lectin like receptor G1
KO	Knock out
LAG-3	Lymphocyte activating 3
LN	Lymph node
MΦ	Macrophage
MEOX1	Mesenchyme Homeobox 1
MHC	Major histocompatibility complex
MIP-1	Macrophage inflammatory protein 1
mLN	Mesenteric lymph node
Mono	Monocyte
ND	Normal diet
NKT	Natural Killer T
NK	Natural killer
Nrp1	Neuropilin-1
PB	Peripheral blood
PDK-1	3-phosphoimositide-dependent protein kinase 1
PG	Prostaglandin
PI3K	Phosphatidylinositol 3 kinase
PIP2	Phosphatidylinositol (4,5)-bisphosphate
PIP3	Phosphatidylinositol (3,4,5)-trisphosphate
pLN	Peripheral (inguinal) lymph node
PPAR-γ	Peroxisome proliferator-activated receptor γ
PTGR	Prostaglandin reductase
RBCL	Red blood cell lysis
RER	Respiratory Exchange Rate
Rosi	Rosiglitazone
RT	Room temperature
SDS-PAGE	Sodium dodecyl sulphate-polyacrylamide gel electrophoresis
siRNA	Small, interfering RNA
SVR	Support vector regression
T2D	Type II diabetes

T_{conv}	Conventional T
TCR	T cell receptor
TGF	Transforming growth factor
T_H	T Helper
TNF-α	Tumor necrosis factor alpha
T_{reg}	Regulatory T
TXA2	Thromboxane
Ucp1	Uncoupling protein 1
VAT	Visceral adipose tissue
WAT	White adipose tissue
WT	Wildtype

Table of Figures

Table of Content

1. Introduction

1.1. The Immune System

The immune system is our primary defense mechanism against invading pathogens and can be divided into two interacting branches: the innate and the adaptive immune system. The innate immune system is older in evolutionary terms and consists of those elements of the immune system which mount an immediate response (Brubaker et al., 2015). The adaptive immune system, on the other hand, is slower to respond but, since it consists of antigen-specific reactions of T- and B- lymphocytes, it is more precise than the innate immune system and has been associated with the development of immunological memory (Bonilla and Oettgen, 2010). Despite the clear distinction between the two branches of the immune system, there is a significant amount of interaction between the innate and adaptive immune system. For instance, dendritic cells (DCs), as members of the innate immune system, respond to environmental cues but also have the capability to capture, process, and present antigens and thus activate the adaptive immune system (Parkin and Cohen, 2001; Steinman, 2006).

1.1.1. Adaptive Immunity

The adaptive immune system consists mainly of B-lymphocytes, which produce antigen-specific antibodies (Hoffman et al., 2016), and antigen-specific T cells. T cells develop in the thymus and can be divided into two major subsets: cytotoxic T lymphocytes (CTLs) and T helper (T_H) cells. These cells differ in their function and, due to the differential expression of the co-receptors cluster of differentiation (CD) 4 and 8 on T_H and CTLs, respectively, in their ability to bind to either major histocompatibility complex (MHC) class II or class I molecules (Broere et al., 2011; Miceli and Parnes, 1991).

After priming in secondary lymphoid organs, CTLs are activated by T-cell receptor (TCR) signaling once they encounter foreign or infected cells. This results in the induction of apoptosis in the opposing cell either via the exocytosis of perforin and granzymes or in a caspase-dependent manner (Broere et al., 2011).

T_H cells, on the other hand, recognize MHC class II molecules which are only expressed by professional antigen presenting cells (APCs), such as macrophages or DCs (Dustin et al., 2006). APCs can take up antigens in peripheral tissues and present the antigen on MHC II molecules. Upon migrating to secondary lymphoid tissues, APCs encounter T_H cells and activate them in an antigen-specific manner. Once activated, T_H cells differentiate

into a variety of different T_H-cell subgroups depending on the microenvironment and are empowered with pathogen-specific reactivity reflected in the production of a variety of different cytokines (Luckheeram et al., 2012; Reinhardt et al., 2006). Activated T_H cells are involved in many immunological processes, such as the activation of macrophages, B cells and CTLs (Broere et al., 2011; Castellino and Germain, 2006; Mills and Cambier, 2003).

A third subgroup of T cells has been described, which is at the interface of innate and adaptive immunity, namely natural killer T (NKT) cells. NKT cells function independently of MHCs. Rather, they rely on the CD1d molecule, which presents glycolipid antigens and, like CTLs, NKT cells have cytotoxic functions (Godfrey et al., 2004). NKT cells can be divided into different subgroups depending on the expression of CD4 and CD8 and differ in their respective cytokine production (Godfrey et al., 2004, 2010).

Finally, γδ T cells comprise the last group of T cells. Unlike the CTLs or T_H they do not express the α and β chains of the TCR but γ and δ TCR chains and therefore recognize a different set of antigens. While αβ TCRs require antigen-presentation via MHCs and recognize mainly non-self antigens, γδ TCRs are activated independently of MHCs and recognize not only pathogenic but also stress antigens. γδ T cells can target cells either directly by inducing cytotoxicity or through the production of a variety of cytokines which, in turn, lead to the activation of other immune cells (Bonneville et al., 2010; Lawand et al., 2017)

1.1.2. Regulatory T cells

T_H cells can be divided into two subgroups: regulatory T (T_{reg}) cells and conventional T (T_{conv}) cells. T_{conv} cells consist of all T_H subgroups, which lead to the activation of the immune system, including for example T_H1 and T_H17 cells (Reinhardt et al., 2006), while T_{reg} cells are vital for the maintenance of peripheral tolerance by acting both on their environment and on other immune cells in an immunomodulatory manner (Sakaguchi et al., 1995; Vignali et al., 2008). If T_{reg} cells can no longer function properly, this results in the development of autoimmunity including the induction of several different autoimmune diseases in the mouse, such as arthritis, gastritis, type I diabetes and pancreatitis (Asano et al., 1996; Papiernik et al., 1997; Sakaguchi et al., 1995; Suri-Payer et al., 1998).

T_{reg} cells can be characterized by the constitutive expression of the interleukin (IL) 2 receptor α-chain, CD25, and the transcription factor forkhead-box-protein P3 (FOXP3).

FOXP3 is necessary for tissue homeostasis as a disruption of FOXP3 leads to the development of severe autoimmune diseases, such as the immunodysregulation polyendocrinopathy enteropathy X-linked (IPEX) syndrome in humans (Vignali et al., 2008). In the mouse, a disruption of Foxp3 leads to the development of the so-called 'scurfy' phenotype which is characterized by a lack of T_{reg} cells and the onset of an ultimately lethal autoimmune disease (Brunkow et al., 2001; Fontenot et al., 2003), caused by hyperactive T_H cells as indicated by increased expression of the activation markers CD69 and CD44 (Fontenot et al., 2003). This indicates that Foxp3 is important for the immunomodulatory function of T_{reg} cells. Further, it was shown that when transducing naïve T_H cells with Foxp3, these cells develop a suppressive function and exhibit an inhibitory effect on cell proliferation (Hori et al., 2003). All in all, this demonstrates that Foxp3 plays a vital role in the development and maintenance of T_{reg} cells (Vignali et al., 2008).

T_{reg} cells exert their immunosuppressive function in a variety of manners. It has been described that T_{reg} cells can interfere with the immune response of other lymphocytes (Sojka et al., 2008). Presence of T_{reg} cells has also been shown to prematurely interrupt the activation of T_{conv} cells, finally resulting in the downregulation of IL-2 mRNA (Sojka et al., 2005) and inducing a completely different transcriptional program compared to uninhibited T_{conv} cells (Sukiennicki and Fowell, 2006).

However, the exact mechanism through which T_{reg} cells function is a matter of debate. It has been described that T_{reg} cells function both in a contact-dependent and contact-independent manner (Vignali et al., 2008). T_{reg} cells have been shown to secrete inhibitory cytokines, such as the transforming growth factor (TGF)-β, IL-10 and IL-35 (Asseman et al., 1999; Collison et al., 2007; Powrie et al., 1996). TGF-β is important for lymphocyte homeostasis by influencing the regulation of their chemotaxis, activation and survival (Li et al., 2005). Furthermore, T_{conv} cells which, due to a mutation of their TGF-β receptor, cannot signal via TGF-β are not impacted by T_{reg} cell suppression (Fahlén et al., 2005). However, T_{reg} cells do not need to produce TGF-β themselves, indicating that T_{reg} cells may influence other cells to produce anti-inflammatory cytokines, like TGF-β and IL-10, to exert their suppressive function (Fahlén et al., 2005; Kullberg et al., 2005). IL-10 has also been implicated in the suppression of T_{conv} cell mediated inflammation and expansion (Sojka et al., 2008). Interestingly, while IL-10 is necessary for the inhibition of antigen-experienced cells, IL-10 is not necessary for the inhibition of naïve T cells (Asseman et al., 2003). The cytokine

IL-35 leads to the suppression of T_{conv} cell proliferation both *in vitro* and *in vivo* and the expression of IL-35 in T cells imparts suppressive properties to these cells (Collison et al., 2007).

Furthermore, T_{reg} cells also seem to exert their function by disrupting the metabolism of other cells. This is achieved either by competing with other cells for growth factors and cytokines or by deregulating the adenosine metabolism (Vignali et al., 2008).

T_{reg} cells, unlike T_{conv} cells, constitutively express the IL-2 receptor CD25 and it has been shown that in co-cultures, T_{reg} cells deprive T_{conv} cells of IL-2 (Barthlott et al., 2005; de la Rosa et al., 2004). Nonetheless, IL-2 deprivation is most likely not the only mechanism in which T_{reg} cells modulate the immune reaction of T_{conv} cells. This reasoning is supported by the fact that the gene expression profile of T_{conv} cells which are undergoing IL-2 deprivation differs greatly from that of T_{conv} cells which are being suppressed by T_{reg} cells (Sukiennicki and Fowell, 2006).

Apart from the competition for IL-2, it has also been described that T_{reg} cells compete for cytokines both *in vivo* and *in vitro* and that the deprivation of these cytokines leads to apoptosis of T_{conv} cells (Pandiyan et al., 2007). However, this mechanism is probably not T_{reg} cell specific but could rather be induced by any T cell which expresses high levels of cytokine receptors on its cell surface (Ge et al., 2004).

Furthermore, it has been shown that the expression of the ectoenzymes CD39 and CD73 on the cell surface of T_{reg} cells leads to the production of adenosine, which suppresses T_{conv} cell function by activating the adenosine receptor A2A on the surface of activated T_{conv} cells (Deaglio et al., 2007). This, in turn, also favors the generation of T_{reg} cells as A2A signaling inhibits IL-6 signaling, which would lead to the differentiation into pro-inflammatory T cells, and instead leads to the secretion of TGF-β, thus promoting the immunosuppressive milieu (Vignali et al., 2008; Zarek et al., 2008). Another manner in which T_{reg} cells interrupt adenosine signaling in T_{conv} cells is by directly introducing cyclic adenosine monophosphate (cAMP), an inhibitor of both proliferation and IL-2 synthesis in T cells, into the cells through gap junctions, thus reducing T_{conv} cell functionality (Bopp et al., 2007).

In addition to modulating the immune response by secreting inhibitory cytokines and competing for proliferation-supporting cytokines, T_{reg} cells also inhibit via cell-cell contacts. Cell-surface bound TGF-β (Nakamura et al., 2001) as well as cytolytic molecules have been implicated in the cell-contact dependent suppressive function of T_{reg} cells. T_{reg} cells can lyse cells (Cao et al., 2007), induce apoptosis in B cells through Fas-Fas ligand interaction (Janssens et al., 2003) and LAG-3, a CD4 homologue which is expressed on the cell surface of activated T_{reg} cells, is implicated in the T_{reg} cell suppressor activity towards T_{conv} cells (Huang et al., 2004). Furthermore, cytotoxic T-lymphocyte antigen 4 (CTLA-4), which is constitutively expressed by T_{reg} cells, also contributes to the suppressive function of T_{reg} cells by influencing T-cell receptor hyposignaling, proliferation, and anergy of target cells (Tai et al., 2012).

However, none of the described mechanisms alone are sufficient to explain the functionality of T_{reg} cells. Rather, it is assumed that T_{reg} cells function in all of these – and possibly more, as of yet undescribed – manners to exert their function (Sojka et al., 2008; Vignali et al., 2008).

1.1.3. Tissue resident Regulatory T cells

In recent years, it has been described that T_{reg} cells differ in their phenotype and function depending on the tissue they reside in (Luu et al., 2017; Zhou et al., 2015), such as a distinct population of T_{reg} cells in the muscle expressing the growth factor amphiregulin are vital for muscle repair (Burzyn et al., 2013). Furthermore, it has been described that disturbing a unique skin-resident T_{reg} cell population expressing high levels of both CD103 and C-C motif chemokine receptor 4 (CCR4) leads to increased inflammation in the skin of these animals indicating that upsetting the balance of tissue-resident T_{reg} cells leads to the induction of tissue-specific inflammation (Ali and Rosenblum, 2017; Sather et al., 2007) .

1.1.3.1. Visceral Adipose Tissue Regulatory T cells

Another subset of tissue resident T_{reg} cells are visceral adipose tissue (VAT) resident T_{reg} cells, first described by Feuerer et al. in 2009 (Feuerer et al., 2009). In contrast to cells from the lymphoid compartment, where T_{reg} cells make up approximately 10-15% of the T_H-cell subgroup, in the VAT the T_H-cell fraction consists of approximately 40-60% of T_{reg} cells. Like T_{reg} cells isolated from the spleen, these cells are effective in suppressing T_{conv} cell proliferation and retain most of the classical T_{reg} cell markers such as CD25, Foxp3 and Ctla-4 (Feuerer et al., 2009).

Analysis of gene expression of VAT-resident T_{reg} cells revealed a significant difference between the expression pattern of these VAT resident T_{reg} cells compared to T_{reg} cells of lymphoid organs, such as the spleen or lymph nodes (LNs). For instance, VAT-resident T_{reg} cells express higher amounts of genes involved in leukocyte migration and extravasation such as CCR2, CCR9 and CXCL10, among others, indicating that VAT-resident T_{reg} cells may be recruited from the periphery based on unique expression patterns of chemokine and cytokine receptors (Cipolletta et al., 2011; Feuerer et al., 2009; Zhou et al., 2015).

Furthermore, the anti-inflammatory cytokine IL-10, as well as several genes downstream of the IL-10 receptor, are highly upregulated in VAT-resident T_{reg} cells, suggesting that VAT-resident T_{reg} cells play an important role in preventing the development of inflammation in the VAT and the induction of inflammation-associated obesity-related metabolic disorders (Feuerer et al., 2009).

VAT-resident T_{reg} cells have also been implicated in the control of the metabolism of mice. Obese animals showed significantly lower VAT-resident T_{reg} cell numbers than lean littermate control animals in three different mouse models. Moreover, a direct correlation could be observed between the number of T_{reg} cells in the VAT and insulin resistance: increased VAT-resident T_{reg} cell numbers lead to a corresponding increase in insulin sensitivity (Feuerer et al., 2009).

1.2. Prostaglandins in the Immune System

Prostaglandins (PGs) are oxygenated polyunsaturated fatty acids containing a cyclopentane ring structure and are potent lipid mediators which play an important role in the immune system (Phipps et al., 1991). PGs are metabolized from arachidonic acid, which is a component of the eukaryotic cell membrane, by cyclooxygenase-1 and -2 (COX-1 and COX-2), thus forming PGG_2, which can be further metabolized by different synthases into a variety of other PGs (Bergstroem et al., 1964; Van Dorp et al., 1964) (Figure 1). These are classified from A to J, according to the structure of the cyclopentane ring (Kawahara et al., 2015).

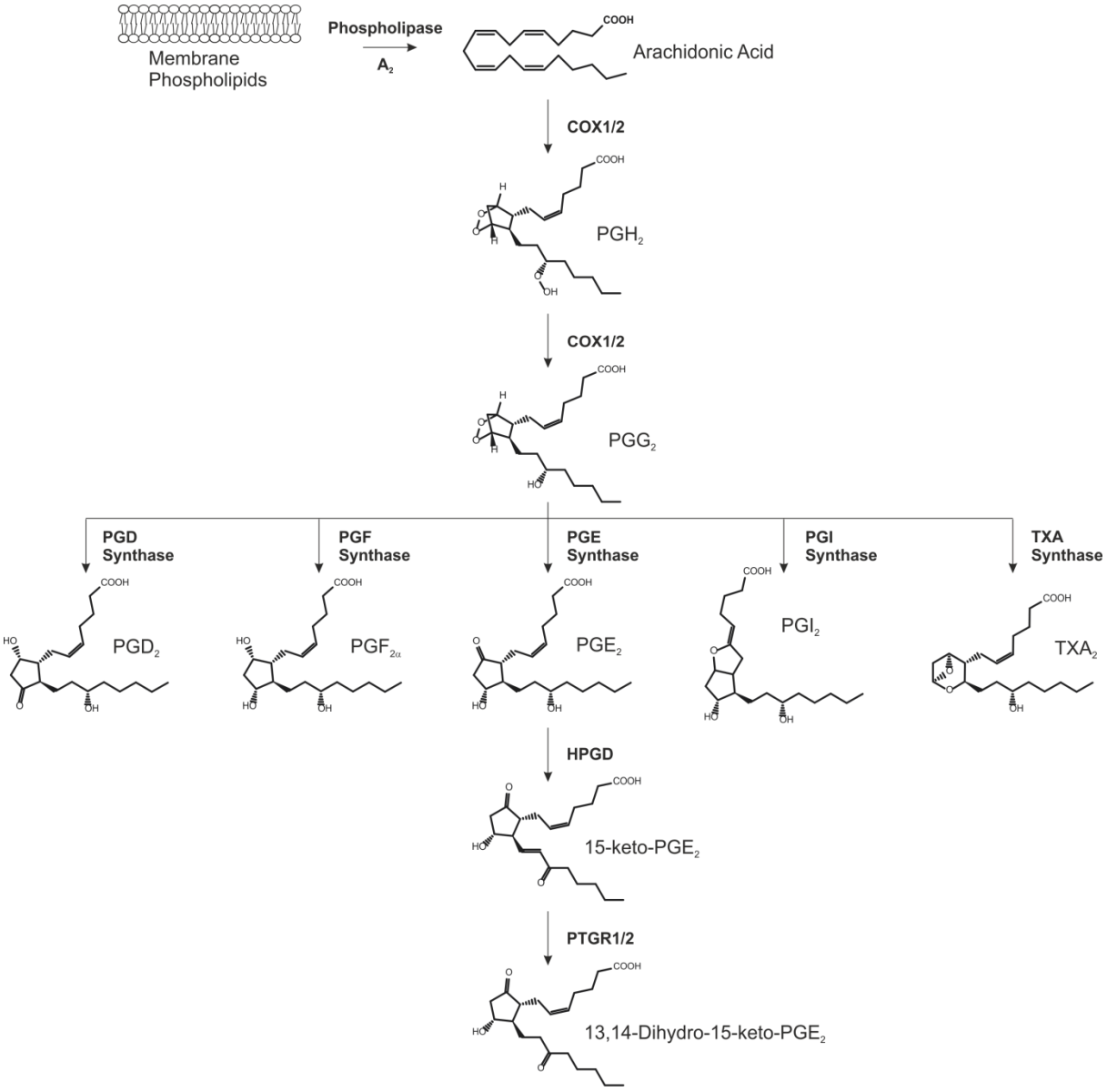

Figure 1: Metabolism of Prostaglandins (PGs)
Arachidonic Acid is metabolized by COX-1 or 2 to PGH_2 and subsequently to PGG_2, which is further metabolized by different synthases to PGD_2, $PGF_{2\alpha}$, PGE_2, PGI_2 and TXA_2. PGE_2 is further metabolized by HPGD into 15-keto PGE_2 which can be further reduced by PTGR1 or 2 into 13,14-Dihydro-15-keto-PGE_2. COX-1/2, Cyclooxygenase 1/2; PGH_2, Prostaglandin H_2; PGG_2, Prostaglandin G_2; PGD_2, Prostaglandin D_2; $PGF_{2\alpha}$, Prostaglandin $F_{2\alpha}$; PGE_2, Prostaglandin E_2; PGI_2, Prostaglandin I_2; PTGR1/2, Prostaglandin Reductase 1/2; TXA_2, Thromboxane A_2. (Figure adapted from Kawahara et al., 2015; Simmons et al., 2004)

PGs have long been known to play a role in the immune system. For instance, they have been shown to affect lymphocyte proliferation (Franks et al., 1971) and thymocyte differentiation (Singh and Owen, 1975). The best described and most abundant of the PGs is PGE_2 (Sreeramkumar et al., 2012). Upon production, PGE_2 is released from the cell and acts in an auto- or paracrine manner via the cell-type specific PGE_2 receptors EP1, EP2 and EP3

(Narumiya, 1994). The three receptors are G-protein coupled receptors which respond to PGE_2 in different manners: signaling via EP1 leads to an increase of free, intracellular Ca^{2+} via G_q, EP2 signaling increases cAMP via G_s while EP3 decreases cAMP via G_i signaling (Buchanan et al., 2006; Fujino et al., 2003; Honda et al., 2006; Regan, 2003) Later, a fourth receptor, EP4, was identified which signals in a similar manner to EP2 and differs only in its ability to activate phosphatidylinositol 3 kinase (PI3K) signaling (Kawahara et al., 2015; Sreeramkumar et al., 2012). However, it has been shown that PGE_2 does not only act in an auto- or paracrine manner but that it can also be taken up by cells via the prostaglandin uptake transporter where it can either act on intracellular EP receptors (Bhattacharya et al., 1998) or interact directly with other signaling molecules, thereby leading to a variety of different biological effects (Lalier et al., 2011).

PGE_2 plays a role in many biological functions. Next to its role in fertility, gastrointestinal integrity, and the regulation of blood pressure, PGE_2, like most other PGs, is also an important mediator of the immune response (Legler et al., 2010; Ricciotti and FitzGerald, 2011). However, the exact manner in which PGE_2 acts within the immune system is still not fully resolved.

Indicative of its role in the immune system is the observation that the presence of pro-inflammatory stimuli can lead to the expression of PGE synthases (Filion et al., 2001), thus leading to an increased production of PGE_2 in pro-inflammatory settings. Interestingly, PGE_2 has been implicated not only in pro- but also in anti-inflammatory situations. PGE_2, in its role as an important pro-inflammatory mediator, leads to an increase in cytokine and chemokine production (Funk, 2001). Furthermore, when PGE_2 is administered to mice it causes increased vasodilation, increased local blood flow and hyperalgesia, leading to increased leukocyte infiltration. Thus, PGE_2 is involved in the development of all four hallmarks of acute inflammation: redness, swelling, pain, and edema (Omori et al., 2014; Sreeramkumar et al., 2012). Conversely, it has been shown that PGE_2 suppresses IL-1β mediated expression of cytokines and chemokines such as IL-8 and Macrophage Inflammatory Protein 1 (MIP-1) and the production of tumor necrosis factor alpha (TNF-α) and Interferon gamma (IFN-γ), thus exerting an anti-inflammatory role (Takayama et al., 2002). Likewise, stimulating DCs with PGE_2 leads to an upregulation of suppressive molecules, inhibiting T-cell proliferation, thus further cementing the immunosuppressive role of PGE_2 (von Bergwelt-Baildon et al., 2006).

Furthermore, it has been shown that all four EP receptors are expressed on the surface of T_H cells (Chemnitz et al., 2006), indicating that PGE_2 can play an important role in T_H cell biology. As a matter of fact, whole transcriptome analysis of T_H cells stimulated with PGE_2 showed that the majority of the genes downstream of the TCR are inhibited by PGE_2 stimulation, leading to the conclusion that PGE_2 interferes with TCR signaling, thus inhibiting the activation of T_H cells (Chemnitz et al., 2006). Moreover, PGE_2 has been implicated in the induction of T-cell anergy (Mannie et al., 1995).

Other data implicate PGE_2 in the differentiation and maintenance of several different T_H-cell subgroups. The presence of PGE_2 favors the differentiation of T_H cells into T_H2 cells over T_H1 cells by inhibiting the production of T_H1 but not T_H2 cytokines (Betz and Fox, 1991). Furthermore, PGE_2 has been shown to enhance T_H17-cell differentiation by increasing the expression of the classical T_H17-cytokine profile by EP2 signaling and inhibiting the expression of immunomodulatory cytokines through EP4 signaling (Boniface et al., 2009).

Additionally, there are conflicting reports indicating that PGE_2 may either be involved in (1) the suppression of T_{reg} cell development by EP2 signaling, leading to the downregulation of classical T_{reg} cell proteins such as CTLA-4 and GITR, as well as the production of the anti-inflammatory cytokine IL-10 (Li et al., 2017) or (2) in enhancing the development of T_{reg} cells by upregulating key genes of the T_{reg} cell signature, such as FOXP3 (Bryn et al., 2008; Sharma et al., 2005).

However, due to these contradictory findings, the exact mechanism in which PGE_2 influences T-cell biology still needs to be further elucidated.

1.2.1. 15-hydroxyprostaglandin dehydrogenase

NAD+-linked 15-hydroxyprostaglandin dehydrogenase (HPGD) is the key enzyme of the PGE_2 metabolism (Figure 1). HPGD oxidizes the prostanoid 15-hydroxyl group to a ketone, thus generating the signaling molecule 15-keto-PGE_2, a metabolite which can no longer bind to the EP receptors, consequently abrogating EP receptor signaling (Tai et al., 2002), and which is rapidly degraded into the unstable metabolite 13,14-Dihydro-15-keto-PGE_2 in the presence of PTGR1 or 2 (Fitzpatrick et al., 1980). Furthermore, a reciprocal regulation with COX-2 seems to indicate that, together with COX-2, HPGD is involved in the regulation of PG levels (Tai et al., 2006; Tong et al., 2006).

HPGD was first characterized in 1964, when it was observed that PGE_1 was converted into its metabolites in lung homogenates unless the homogenate was boiled, thus indicating an enzymatic reaction is responsible for the metabolism of the PG (Samuelsson, 1964). Subsequently, HPGD was isolated from swine lung (Anggård, 1966) and has since been found to be expressed ubiquitously in mammalian tissues (Bergholte and Okita, 1986; Braithwaite and Jarabak, 1975; Chang et al., 1990; Lee and Levine, 1975).

A second version of HPGD exists: NADP+-dependent HPGD type II. However, HPGD type II appears to be less active than the type I enzyme (Krook et al., 1993). Furthermore, NADP+-dependent HPGD is far less specific for prostaglandins. Moreover, the two enzymes are only about 20% homologous, indicating an early evolutionary divergence between the two enzymes (Wermuth, 1992). Additionally, the physiological function of HPGD type II is unclear since it does not seem to metabolize PGs *in vivo* as the K_M value for all prostaglandins is too high (Tai et al., 2006). A possible alternative substrate for HPGD type II may be quinines (Wermuth, 1992; Wermuth et al., 1986). Furthermore, compared to HPGD type I, HPGD type II is relatively lowly expressed in immune cells, including T_{reg} cells, with the highest expression observed in naïve T_H cells (Heng et al., 2008).

1.2.1.1. The role of HPGD in disease

Even though it has long since been known that HPGD is expressed in monocytes (Maddox and Serhan, 1996) and that its expression is reduced in tumor-infiltrating macrophages (Eruslanov et al., 2009), no functional role for HPGD has been described in immune cells.

However, HPGD has been implicated in several different types of cancer. An inhibition of HPGD leads to increased inflammation and decreased tumor formation (Arima et al., 2019). HPGD is markedly downregulated in colonic epithelial cells of colon cancer patients compared to healthy controls and in mice Hpgd expression inhibits tumor formation in the colon (Myung et al., 2006; Yan et al., 2004). A similar observation has been made in breast cancer: the HPGD promoter is methylated in around 30% of primary tumors leading to epigenetic silencing of HPGD in breast cancer. Furthermore, an upregulation of HPGD in mice leads to decreased tumor formation while a downregulation of the enzyme correlates with increased cell proliferation (Wolf et al., 2006). In line with this, it has been shown that an inhibition of HPGD can lead to tissue regeneration following liver injury(Zhang et al., 2015).

Interestingly, it has also been shown that HPGD, through the metabolism of PGE_2 into 15-keto-PGE_2, can inhibit the growth of hepatocellular carcinoma (Lu et al., 2014).

Next to its role in cancer inhibition, HPGD is also necessary for reproduction. This is unsurprising as PGs control both ovulation and menstruation and play a role in the establishment of pregnancy and initiation of labor (Arosh et al., 2004a, 2004b; Challis et al., 1999; Kang et al., 2005). It has been suggested that HPGD is the key enzyme which controls PGE_2 levels during pregnancy, especially during the recognition of pregnancy (Parent et al., 2006; Tai et al., 2006). Thus, a loss of HPGD can lead to the induction of pre-term birth in mice (Kishore et al., 2017; Roizen et al., 2008). Furthermore, a loss of HPGD leads to several congenital defects such as the induction of primary hypertrophic osteoarthropathy (Uppal et al., 2008) and a patent ductus arteriosus (Coggins et al., 2002).

1.3. Interplay of Metabolism and the Immune System

Metabolism is a complex system of catabolic, anabolic and transformative reactions within a cell necessary to maintain life in any organism. In this context, insulin signaling is a vital pathway which regulates both glucose and lipid metabolism (Boucher et al., 2014; Saltiel and Kahn, 2001).

1.3.1. The Role of Insulin Signaling in the Metabolism

Insulin signaling is vital to maintain glucose homeostasis and is mainly influenced by fasting states (Baeshen et al., 2014). Insulin is produced in the pancreas by beta cells as a single polypeptide. Increased blood glucose levels following the digestion of carbohydrates lead to the release of insulin and the subsequent uptake of glucose into cells. Insulin signaling via the insulin receptor (IR) induces cellular processes that increase the usage or storage of glucose in the cell (Baeshen et al., 2014; DeFronzo et al., 2015).

When insulin binds to the IR, the receptor forms a dimer and the intracellular tyrosine kinase domain auto-phosphorylates (Kasuga et al., 1982), leading to recruitment and phosphorylation of scaffold proteins, mainly insulin receptor substrate (IRS) 1 and 2. Whereas IRS1 is important for growth and peripheral insulin signaling, IRS2 is involved in the control of body weight, glucose homeostasis and fertility (Schubert et al., 2003). Association with the phosphorylated IRS molecules leads to the activation of PI3K which phosphorylates phosphatidylinositol (4,5)-bisphosphate (PIP_2), an inositol phospholipid of the plasma membrane, into phosphatidylinositol (3,4,5)-trisphosphate (PIP_3). This phosphorylation leads

to the recruitment of both 3-phosphoinositide-dependent protein kinase 1 (PDK-1) and the kinase AKT and subsequent phosphorylation and activation of AKT by PDK-1. AKT has many downstream substrates such as BCL2 Associated Agonist Of Cell Death (BAD), which plays an important role in cell survival, or Glycogen Synthase Kinase (GSK) 3β, which regulates growth and glycogen synthesis (Figure 2) (Boucher et al., 2014; White, 2003). Insulin signaling varies depending on the cell type; for instance insulin is most important for glucose uptake in muscle cells, and, to a lesser degree, adipocytes (DeFronzo et al., 2015), while osteocytes are largely unaffected by insulin signaling (Sheng et al., 2014).

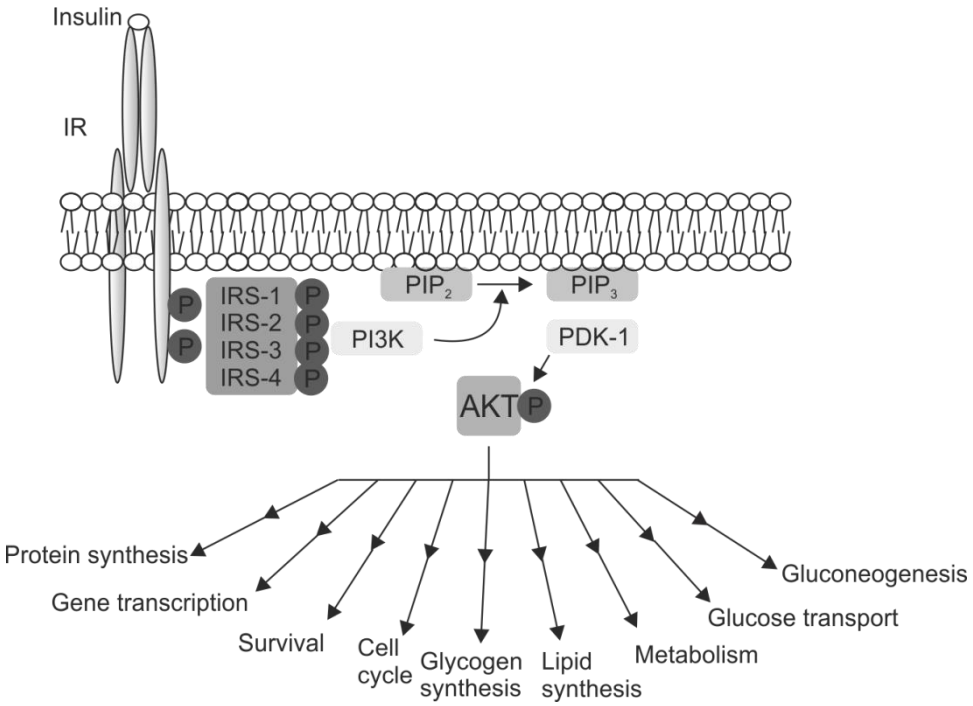

Figure 2: Insulin Signaling via AKT.
Insulin binding to the insulin receptor (IR) induces autophosphorylation of the receptor which, in turn, leads to the recruitment and phosphorylation of the insulin receptor substrates (IRS) 1 – 4. These phosphorylated substrates activate the phosphatidylinositol (4,5)-bisphosphate (PIP_2), an inositol phospholipid of the plasma membrane, into phosphatidylinositol (3,4,5)-trisphosphate (PIP_3). PIP_3 recruits the 3-phosphoimositide-dependent protein kinase 1 (PDK-1) and the kinase AKT. Phosphorylation of AKT by PDK-1 leads to the activation of AKT and subsequent downstream signaling is important for protein synthesis and induces gene transcription of important genes for survival and cell cycle progression. Furthermore, AKT signaling is vital for the cell metabolism as it controls gluconeogenesis, glucose transport as well as both glycogen and lipid synthesis. (Figure adapted from Boucher et al., 2014)

If insulin signaling is disrupted, the resulting hyperglycemia can lead to a host of different diseases, including but not limited to dyslipidemia, hypertension, cardiovascular disease, stroke, kidney disease, female infertility, neurodegeneration and the development of diabetes (White, 2003). Globally, metabolic disorders, such as type II diabetes (T2D), are on the rise. According to the World Health Organization, 60 million people were afflicted with diabetes in the European Region as of 2010. Worldwide, 3.4 million people annually die of diabetes, a number that is estimated to double by 2030 (World Health Organization (WHO), 2010). These statistics do not differentiate between type I diabetes and T2D, yet as approximately 90% of all diagnosed cases of adult diabetes are T2D, the current rise in diabetes is most likely due to an increase in T2D (DeFronzo et al., 2015; NCD Risk Factor Collaboration (NCD-RisC), 2016). This has led to a refocusing of research on metabolism and the underlying signaling pathways, such as insulin signaling (Boucher et al., 2014).

1.3.1.1. Type II Diabetes

Diabetes can be divided into three subgroups: gestational diabetes, Type I diabetes and T2D. Gestational diabetes occurs in approximately 5% of all pregnancies. During pregnancy, due to hormonal changes, maternal tissues become increasingly insensitive to insulin leading to an increase of maternal insulin secretion of about 200% in order to maintain glucose homeostasis. Gestational diabetes develops when insulin secretion is not upregulated and thus the insulin sensitivity is not compensated for (Barbour et al., 2007; Kampmann et al., 2015).

Type I diabetes, on the other hand, is an autoimmune disease leading to the destruction of beta cells in the pancreas. Thus, not enough insulin is produced, leading to hyperglycemia and related symptoms (Katsarou et al., 2017).

The most prevalent form of diabetes, however, is T2D which accounts for an estimated 90% of all cases of diabetes (DeFronzo et al., 2015). The occurrence of T2D is heavily influenced by lifestyle: a sedentary lifestyle, smoking, alcohol consumption, and an unhealthy diet are known risk factors for T2D (Hu et al., 2001). As such, obesity has been shown to contribute to more than 50% of T2D cases (DeFronzo et al., 2015).

T2D patients exhibit insulin insensitivity caused by insulin resistance and reduced insulin production (Kahn, 1994) caused by a combination of genetic and environmental influences. Insulin resistance can be induced by the activation of different protein kinases which interfere with the canonical insulin signaling pathway thus exploiting negative

feedback mechanisms to inhibit insulin signaling, resulting in insulin insensitivity (DeFronzo et al., 2015; Olokoba et al., 2012). Beta cell dysfunction, on the other hand, can also be induced by many different factors, such as increased oxidative or endoplasmatic reticulum stress as well as increased inflammation. In healthy humans, oxidative glucose metabolism in beta cells leads to an increase of intracellular ATP causing a closure of potassium channels. This, in turn, leads to an influx of calcium and the subsequent depolarization of the cell membrane, inducing the exocytosis of insulin. However, if the oxidative potential is somehow disturbed, the entire process is disrupted leading to a dysregulation of insulin production, which can lead to the induction of T2D (DeFronzo et al., 2015)

During fasting, glucose and glucagon levels rise. In patients suffering from T2D, these levels can no longer be suppressed with a meal due to increasing insulin insensitivity and inadequate insulin levels. This leads to hyperglycemia and related acute symptoms, such as weakness, weight loss and blurred vision (DeFronzo et al., 2015; Olokoba et al., 2012) and retinopathy, nephropathy and neuropathy as long-term consequences of insulin resistance (White, 2015).

1.3.2. Peroxisome Proliferator-Activated Receptor γ Signaling

The nuclear receptor peroxisome proliferator-activated receptor-γ (PPAR-γ) is a transcription factor which is mainly expressed in brown and white adipose tissue and plays a vital role in insulin sensitivity, adipocyte differentiation, and in lipid homeostasis (Ahmadian et al., 2013; Staels and Fruchart, 2005). When PPAR-γ is activated by ligand binding, it recruits co-activator proteins and heterodimerizes with the retinoid-X receptor. These heterodimers can bind to genomic peroxisome proliferator-response elements, thus promoting or repressing gene expression (Ahmadian et al., 2013; Staels and Fruchart, 2005).

Most genes downstream of PPAR-γ are relevant for glucose homeostasis and fatty acid uptake and storage but also inflammation. For this reason, Ppar-γ has been described as a metabolic master-regulator (Ahmadian et al., 2013; Staels and Fruchart, 2005). A further indication for its role in the metabolism is that thiazolidinediones, a class of PPAR-γ ligands, have found use as antidiabetic drugs (Lehmann et al., 1995).

Most PPAR-γ ligands are anti-inflammatory in nature. Thiazolidinediones, for example, inhibit pro-inflammatory cytokine production in activated lymphocytes, monocytes and microglia (Jiang et al., 1998; Lombardi et al., 2008; Schmidt et al., 2004). Furthermore,

both human and murine studies showed that a stimulation with thiazolidinediones leads to a PPAR-γ-dependent upregulation of anti-inflammatory processes (Luo et al., 2006; Yu et al., 2009).

Another ligand of PPAR-γ, which has been identified is 15-keto-PGE_2, the main metabolite generated by the enzymatic activity of HPGD. In 3T3-L1 cells, 15-keto-PGE_2 has been shown to act as a PPAR-γ ligand, thereby increasing 3T3-L1 adipogenesis and activating other PPAR-γ downstream targets. Furthermore, overexpressing one of the 15-keto-PGE_2 metabolizing enzymes, Prostaglandin Reductase (PTGR) 1, leads to the degradation of 15-keto-PGE_2 and the ablation of PPAR-γ signaling. Conversely, overexpressing HPGD leads to increased generation of 15-keto-PGE_2 from PGE_2 and thus increased PPAR-γ signaling (Chou et al., 2007), thus implicating the enzymatic activity of HPGD in the induction of PPAR-γ signaling.

1.3.3. Metabolic Signaling and VAT-resident T_{reg} cells

1.3.3.1. Insulin signaling and VAT-resident T_{reg} cells

VAT-resident T_{reg} cells contribute to the prevention of obesity-related diseases. It has been described that VAT-resident T_{reg} cells confer anti-inflammatory properties and that these successfully improve insulin sensitivity and decrease the severity of other metabolic disorders caused by obesity (Zhou et al., 2015).

Furthermore, it has been described that female animals are protected against metabolic disorders induced by feeding of a high caloric diet by increasing the levels of VAT-tissue resident T_{reg} cells (Ingvorsen et al., 2017; Pettersson et al., 2012), while a loss of VAT-resident T_{reg} cells causes a decrease in insulin sensitivity and an upregulation of inflammation in the VAT (Cipolletta et al., 2011). Moreover, the adoptive transfer of T_{reg} cells decreased insulin resistance in obese mice (Ilan et al., 2010), indicating that VAT-resident T_{reg} cells might play a role in delaying the onset of obesity-related diseases.

Conversely, the genetic prevention of the development of the population of VAT-resident T_{reg} cells leads to a marked improvement of age related insulin resistance in aged animals while they remain susceptible to obesity-related insulin resistance (Bapat et al., 2015). This could be explained by the fact that in this model, a loss of VAT-resident T_{reg} cells leads to a completely different microenvironment prompting differing reactions.

Alternatively, these data could also indicate that the mechanisms of age-related and obesity-related insulin resistance are distinct.

1.3.3.2. Ppar-γ signaling and VAT-resident T_{reg} cells

Ppar-γ has been shown to interact with Foxp3 in VAT-resident T_{reg} cells to induce a VAT-specific T_{reg} cell gene signature (Cipolletta et al., 2012; Zhou et al., 2015). A T_{reg} cell specific deletion of Ppar-γ had no effect on the T_{reg} cell fraction in lymphoid compartments, while it resulted in a distinct decrease of VAT-resident T_{reg} cells to about 10% of the T_H-cell compartment compared to the 40-60% of VAT-resident T_{reg} cells in control animals. Furthermore, these Ppar-γ-deficient VAT-resident T_{reg} cells also exhibited reduced mean fluorescence intensity of Foxp3. Moreover, a deletion of Ppar-γ in T_{reg} cells altered the expression of VAT-resident T_{reg} cells to more closely resemble that of lymphoid-organ resident T_{reg} cells, indicating that Ppar-γ is important for the development and maintenance of VAT-resident T_{reg} cells (Cipolletta et al., 2012). Further analysis of these VAT-resident T_{reg} cell deficient animals revealed reduced age-induced insulin resistance yet unaltered susceptibility to obesity (Bapat et al., 2015), further establishing the vital role that VAT-resident T_{reg} cells play in the metabolism (Cipolletta et al., 2012). Recent studies have shown that this VAT-resident specific T_{reg} cell signature is already established in the spleen and then reinforced through signals from the micromilieu in VAT (Li et al., 2018).

Interestingly, this VAT-resident T_{reg} cell signature is lost in obese mice. However, these mice still express a distinct signature from splenic T_{reg} cells, characterized by altered expression of several different genes as well as a change in the phosphorylation of PPAR-γ (Cipolletta et al., 2015).

In addition to its direct influence on VAT-resident T_{reg} cell function, Ppar-γ signaling also influences the expression of the scavenger receptor CD36 on macrophages, which mediates the uptake of low-density lipoproteins, fatty acids, and phospholipids (Tontonoz et al., 1998). T_{reg} cell differentiation has been shown to rely selectively on exogenous lipid metabolism rather than glucose (Michalek et al., 2011). Thus, the mechanism by which Ppar-γ influences the differentiation of VAT-resident T_{reg} cells could also involve altering the lipid composition of the microenvironment by affecting CD36 expression on macrophages (Sugii et al., 2009; Zhou et al., 2015).

1.4. Mesenchyme Homeobox 1

Mesenchyme Homeobox 1 (MEOX1) is a transcription factor which is required for correct gene expression in all somatic compartments (Bayrakli et al., 2013). Transcription factors containing Homeobox (HOX) domains have been first described in drosophila and have been shown to play an important role in the shaping of animal structures by inducing different programs in the early development of both mammals and insects by binding to DNA domains through helix-turn-helix structures (Alonso, 2002).

As such, it is unsurprising that MEOX1 has been shown to be one of the transcription factors involved in the epithelial-to-mesenchymal transition (Sun et al., 2016). Mutations leading to the loss of MEOX1 mRNA cause Klippel-Feil-Syndrome, a segmentation defect in the cervical spine which is characterized by a short neck, limited neck movement, and a low hairline (Bayrakli et al., 2013; Mohamed et al., 2013)

Moreover, MEOX1 has been implicated in breast cancer development as it is located in the breast cancer 1 (BRCA1) region, which encodes for several different tumor suppressor genes. Mutations in this region highly increase the risk for breast and ovarian cancer (Futreal et al., 1994). Furthermore, MEOX1 has been shown to be involved in both the regulation of breast cancer stem cells and in mesenchymal-like cell proliferation and increased MEOX1 expression can be correlated with breast cancer stage, lymph node metastasis and poor survival prognosis (Sun et al., 2016).

However, as of yet, MEOX1 has not been described in the context of T-cell biology or immunology.

1.5. Aim of this thesis

The immunomodulatory effect of T_{reg} cells is one of the main ways in which the immune system self-regulates. However, even though T_{reg} cells were first hypothesized in the early 1970s, we still do not completely understand their functionality, especially their divergent functions depending on their tissue of residence.

In this thesis, we attempted to gain a better understanding of T_{reg} cell biology by analyzing T_{reg} cells in the VAT, a PGE_2-rich environment. We focused especially on the role of HPGD, an enzyme which we found to be highly expressed in T_{reg} cells and which is important in the metabolism of PGE_2.

To more closely evaluate the role of HPGD in T_{reg} cell biology, we utilized a T_{reg} cell specific Hpgd knockout mouse line generated by crossing two previously published lines (Roizen et al., 2008; Rubtsov et al., 2008) and analyzed the effect the loss of Hpgd has on T_{reg} cell functionality, on the overall makeup of the immune-cell compartment, as well as on the metabolism of these animals. Furthermore, we analyzed the role of HPGD in T_{reg} cells isolated from humans suffering from T2D, a very common metabolic disorder, to determine whether the metabolic role of HPGD in T_{reg} cells is conserved between the species.

Finally, we attempted to understand T_{reg} cell signaling upstream of HPGD by studying the effect of the transcription factor MEOX1, which we found to be highly upregulated in human T_{reg} cells and regulated in a similar manner to HPGD.

2. Materials

2.1. Antibodies

Table 2: List of murine antibodies for flow cytometry

Epitope	Clone	Company	Dilution
B220	RA3-6B2	Biolegend	1:200
CD11b	M1/70	Biolegend	1:200
CD11c	N418	Biolegend	1:400
CD127	A7R34	Biolegend	1:200
CD14	Sa14-2	Biolegend	1:200
CD19	eBio1D3	eBioscience	1:200
CD25	PC61	Biolegend	1:200
CD3	17A2	Biolegend	1:200
CD4	RM4-5	Biolegend	1:200
CD44	IM7	Biolegend	1:200
CD45	30-F11	Biolegend	1:200
CD62L	MEL-14	eBioscience	1:200
CD69	H1.2F3	eBioscience	1:200
CTLA4	UC10-4B9	eBioscience	1:100
Eos	ESB7C2	eBioscience	1:200
F4/80	BM8	Biolegend	1:100
Foxp3	FJK-16s	eBioscience	1:100
GFP	polyclonal	Invitrogen	1:300
GITR	DTA-1	Biolegend	1:200
GR-1	RB6-8C5	eBioscience	1:200
Helios	22F6	eBioscience	1:200
I-A/I-E	M5/114.15.2	Biolegend	1:200
ICOS	15F9	eBioscience	1:200
Ki67	SolA15	eBioscience	1:200
KLRG1	2F1	eBioscience	1:200
Ly6C	HK1.4	Biolegend	1:200
Ly6G	1A8	eBioscience	1:200
Neuropilin-1	3E12	Biolegend	1:100

NK1.1	PK136	Biolegend	1:200
NKp46	29A1.4	Biolegend	1:100
ST2	DIH9	Biolegend	1:100

Table 3: List of human antibodies for flow cytometry

Epitope	Clone	Company	Dilution
CD127	HCD127	Biolegend	1:100
CD25	BC96	Biolegend	1:100
CD3	UCHT1	Biolegend	1:200
CD4	RPA-T4	Biolegend	1:200
Foxp3	PCH101	eBioscience	1:100
MEOX1	ab23279	Abcam	1:25

Table 4: List of secondary antibodies for flow cytometry

Epitope	Clone	Company	Dilution
Goat aRabbit IgG	Oligoclonal	Invitrogen	1:500

Table 5: List of human antibodies used for bead coating

Epitope	Clone	Company
CD3	OKT3	Janssen-Cilag GmbH
CD28	9.3	kind gift of James Riley, UPenn
MHCI	W6/32	Hybridoma

Table 6: List of western blot primary antibodies

Epitope	Cat. No.	Company	Dilution
pAKT (Ser 473)	#9271	Cell Signaling	1:1000
AKT	#4685	Cell Signaling	1:500
MEOX1	ab23279	Abcam	1:1000
β-Actin	MAB1501	Sigma-Aldrich	1:5000

Table 7: List of western blot secondary antibodies

Epitope	Cat. No.	Company	Dilution
Mouse IRDye800	926-32210	LI-COR Biosciences	1:5000
Rabbit IRDye680	925-68071	LI-COR Biosciences	1:5000
Rabbit IgG-HRP	GENA9340	Sigma-Aldrich	1:1000
Mouse IgG-HRP	GENXA931	Sigma-Aldrich	1:1000

Table 8: List of Immunohistochemistry antibodies

Epitope	Clone	Cat. No.	Company	Dilution
F4/80	CI:A3-1	ab6640	Abcam	1:50
Rabbit anti-rat IgG, biotin	polyclonal	31834	Thermo Fisher Scientific	1:5000

2.2. Buffers

Table 9: List of buffer compositions

Buffer	Component
10x Wet blot Buffer	250 mM Tris Base 1.92 M glycine in H_2O
1x Laemmli Running Buffer	1x 10x Laemmli Running Buffer in H_2O
1x Wet Blot Buffer	1x 10x Wet Blot Buffer 20% (V/V) methanol in H_2O
4% PFA solution	4% (w/V) paraformaldehyde in PBS, pH adjusted to 6.9
5x Laemmli Loading Buffer	156.25 mM Tris-HCl, pH 6.8 5% (w/V) SDS 54% (V/V) glycerol 0.0025% (w/V) bromphenol blue 12.5% β-mercaptoethanol in H_2O

Adipocyte Differentiation Medium	1µM Dexamethasone 0.5mM Methylisobutylxanthine (IBMX) 1µg/ml bovine Insulin 10% FCS in DMEM
Adipocyte Maintenance Medium	1µg/ml bovine Insulin 10% FCS in DMEM
AT-Digestion Buffer	20 mg/ml BSA 0.1 mg/ml collagenase type II 20 µg/ml DNAseI in DMEM
Digestion Buffer	10 mM HEPES 0.5 mg/ml collagenase type IV 0.05 mg/ml DNAseI in RPMI
Intestinal Digestion Buffer	0.2U/ml Liberase TM 200U/ml DNAse 10mM HEPES 100U/ml Penicillin 100µg/ml Streptomycin in HBSS
Intestinal Wash Buffer I	5mM DTT 2% FCS 100U/ml Penicillin 100µg/ml Streptomycin in HBSS
Intestinal Wash Buffer II	5mM EDTA 2% FCS 100U/ml Penicillin 100µg/ml Streptomycin in HBSS

Intestinal Wash Buffer III	10mM HEPES 100U/ml Penicillin 100µg/ml Streptomycin in HBSS
MACS Buffer	0.5% (w/V) BSA 2 mM EDTA in PBS
MRC Buffer	50 mM Tris-HCl, pH 7.5 1 mM EGTA, pH 8.0 1 mM EDTA, pH 8.0 10 mM β-glycerol phosphate 50 mM sodium fluoride 5 mM sodium pyrophosphate 1 mM sodium vanadate 270 mM sucrose 1% (V/V) Triton-X 100
PBST	0.1% (V/V) Tween-20 in PBS
RIPA Buffer	10 mM Tris HCl, pH 8.0 1 mM EDTA 140 mM NaCl 1% (V/V) Triton-X 100 0.1% (w/V) SDS 0.1% (w/V) sodium deoxycholate in H_2O
Red Blood Cell Lysis (RBCL) Buffer	155 mM ammonium chloride 10 mM potassium hydrogen carbonate 0.1 mM EDTA 0.5% (w/V) SDS in H_2O

2.3. Disposables

Table 10: List of disposables used

Kit	Manufacturer
0,2 ml PCR reaction tubes	Eppendorf GmbH
0,5-2,0 ml reaction tubes	Eppendorf GmbH
10 cm plates	Sarstedt
12-well tissue culture plates	Sarstedt
15 ml Falcon tubes	Sarstedt
19 G needle	VWR
24-well tissue culture plates	Sarstedt
48-well tissue culture plates	Sarstedt
50 ml Falcon tubes	Sarstedt
6-well tissue culture plates	Sarstedt
27 G needle	VWR
96 well half-area plate	Greiner
96 well suspension plate	Sarstedt
96-well tissue culture plates	Sarstedt
Cell stainer (100 µm)	Greiner
LightCycler 480 Multiwell Plate and sealing foil	Roche Diagnostics
MACS C-Tubes	Miltenyi Biotec
MACS LS columns	Miltenyi Biotec
MACS M-Tubes	Miltenyi Biotec
Nitrocellulose-membrane Hybond-C Extra	GE healthcare
Pipette tips (10, 200 & 1,000 µl)	Sarstedt
Pre-Separation Filters	Miltenyi Biotech, Bergisch Gladbach (DE)
Serological pipettes (2, 5, 10 & 25 ml)	Sarstedt
Syringe (2, 5, 10 and 50 ml)	Braun
Z Gel Tubes	Sarstedt

2.4. Enzymes

Table 11: List of enzymes used

Enzyme	Supplier
Collagenase Type II	Sigma Aldrich
Collagenase Type IV	Sigma Aldrich
DNAseI	Sigma Aldrich
Liberase TM	Roche Diagnostics
MyTaq™ HS DNA Polymerase	Bioline

2.5. Equipment

Table 12: List of equipment used

Equipment	Manufacturer
AccuChek Avia	Roche Diagnostics
Analysis Scale MS104S	Mettler Toledo
Centrifuge 5810R	Eppendorf GmbH
Centrifuge 5815R	Eppendorf GmbH
Centrifuge AvantiTM J-20 XP	Beckman Coulter
Centrifuge Mikro-200R	Hettich
Centrifuge Rotina 420R	Hettich
CO2 Incubator	Heraeus Christ Instruments
Dynal magnet MPC-S	Dynal Biotech
Electroporator	Amaxa
Flow cytometer / cell sorter FACS Aria III	BD Biosciences
Flow cytometer FACS CANTO	BD Biosciences
Flow cytometer FACS LSR II	BD Biosciences
Gene pulser XCell	BioRad Laboratories
GentleMACS dissociator	Miltenyi Biotec
Magnet MACS Multi Stand	Miltenyi Biotec
Microplate reader Infinite M200	Tecan Austria GmbH
Mini-& MidiMACS Separation Units	Miltenyi Biotec
Mini-Protean Electrophoresis System	Bio-Rad Laboratories
Multi-Detection Microplate Reader Synergy HT	BioTek Instruments

Odyssey Infrared Imaging System	LI-COR Biosciences
Pharmacia Pump P-1	Pharmacia
pH-meter S20-SevenEasy	Mettler Toledo
Pipette Controller Accu Jet Plus	Brand GmbH
Pipette Multipette Plus	Eppendorf GmbH
Pipette Set Ergo One	Starlab
PowerPac HC Power Supply	Bio-Rad Laboratories
Real-time PCR system LightCycler 480	Roche Diagnostics
Roller Mixer SRT9D Stuart	Bibby Scientific
Scale EL2001	Mettler Toledo
Shaking incubator	Stuart
Spectrophotometer NanoDrop 2000	Thermo Scientific
Steril work bench	BDK
Vortexer	Velp Scientifica
Water bath	Memmert

2.6. Kits

Table 13: List of kits used

Kit	**Manufacturer**
12-230 kDa Wes Separation Module kit	Protein Simple
CD4 M-pluriBeads Kit	PluriSelect
CD4+ T cell isolation kit II, mouse	Miltenyi Biotech
Transcription factor staining buffer set	eBioscience
Pierce BCA Protein Assay Kit	Thermo Fisher Scientific
Prostaglandin E Metabolite EIA Kit	Cayman Chemicals
Transcriptor 1st Strand cDNA Synthesis Kit	Roche
Ultrasensitive Mouse Insulin ELISA	Mercodia

2.7. Mouse Lines

Table 14: List of mouse lines used

Mouse Line	Reference
CD4-Cre	Lee et al., 2001
Foxp3-YFP-Cre	Rubtsov et al., 2008
Hpgd flox	Roizen et al., 2008
Ppar-γ flox	Akiyama et al., 2002

2.8. Cell Lines

Table 15: List of cell lines used

Cell Line	Reference
HEK293T	ATCC CRL-11268
3T3-L1	ATCC CL-173

2.9. Oligonucleotides

Table 16: List of murine qRT-PCR primer sequences

Target	Sequence	Probe
β-Actin	forward: 5'-CTA AGG CCA ACC GTG AAA AG-3' reverse: 5'-ACC AGA GGC ATA CAG GGA CA-3'	#64
Ap2	forward: 5'-GGA TGG AAA GTC GAC CAC AA-3' reverse: 5'-TGG AAG TCA CGC CTT TCA TA-3'	#31
Angptl4	forward: 5'-GGG ACC TTA ACT GTG CCA AG-3' reverse: 5'-GAA TGG CTA CAG GTA CCA AAC C-3'	#83
Foxp3	forward: 5'-ACC ACA CTT CAT GCA TCA GC-3' reverse: 5'-CCA GTG GCA GCA GAA GGT-3'	#75
Hpgd	forward: 5'-TCA GAA GAC ACT GTT CGT CCA-3' reverse: 5'-TCC AAT CTT CCG AAA TGG TC-3'	#46
Ppar-γ	forward: 5'-TTA TAG CTG TCA TTA TTC TCA GT-3' reverse: 5'-GAC TCT GGG TGA TTC AGC TTG-3'	#62
Ptgr1	forward: 5'-GAC TGA GCT CCC ACC CTT AAA-3' reverse: 5'-GAC TGA GCT CCC ACC CTT AAA-3'	#18
Ptgr2	forward: 5'-GGA GGT GAC ATC AGC AAC G-3' reverse: 5'-CTG AGA AAT CTG ACC ACA CAG G-3'	#5

Insr1	forward: 5’-CGG TAG CCT GAT CAT CAA CAT-3’ reverse: 5’-TCT TCA ATG AGG CCA AGG TTA-3’	#78
Irs1	forward: 5’- CTA TGC CAG CAT CAG CTT CC-3’ reverse: 5’- TTG CTG AGG TCA TTT AGG TCT TC-3’	#71
Irs2	forward: 5’- TCC AGG CAC TGG AGC TTT-3’ reverse: 5’-GGC TGG TAG CGC TTC ACT-3’	#53

Table 17: List of human qRT-PCR primer sequences

Target	Sequence	Probe
B2M	forward: 5’-TTC TGG CCT GGA GGC TAT-3’ reverse: 5’-TCA GGA AAT TTG ACT TTC CAT TC-3’	#42
FOXP3	forward: 5’-ACC TAC GCC ACG CTC ATC-3’ reverse: 5’-TCA TTG AGT GTC CGC TGC T-3’	#50
HPGD	forward: 5’- GGT TCC ACT GAT AAC AGA AAC CA-3’ reverse: 5’-TTT GGT CAA TAA TGC TGG AGT G-3’	#48
MEOX1	forward: 5’-GAC TGC AAA AGG GGA CAA GA-3’ reverse: 5’-CAG CAA GAG CTT AAA TCC ATC C-3’	#69
PTGR1	forward: 5’-GCA GCC AAA AGA TTG AAG GA-3’ reverse: 5’-GGC TAC ATT TTT ACT TTC CAC AAC T-3’	#43
PTGR2	forward: 5’-CGG TAA TAA ATG GGT TGG AAA A-3’ reverse: 5’-CTG CTT TCC AAT GTT ACC TCC T-3’	#24

Table 18: List of siRNA sequences

Target	Sequence	
FOXP3	sense:	5’-GCA CAU UCC CAG AGU UCC-3’
	antisense:	5’-AGG AAC UCU GGG AAU GUG C-3’
MEOX1	sense:	5’-CAC UGC CAA UGA GAC AGA GAA GAA A-3’
	antisense:	5’-UUU CUU CUC UGU CUC AUU GGC AGU G-3’
Scrambled	sense:	5’-UUC UCC GAA CGU GUC ACG U-3’
	antisense:	5’-ACG UGA CAC GUU CGG AGA A-3’

Table 19: List of primers for Hpgd genotyping

Primer	Sequence
sense:	5'-TCT TTA GTC TGA ACC AAT CC-3'
antisense 1:	5'-AGA AGA AGA CAG GCA AAT AA-3'
antisense 2:	5'-GCA TGA CTG TCA TTG AAA CT-3'

2.10. Reagents

Table 20: List of reagents and suppliers

Reagent	Supplier
10% SDS	Applichem
15-keto-PGE_2	Cayman Chemical
30 % Acrylamide/bis Solution 29:1	Bio-Rad Laboratories
480 Probe Master	Roche Diagnostics
6x Purple Loading Dye	Fermentas GmbH
Agarose	Applichem
Ammonium persulfate (APS)	Sigma-Aldrich
Ammoniumacetate	Merck
BD Pharm Lyse Buffer	BD Biosciences
Bovine serum albumin (BSA)	Sigma-Aldrich
Bromophenole blue	Roth
CD14+ Microbeads	BD Biosciences
CD25+ Microbeads II	BD Biosciences
Cell Proliferation Dye eFluor 670	eBioscience
CFSE	Sigma-Aldrich
Chloroform	Applichem
Complete mini Protease Inhibitor cocktail tablets	Roche Diagnostics
CountBright Absolute Counting Beads	Invitrogen Life Technologies
Dimethyl sulfoxide (DMSO)	Sigma-Aldrich
DSS	Sigma Aldrich
Dulbecco's Modified Eagle Medium (D-MEM)	PAA Laboratories GmbH
Dynabeads M-450 Tosylactivated	Thermo Fisher Scientific
ECL Western Blotting Substrate	Promega
EDTA	Sigma-Aldrich

EGTA	Sigma-Aldrich
Ethanol	Roth
Fc receptor blocking reagent, human	Miltenyi Biotec
Fc receptor blocking reagent, murine	Biolegend
Fetal calf serum (FCS)	Sigma-Aldrich
Forane (Isolfourane)	Baxter
Formaldehyde solution (37 %)	Sigma-Aldrich
Gibco distilled water (RNase/ DNase free)	Invitrogen Life Technologies
Glucose	Merck
Glutamax (100 x)	Invitrogen Life Technologies
Glycerol (87 %)	Applichem
Glycine	Sigma Aldrich
GM-CSF	ImmunoTools
HEPES	Applichem
IL-2	ImmunoTools
IL-4	ImmunoTools
Insuman Rapid (40 I.E./ml)	Sanofi
Isopropanol	Applichem
Laemmli buffer for SDS-PAGE (10x)	Serva
Methanol	Roth
Near-IR fixable live dead stain	Invitrogen Life Technologies
O'GeneRuler 1 kb Plus DNA-Ladder	Fermentas GmbH
O'GeneRuler 50bp DNA-Ladder	Fermentas GmbH
Odyssey Two-Color Molecular Weight Marker	Licor Biosciences
Pancoll human (density 1.077 g/L)	PAN Biotech GmbH
Paraformaldehyde	Sigma-Aldrich
Penicillin/Streptomycin	Gibco
PGD_2	Cayman Chemical
PGE_2	Sigma-Aldrich
PGF_{2a}	Cayman Chemical
PGJ_2	Cayman Chemical
Phosphate buffered saline (PBS)	PAA Laboratories GmbH
PhosStop (Phosphatase Inhibitor)	Roche Diagnostics

Propidium iodide (PI)	Sigma-Aldrich
Qiazol (Trizol)	Qiagen
Re-Blot plus mild solution (Chemicon)	Merck
rmGM-CSF	Peprotech
rmIL4	Peprotech
rmM-CSF	Peprotech
RPMI cell culture medium (1640)	Pan Biotec
SeeBlue Plus 2 standard	Thermo Fisher Scientific
siRNA-buffer	Dharmacon
Skim Milk powder	Roth
Sodium dodecylsulfate (SDS) powder	Roth
Sodium fluoride	Sigma-Aldrich
Sodium hydroxide (NaOH)	Merck
Sodium pyrophosphate	Sigma-Aldrich
Sodium vanadate	Sigma-Aldrich
SYBR Green Master Mix	Fermentas
TEMED	Applichem
Tris	Applichem
Tris-HCl	Applichem
Triton X-100	Applichem
Turbofect *in vitro* Transfection Reagent	Fermentas GmbH
Tween 20	Applichem
X-vivo 15 cell culture medium	Lonza
β-Glycerol Phosphate	Sigma-Aldrich
β-Mercaptoethanol	Applichem

2.11. Software

Table 21: List of software used

Software	Developer
Compass for Simple Western, Version 3.0	Protein Simple
CorelDRAW, Version 19.1.0.419	Corel Corporation
Flow Jo, Version 10.4.2	FlowJo, LLC
GraphPad Prism 7.02	Graph Pad Software, Inc
Image J Fiji, Version 1.51s	Schindelin et al., 2012
LightCycler 480 Software, Version 1.5.0.39	Idaho Technology, Inc

3. Methods

3.1. Isolation of murine cells and serum

Prior to cell isolation, mice were anesthetized by isoflourane inhalation and sacrificed by cervical dislocation unless perfusion was required, in which case mice were anesthetized with 100 mg/kg bodyweight ketamine and 10 mg/kg bodyweight xylazine and perfused with 20 ml PBS through the left ventricle under animal license AZ 84-02.04.2016.A284.

3.1.1. Isolation of cells from bone marrow

Mice were sacrificed by cervical dislocation and the femurs and tibias were excised. Bone marrow (BM) was flushed out of the bones with MACS buffer and collected in a reaction tube. Cells were centrifuged at 400 g for 5 min at 4° C and resuspended in 1 ml of RBCL buffer. Cells were incubated for 2 min at room temperature (RT) while shaking gently. The lysis was stopped with 5 ml PBS and repeated if necessary. Cells were washed twice in PBS by centrifuging at 400 g for 5 min at 4°C, removing the supernatant and repeating the centrifugation step. After washing, the supernatant was removed and cells were used for subsequent experiments.

3.1.2. Isolation of cells and serum from blood

Mice were euthanized by inhalation of an isofluorane overdose and blood was drawn directly from the heart by cardiac puncture. For cell isolation, blood was transferred to a reaction tube and RBCL was performed as with cells isolated from the BM (see section 3.1.1). Cells were washed and resuspended in PBS for subsequent staining. For serum isolation, blood was and transferred into Z-Gel tubes containing a gel with clotting factors. After 5 min of incubation at RT, tubes were centrifuged at maximum speed for 5 min and the serum was transferred into a new tube and stored at -80°C until use.

3.1.3. Isolation of cells from the kidney

Mice were perfused, the kidneys were excised and their capsule was removed with the help of a forceps. The kidneys were subsequently homogenized and digested in 3 ml digestion buffer at 37°C for 45 min. The reaction was stopped with 5 ml PBS and the homogenate was resuspended and filtered through a 100 µm mesh. The homogenate was then layered onto 5 ml pancoll and centrifuged at 700 g for 20 min with the brake disengaged. The interphase containing the cells was collected and washed with PBS by centrifuging at 500 g for 7 min before resuspending in PBS for staining.

3.1.4. Isolation of cells from the lung

Mice were perfused and the lung was excised and homogenized through a 100 µm mesh. The homogenate was then layered onto a pancoll gradient and cells were collected as in 3.1.3. Washed cells were resuspended in PBS for staining.

3.1.5. Isolation of cells from LNs

Mice were sacrificed by cervical dislocation and LN were excised and homogenized through a 100 µm mesh. Cells were washed once with 10 ml PBS and centrifuged at 400 g for 5 min at 4°C and resuspended in PBS for staining.

3.1.6. Isolation of cells from the spleen

Mice were sacrificed by cervical dislocation and the spleen was excised and homogenized through a 100 µm mesh. If splenic myeloid cells were analyzed, the tissue was resuspended in 3 ml digestion buffer and digested at 37°C for 45 min before RBCL. The digestion was omitted if only T cells were analyzed by flow cytometry. RBCL was performed as described for the BM (see section 3.1.1). Cells were washed and then resuspended in PBS for subsequent staining or sorting.

3.1.7. Isolation of cells from adipose tissue

Mice were perfused and adipose tissue was excised. If adipose tissue was isolated in order to stain for ST2, the tissue was cut into small pieces and transferred into 10 ml of AT-digestion buffer and incubated for 45 min at 37°C. The reaction was then stopped with 40 µl 0.5M EDTA and incubated at RT for 2 min before transferring the homogenate through a 100 µm mesh into a new reaction tube. Cells were centrifuged at 400 g for 5 min and washed once with PBS before resuspending in PBS for ST2 staining.

If cells were isolated for other stainings, adipose tissue was transferred into GentleMACS C Tubes with 3 ml of digestion buffer and homogenized on the GenlteMACS dissociator using the ‘m_brain_1’ program. After incubating at 37°C for 15 min, the sample was dissociated again, this time using the ‘m_brain_2’ program followed by another 15 min of incubation at 37°C. After the last incubation step, cells were transferred through a 100 µm mesh, centrifuged at 400 g for 5 min and washed with PBS before staining for flow cytometry or sorting.

3.1.8. Isolation of cells from the colon

The colons were removed from animals and associated patches of adipose tissue removed before flushing the intestinal content and cutting the colon into small pieces. To remove the mucosal layer, colon pieces were incubated in intestinal wash buffer I for 20 min at 37° C at 200 rpm. Epithelial cells were removed by washing the tissue in intestinal wash buffer II three times for 15 min each at 37°C at 200 rpm. EDTA and FCS were removed by washing in intestinal wash buffer III for 10 min at 37°C, 200 rpm. The tissue was then digested in intestinal digestion buffer for 45 min at 37°C, 200 rpm after which the reaction was stopped with MACS buffer. Cells were filtered through a 70 µm mesh and washed twice with HBSS containing 2% FCS before staining for flow cytometry.

3.1.9. Isolation of cells from the skin

To isolate cells from the skin, a $2cm^2$ area of the skin from the trunk of the animals was depilated, excised and lightly defatted. The tissue was minced and digested in PBS containing 0.8 U/mL Liberase and 200U/mL DNAse I at 37°C, 150 rpm for 90 min. A single cell suspension was then generated by pipetting up and down and filtering cells through a 70 µm cell mesh before proceeding to FACS staining.

3.2. Isolation of cells from human peripheral blood

All experiments conducted with human samples were performed in compliance with the institutional review boards and covered by Reg. No. 017-12-23012012 (T2D patient blood samples) or 288/13 (isolation of cells from buffy coats). All donors provided written and informed consent.

For experiments with cells from healthy individuals or T2D patients depicted in Figure 40, cells were isolated from whole blood while all other experiments were conducted with cells isolated from buffy coats. For analysis of T-cell populations, samples were enriched for $CD4^+$ T cells using $CD4^+$ pluribeads according to manufacturer's instructions. Samples were then either stained with antibodies and sorted using the BD FACS ARIA III or further purified using human CD25 microbeads according to manufacturer's instructions. Both the $CD25^+$ fraction, containing the T_{reg} cells, and the $CD25^-$ fraction, containing the T_{conv} cells, were collected for subsequent analysis.

3.3. Antibody staining for flow cytometry

3.3.1. Extracellular staining

After cell isolation, cells were stained with antibodies binding to cell-surface proteins. Thus, cells were transferred into a 96-well plate and resuspended in PBS to a final reaction volume of 50 µl. A master mix containing FC receptor block, fluorochrome-coupled antibodies and, if required, near-IR fixable live-dead stain was prepared and added to the reaction to yield final dilutions of 1:300 for the FC receptor block, between 1:50 and 1:400 for the antibodies and 1:1,000 for the live-dead stain. Cells were then incubated at 4°C for 20 min in the dark. Cells were washed with PBS and centrifuged at 400 g for 5 min. The supernatant was decanted and cells were resuspended in 200 µl PBS prior to acquiring them on a flow cytometer. If cells were not immediately acquired, they were stored at 4°C in the dark. If cells were stored for longer than a few hours, cells were fixed as described in section 3.3.3.

3.3.2. Sorting of human and murine T cells

Cells were stained as described in section 3.3.1. Human cells were stained for CD3, CD4, CD25 and CD127. The following populations were isolated using a BD FACS Aria III sorter: $CD3^+CD4^+CD25^+CD127^-$ T_{reg} cells and $CD3^+CD4^+CD25^-CD127^+$ T_{conv} cells. Murine cells expressing YFP under the control of the Foxp3 promoter were stained for CD45, CD3, CD4 and CD25, as described in section 3.3.1. T_{reg} cells, defined as $CD45^+CD3^+CD4^+CD25^+$ and YFP^+, and T_{conv} cells, defined as $CD45^+CD3^+CD4^+CD25^-$ and YFP^-, were sorted. To sort for naïve T cells, cells were additionally stained for CD44 and CD62L. Naïve T cells were defined as $CD45^+CD3^+CD4^+CD25^-YFP^-CD44^-CD62L^+$ and sorted using a BD FACS Aria III cell sorter.

Murine cells sorted from the spleen were pre-enriched using the $CD4^+$ T cell isolation kit II according to manufacturer's instructions. Cells isolated from either the VAT or the kidney were pre-enriched by sorting for $CD45^+$ cells prior to sorting for T_{reg} or T_{conv} cell populations.

3.3.3. Intracellular YFP staining

After extracellular staining, cells were centrifuged at 400 g for 5 min at 4°C and then fixed in 200 µl 4% PFA buffer for 10 min on ice in the dark. Following the fixation step, cells were centrifuged at 700 g for 2 min at 4°C and washed twice in 1x Permeabilization Buffer. Cells were then counterstained with a flourochrome coupled anti-GFP antibody, which is

cross-reactive for YFP, at a final concentration of 1:300 at RT for 30 min. After washing once with 1 x Permeabilization Buffer, cells were fixed and stained for intracellular transcription factors as described in section 3.3.4.

3.3.4. Intracellular transcription factor staining

Intracellular transcription factor staining of cells was performed using the transcription factor staining buffer set in a 96-well plate according to the manufacturer's instructions.

3.3.5. MEOX1 staining

MEOX1 staining was performed using the intracellular transcription factor staining buffer set as described in section 3.3.4. After washing once with 1x Permeabilization Buffer, cells were stained with a fluorochrome-coupled goat anti-rabbit secondary antibody for 1hr at room temperature. Subsequently, cells were washed once with 1X Permeabilization Buffer and once in PBS.

3.3.6. CD1d Tetramer staining

CD1d staining was performed using tetramers loaded by the NIH tetramer core facility. Cells were resuspended in 200µl of PBS and stained with either empty tetramer or CD1d loaded, fluorescently labeled tetramers in a dilution of 1:400 for 15 min at RT. Cells were then washed in PBS and resuspended in PBS prior to acquiring on a flow cytometer.

3.3.7. FOXP3 staining of T2D samples

For FOXP3 staining of T2D patient samples and healthy control samples, 1ml of peripheral blood was used per staining and surface antibodies were added to whole blood samples in adequate dilutions. Subsequently, red blood cells were lysed using the BD Pharm Lyse Buffer according to the manufacturer's instructions. If necessary, lysis was repeated. Subsequently, cells were fixed, permeabilized and stained as described in section 3.3.4.

3.3.8. Quantification of cell numbers by flow cytometry

To quantify cells, CountBright counting beads were added to the cells prior to antibody staining. Absolute cell numbers could be calculated based on the following formula:

$$\text{absolute cell number} = \frac{\text{cells aquired by flow cytometer x total beads added to reaction}}{\text{beads aquired by flow cytometer}}$$

3.4. ELISAs

3.4.1. Metabolite assay

To determine the ability of human T_{reg} and T_{conv} cells to metabolize PGE_2, human T_{reg} and T_{conv} cells were isolated as described in section 3.2. Cells were then stimulated with 100 U/ml of IL-2 and 1 µM PGE_2 for 24 hours before assessing the amount of PGE_2 metabolite in the cell supernatant with the Prostaglandin E Metabolite EIA Kit according to the manufacturer's instructions.

3.4.2. Insulin ELISA

Animals were fasted overnight and blood was drawn. Serum was collected as described in section 3.1.2. Insulin levels were determined with the Ultrasensitive Mouse Insulin ELISA performed in 96-well half-area plates according to manufacturer's specifications.

3.5. Cell culture

Cells were cultured in an incubator at 37°C with 5% CO_2. Human primary T cells were cultured in X-Vivo 15 medium supplemented with 10% FCS and 1% Glutamax. In contrast, murine T cells were cultured in IMDM supplemented with 10% FCS, 1% Glutamax, 55 µM β-Mercaptoethanol, 0.5 mM Sodiumpyruvate, 1% Non-essential amino-acids and 5 mM HEPES. Meanwhile, HEK293T and 3T3-L1 cells were cultured in DMEM supplemented with 10% FCS, 1% Glutamax and 1% Penicilin/Streptomycin. Both cell lines were allowed to grow to a confluency of approximately 70% before passaging.

3.5.1. Suppression assays

To analyze the suppressive capability of T_{reg} cells, human and murine T_{reg} and T_{conv} cells were isolated as described in section 3.3.2. Human T_{conv} cells were then stained with CFSE at a final concentration of 5.5 mM for 8 min in the dark at RT. The staining was stopped with FCS and the cells were washed twice with full medium. Murine T_{conv} cells were stained with eFlour670 according to manufacturer's specifications.

T_{conv} cells were then co-cultured with T_{reg} cells in different ratios and either CD3/CD28/MHC-I coated beads for human or Mouse T-Activator CD3/CD28 Dynabeads for T-Cell Expansion and Activation for murine cells, respectively, were added at a ratio of 1 bead for every 3 cells. Cells were then cultivated in the presence or absence of different prostaglandins for 3 days before measuring the proliferation on a flow cytometer by

determining proliferation-dependent CFSE dilution as a measure of the rate of T_{conv} proliferation where a higher dilution is indicative of more proliferation.

3.5.2. Transfection of HEK293T cells

To transfect cells, $2.5x10^5$ HEK293T cells were seeded in 6-well plates and cultivated overnight to reach a confluency of approximately 70 – 80%. The transfection was carried out using the Turbofect *in vitro* Transfection Reagent according to the manufacturer's specifications.

Transfection efficiency was assessed by analyzing GFP expression by flow cytometry after 24 hours. Cells were analyzed for gene expression by qRT-PCR as described in section 3.7 after 48 hours.

3.5.3. siRNA knockdown

3.5.3.1. Preparation of siRNA

Single-stranded siRNA was dissolved to a final concentration of 500 µM in sterile H_2O and annealed by combining 30 µl of both the sense and antisense siRNA together with 15 µl 5x siRNA-buffer. The mixture was then heated to 90°C for 1 minute and subsequently cooled down to RT over the span of an hour. Afterwards, the mixture was heated to 90°C again and then incubated at 37°C for 1 hour. The annealed oligos were stored at -80°C until use.

3.5.3.2. Transfection of siRNA into primary human T cells

To perform a knockdown of the target gene, siRNA specific for the gene of interest was introduced into primary T_{reg} or T_{conv} cells, isolated as described in section 3.2. As a control, scrambled siRNA was transfected instead of the specific siRNA.

Briefly, $5x10^6$ cells were resuspended in 100 µl human T cell nucleofector solution with 5 µl of the annealed siRNA in an electroporation cuvette. The cells were then transfected using the U14 program on an AMAXA electroporator. Subsequently, cells were transferred into a 24-well plate with prewarmed X-Vivo 15 medium, supplemented with 10% FCS and 1% Glutamax. After 48 hours, RNA was isolated and gene expression was analyzed by qRT-PCR as described in section 3.7.

3.5.4. IL-2 time kinetics of human primary T_{reg} cells

Human primary $CD4^+CD25^+$ T_{reg} cells were isolated as described in section 3.2. Cells were seeded onto 96-well plates at a final concentration of $2x10^5$ cells/well and stimulated with either 0, 10, 100 or 1,000 U/ml of IL-2. Cells were harvested after 0, 12, 24, 48 and 72 hours with Trizol, RNA was isolated and gene expression was analyzed by qRT-PCR as described in section 3.7.

3.5.5. Differentiation of human monocytes

To differentiate human monocytes into macrophages or dendritic cells, blood from human buffy coats was layered over pancoll and centrifuged at 900 g for 25 min without a brake and the PBMCs located at the interphase were collected. Monocytes were then isolated from the PBMC population by using human CD14 MACS beads according to the manufacturer's instructions. Cells were subsequently differentiated into macrophages or dendritic cells as previously published using a cocktail of 500U/ml GM-CSF for macrophage differentiation or 800 U/ml GM-CSF and 500 U/ml IL-4 for dendritic cell differentiation for 6 days with a medium change after three days (Xue et al., 2014).

3.5.6. Differentiation and stimulation of 3T3-L1 cells into adipocytes

Prior to differentiation, cells were allowed to reach 100% confluency for 48 hours. Cells were then stimulated with adipocyte differentiation medium for 48 hours. After 48 hours, adipocyte differentiation medium was exchanged for adipocyte maintenance medium and cells were allowed to further differentiate for another 6 days before stimulating cells with either 1 µM 15-keto-PGE_2, 1 µM Rosiglitazone or DMSO as vehicle control. Cells were then harvested and lyzed in Trizol for subsequent qPCR analysis (see section 3.7).

3.5.7. Differentiation and stimulation of bone-marrow derived macrophages (BMDMs) and dendritic cells (BMDCs)

Isolation of cells from the BM was performed as described above (see chapter 3.1.1). For differentiation into BMDMs, cells were then differentiated for 6 days in DMEM containing 10% FCS and 20 ng/ml rmM-CSF. Cells were then stimulated with 1 µM 15-keto-PGE_2, 1 µM Rosiglitazone or DMSO as vehicle control overnight before harvesting and lysis in Trizol for qPCR analysis (see section 3.7).

To analyze the effect of 15-keto-PGE_2 and Rosiglitazone on the differentiation of BMDCs, cells were stimulated with 20 ng/ml rmGM-CSF and 2 ng/ml IL-4 in DMEM

containing 10% FCS. After 3 days, 1 µM 15-keto-PGE_2, 1 µM Rosiglitazone or DMSO as vehicle control was added to the differentiation. After another 3 days, cells were stained with antibodies for flow cytometric analysis as described above (see section 3.3.1).

3.6. *In vivo* assays

Mice used for experiments were housed under specific pathogen-free conditions. All experiments conducted followed the principles of laboratory animal care as elucidated by the NIH (NIH, 2011). All experiments were approved by the Animal Care Commission of North Rhine-Westphalia. Mice were used between 6 and 10 weeks of age, unless denoted as aged animals in which case they were defined as more than 40 weeks old. All mice, unless otherwise specified, were male.

3.6.1. DSS colitis

The induction of DSS colitis in animals was approved by the commission for animal care under the animal license AZ 84-02.04.2011.A167. Colitis was induced by replacing the drinking water of the animals with a 5% (w/v) DSS solution in distilled water. Female animals with Hpgd competent or deficient T_{reg} cells were given *ad libitum* access to the DSS solution for 6 days and scored and weighed daily to track disease progression.

Animals were sacrificed after 6 days and 10 µl serum and 10 mg colon were harvested and used for MS at the Institute of Clinical Pharmacology in Frankfurt by the group of N. Ferreirós to analyze PGE_2 levels as previously described (Lacroix et al., 2015; Schmitz et al., 2014).

3.6.2. Adoptive transfer colitis

Adoptive transfer experiments were conducted as approved by the relevant authorities under AZ 84-02.04.2013.A248. Cells were isolated from the spleen of animals with either Hpgd-deficient or competent T_{reg} cells and naïve T cells or T_{reg} cells were isolated as described in section 3.3.2.

Colitis was induced by intravenously injecting either $1x10^6$ naïve T cells or $1x10^6$ naïve T cells and $2.5x10^5$ either Hpgd-competent or deficient T_{reg} cells into $Rag2^{-/-}$ animals. Animals were weighed and scored three times a week for six weeks until they were sacrificed for analysis.

Flow cytometric analysis was performed on LNs and spleen as described above (see sections 3.1.5, 3.1.6 and 3.3).

For histological analysis and scoring, the colon was excised, cleaned, and stored in 4% PFA solution. Colons were then embedded in paraffin and stained with hematoxylin and eosin and disease severity was scored by the group of C. Wickenhauser at the University Hospital of Halle, Institute of Pathology as described previously (Beyer et al., 2011).

3.6.3. Adoptive transfer experiments

Adoptive transfer experiments were conducted in the same manner as adoptive transfer colitis. However, in addition to injecting $1x10^6$ naïve T cells and $2.5x10^5$ Hpgd-competent or Hpgd-deficient T_{reg} cells into $Rag2^{-/-}$ animals, $2.5x10^5$ Hpgd-competent RFP^+ T_{reg} cells were co-transferred to avoid the development of colitis. Recipient mice were weighed and scored three times a week and sacrificed after 6 weeks. Flow cytometric analysis was performed as described in section 3.6.2 and T_{reg} cells were sorted from mLN for subsequent transcriptomic analysis (see section 3.7.5).

3.6.4. High fat diet experiments

High fat diet experiments were conducted according to animal license AZ 84-02.04.2016.A282. Animals were put on a low caloric diet for 2 weeks at 3 weeks of age, after which they either continued to be fed the low caloric diet or were switched to a high caloric diet for the next 15 weeks. Animals were weighed and scored once a week for the duration of the experiment. Glucose and insulin tolerance were tested as described in section 3.6.5.

3.6.5. Insulin and glucose tolerance tests

Animals were tested for their tolerance towards insulin and glucose as approved by the committee for animal care in the license AZ 84-02.04.2016.A282. Animals were fasted either overnight or for 4 hours to analyze glucose or insulin tolerance, respectively. Animals were then weighed and their fasting glucose levels were determined by drawing one drop of blood from the tail vein and measuring glucose content with an Accu-Chek Aviva. Either 2 g glucose/kg bodyweight or 1 U insulin/kg bodyweight were injected intraperitoneally and glucose levels were measured 20, 40, 60, 80, 120, and 240 min post injection to test glucose tolerance or 15, 30, 60, 120, and 240 min post injection for insulin tolerance.

3.6.5.1. Calculating the Homeostatic Model Assessment for Insulin Resistance

To determine the Homeostatic Model Assessment for Insulin Resistance (HOMA-IR), the fasting glucose and insulin were determined after an overnight fasting period as described. The following formula was used to calculate the HOMA-IR:

$$\mathrm{HOMA-IR} = \frac{\text{fasting glucose } \left(\frac{\mathrm{mg}}{\mathrm{ml}}\right) \cdot \text{fasting insulin } \left(\frac{\mathrm{mg}}{\mathrm{ml}}\right)}{405}$$

3.7. RNA isolation, cDNA synthesis, qRT-PCR and SmartSeq2

3.7.1. RNA isolation

Protocols for RNA isolation differ depending on whether RNA was extracted from whole tissues, from cell suspensions containing fewer than 10,000 cells or from cell suspensions containing more than 10,000 cells.

When isolating RNA from whole tissue samples, samples were harvested from animals and flash frozen in liquid nitrogen. Prior to RNA extraction, tissue was transferred into gentleMACS M Tubes with 500 µl Trizol and dissociated on a gentleMACS dissociator using the program 'm_protein_1'. Subsequently, samples were incubated at RT for at least 5 min to allow for complete dissociation. After dissociation, 200 µl chloroform was added per ml of trizol and vortexed. The mixture was incubated at RT for 3 min before centrifuging at 4°C for 10 min at 12,000 g. The aqueous phase was collected and transferred into a new reaction tube containing 400 µl isopropanol and the RNA was precipitated at -20°C for 2 hours. After precipitation, samples were centrifuged at 12,000 g for 30 min at 4°C and the supernatant was decanted followed by two washing steps with 800 µl of 80% Ethanol. After washing, pellets were air-dried for approximately 20 min and solved in 20 µl RNAse and DNAse free water. RNA concentrations were determined using a spectrophotometer.

Cell suspensions containing more than 10,000 cells were resuspended in 500 µl Trizol and incubated at RT for 5 min. RNA isolation was performed following the same protocol as for the isolation of RNA from whole tissue samples.

If fewer than 10,000 cells were isolated, RNA was extracted using the RNeasy Micro Kit according to the manufacturer's instructions.

3.7.2. cDNA synthesis

Isolated RNA was converted into cDNA using the Transcriptor First Strand cDNA Synthesis Kit. Ideally, at least 200 ng of RNA was used for the conversion reaction, however as little as 50 ng input material can yield cDNA with adequate quality for qRT-PCR.

The RNA was adjusted to a final volume of 12 µl and 50 pmol oligo(dT) primer was added yielding a final volume of 13 µl. Denaturing and oligo annealing was performed at 65°C for 15 min. For the reverse transcription reaction 0.5 µl RNAse Inhibitor, 2 µl 10mM dNTPs, 0.5 µl reverse transcriptase and 4 µl of 5 x reaction buffer were added, yielding a final volume of 20 µl. Reverse transcription was carried out at 55°C for 30 min followed by heat inactivation at 85°C for 5 min.

3.7.3. qRT-PCR reaction

Prior to setting up the qRT-PCR reaction, cDNA was diluted to a final volume of 100 µl. qRT-PCR reactions were either carried out using the Roche 480 Probe master system (reaction set-up Table 22, qRT-PCR program Table 23) or the SYBR green system (reaction set-up Table 24, qRT-PCR program Table 25). All samples were pipetted at least in duplicates to ensure reproducibility.

Table 22: Roche Probe Master reaction set-up

Component	Volume [µl]
Universal ProbeLibrary probe	0.1
Primer Mix (10µM each)	0.2
H_2O	0.5
Roche 480 Probe Master	5
cDNA	4

Table 23: Roche Probe Master qRT-PCR program

	T[°C]	t[sec]	#cycles
Pre-Incubation	95	600	1
Amplification	95	10	
	60	30	50
	72	1	
Cooling	20	30	1

Table 24: SYBR green qRT-PCR reaction set-up

Component	Volume [µl]
Primer Mix (10µM each)	0.2
H_2O	2.8
SYBR Green Master Mix	5
cDNA	2

Table 25: SYBR green qRT-PCR program

	T[°C]	t[sec]	#cycles
Pre-Incubation	95	600	1
Amplification	95	15	
	60	30	50
	72	30	
Melting Curve	95	5	
	65	60	1
	97	cont	
Cooling	37		

3.7.4. qRT-PCR data analysis

For data analysis, the expression of a reference gene was analyzed in parallel with the gene of interest: B2M in humans and β-actin for murine samples. The relative expression was calculated by applying the formula $2^{-\Delta ct}$, where Δct is the difference between the threshold cycle of the gene of interest and the reference gene.

3.7.5. SmartSeq2

RNA was isolated as described above (see section 3.7.1) and the samples were further processed for transcriptome analysis using the previously published SmartSeq2 protocol (Picelli et al., 2013). Denaturation was performed at 95°C for 2 min in Denaturing Reaction Mix (see Table 26) followed by reverse transcription at 42°C for 90 min (see Table 27). For pre-amplification, commercially available KAPA HiFi HotStart ReadyMix with 1 nm ISPCR primer was used. Cycle conditions are listed in Table 28. The reaction was purified using AMPure XP beads and quality was assessed using a Tapestation HighSensitivity D5000 assay according to manufacturer's instructions. Subsequently, the Nextera XT DNA Library Preparation Kit was used to prepare the library. Samples were sequenced on an Illumina NextSeq 500 instrument using High Output v2 chemistry. RNA-seq data was demultiplexed using bcl2fastq2 v2.20 and pseudo aligned to Mus musculus GRCm38 transcriptome using kallisto v.0.44.0. Genes that were up- or down-regulated between KO and WT samples were

identified (FC > |2.0|, p-value < 0.05, FDR-corrected). Differentially expressed genes were compared to a previously published T_{reg} cell signature (Hill et al., 2007) and plotted as a Z-normalized Heatmap.

Table 26: Denaturing Reaction-Mix

Component	Amount
RNA	500pg
dNTP	0.05M
anchored oligodT primer	2µM
RNAse Inhibitor	1U/µl
Triton X-100	0.1%
in H_2O	

Table 27: Reverse Transcription Reaction Mix

Component	Amount
Template Switching Oligo	1µM
DTT	5mM
$MgCl_2$	14mM
Betaine	1M
RNAse Inhibitor	1U/µl
Superscript II reverse transcriptase	5 U/µl
in 1X Superscript II Buffer	

Table 28: Pre-Amplification Cycle Conditions

	T[°C]	t[sec]	#cycles
Pre-Incubation	98	180	1
Amplification	98	20	
	67	20	16
	72	360	
Cooling	8	hold	1

3.8. Immunohistochemistry staining of VAT

VAT was embedded in paraffin, sectioned and stained for F4/80, hematoxylin and eosin by the group of C. Wickenhauser from the Institute of Pathology at the University Hospital of Halle as described by Eming and colleagues (Eming et al., 2007).

3.9. Immunoblotting

3.9.1. Protein Isolation

Mice were challenged with 0.5 U/kg bodyweight insulin by intraperitoneal injection after a 4 hour fasting period as described in the animal license AZ 84-02.04.2016.A282. Mice were sacrificed after 3 min and organs were harvested and flash frozen in liquid nitrogen. Subsequently, samples were either stored at -80°C or further processed by transferring the tissue into gentleMACS M Tubes with 500µl of either RIPA or MRC buffer supplemented with proteinase phosphatase inhibitors. Tissues were dissociated on a gentleMACS dissociator using the program 'm_protein_1' and incubated on ice for 30 min. Samples were centrifuged at 1,000 g for 10 min at 4°C and the supernatant was transferred into a new reaction tube. This centrifugation step was repeated three times to remove any traces of fat or tissue remnants.

To isolate protein from cell suspensions, cells were pelleted and resuspended in RIPA buffer supplemented with proteinase inhibitor and, if necessary, phosphatase inhibitor and incubated on ice for 30 min. After the incubation, samples were centrifuged at 1,000 g for 10 min and transferred to a new reaction tube.

To determine the protein concentration of the resulting sample, the Pierce BCA Protein Assay Kit was used according to manufacturer's instructions.

3.9.2. Sodium dodecyl sulfate polyacrylamide gel electrophoresis (SDS-PAGE)

Between 20 and 50 µg of protein were denatured by adding 5x Laemmli loading buffer and incubated at 95°C for 10 min. Samples and a size marker were loaded onto a gel consisting of a 10% separation gel overlaid with a 4% stacking gel (For gel composition, see Table 29). Electrophoresis was performed at 80 V for 20 min to allow for adequate focusing of the protein bands. Subsequently, the voltage was increased to 130 V and continued for another hour.

Table 29: Reaction set-up for SDS-PAGE gel

Component	4% stacking gel [V in ml]	10% separation gel [V in ml]
H_2O	1.83	2.01
1M Tris-HCl (pH 6.8)	0.83	-
1.5M Tris-HCl (pH8.8)	-	1.25
10% SDS	0.025	0.05
30% Acrylamide	0.42	1.67
10% APS	0.017	0.017
TEMED	0.003	0.007

3.9.3. Immunoblotting and detection

Gels were blotted onto nitrocellulose membranes in wet blotting buffer at 0.2 A for 2 hours. Subsequently, the membrane was blocked in 5% milk in PBST for 1 hour. The blot was incubated overnight in primary antibody, diluted in 5% milk in PBST and subsequently washed 3 times for 10 min in PBST followed by incubation in secondary antibody for 1 hour at RT in either PBST when using horse-radish-peroxidase (HRP) coupled secondary antibodies or in LICOR buffer when using fluorescence coupled secondary antibodies. Following the secondary antibody incubation, protein signals were either detected on the LICOR Odyssey Imaging System or, when using HRP-conjugated secondary antibodies, developed using ECL according to manufacturer's instructions and imaged on a Chemidoc XRS (Bio-Rad).

If the same blot was probed for a second protein of a similar size, the blot was stripped using Re-blot mild solution according to the manufacturer's instructions. After stripping, the blot was blocked in 5% milk in PBST again prior to probing with a different antibody.

3.9.4. Automated Western Blots

Samples with limited protein amounts were run on the WES system (Protein Simple), a capillary Western blot system with a far lower detection limit than the traditional western. WES runs were performed according to manufacturer's instructions.

3.10. Genotyping

For genotyping, ear-clippings were digested at 55°C for at least 1 hour in DirectPCR Lysis Reagent Tail (Peqlab) with 0.2 mg/mL Proteinase K according to the manufacturer's instructions. The reaction was stopped by heat inactivation at 85°C for 45 min. Genotyping was performed with the MyTaq HS DNA Polymerase (Bioline).

3.11. CIBERSORT

Two publicly available datasets containing PBMC samples from T2D patients as well as healthy control patients (GSE9006 and E-MTAB-1954) were analyzed using the CIBERSORT (cell-type identification by estimating relative subsets of RNA transcripts) algorithm. The algorithm can enumerate immune cell populations based on distinct gene signatures and was first published by Newman et al. in 2015 (Newman et al., 2015).

3.12. Statistical Analysis

Statistical analysis was performed using GraphPad Prism software version 7.0. To allow for statistical testing, the number of samples was always at least 3. Statistical differences were analyzed using the Student's t-test or the Mann-Whitney test when analyzing differences between two groups. When more than two groups were analyzed, analysis of variance (ANOVA) tests were applied. Statistical significance was denoted as n.s. (not significant) when $p \geq 0.05$, * when $p < 0.05$, ** when $p < 0.005$ and *** when $p < 0.001$. Unless otherwise denoted, mean and standard error of the mean (SEM) were depicted.

4. Results

4.1. HPGD is upregulated and enzymatically active in human T_{reg} cells

T_{reg} cells are vital to maintain control of immune responses and to ensure that immune homeostasis is preserved, thus preventing or reducing the induction of autoinflammatory diseases. While a lot of research has been conducted to understand the functionality of T_{reg} cells, the function of these cells in specific environmental settings, such as the PGE_2-rich VAT, still remains unclear. Previous work performed by E. Schönfeld and Y. Thabet could demonstrate that HPGD, the primary enzyme of PGE_2 metabolism, is significantly upregulated in human T_{reg} cells compared to T_{conv} cells (Figure 3 A and B).

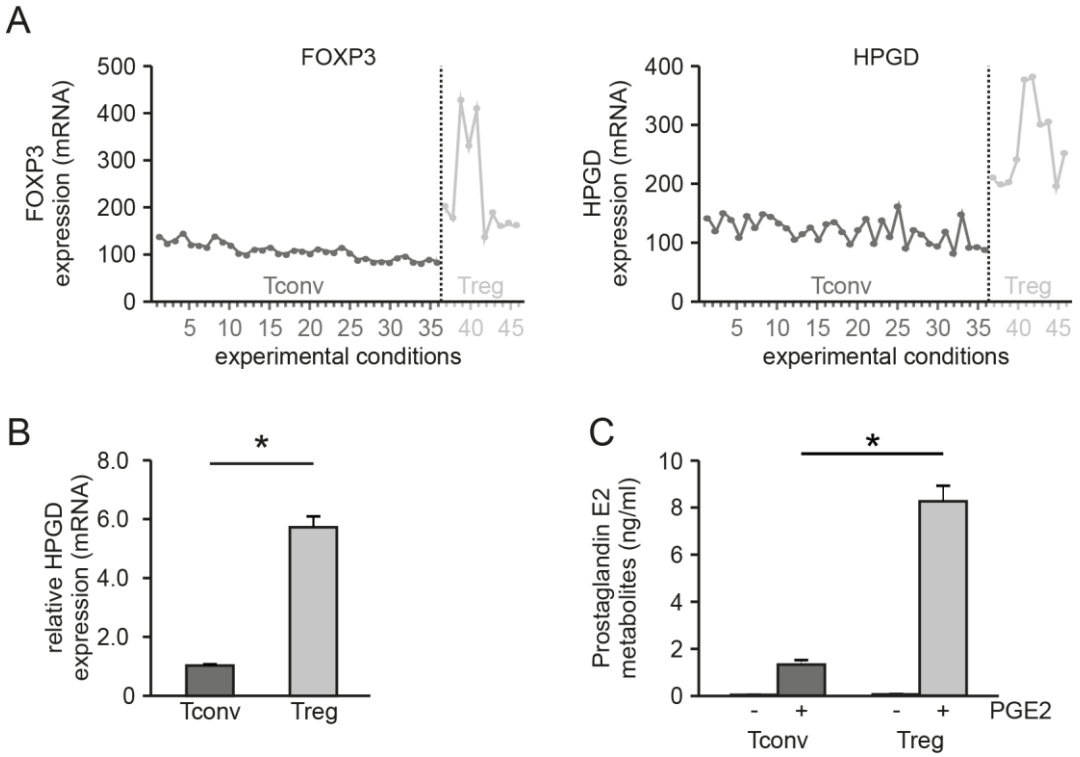

Figure 3: HPGD is expressed and enzymatically active in human T_{reg} cells.
A) Microarray data are published under GEO accession number GSE15390. mRNA expression levels of FOPX3 (left panel) and HPGD (right panel) were compared across the different experimental conditions. **B)** Human regulatory and conventional T (T_{reg} and T_{conv}) cells were isolated and relative HPGD mRNA expression was analyzed by qRT-PCR. Mean HPGD expression of T_{conv} cells was normalized to 1. **C)** Human T_{reg} and T_{conv} cells were cultured in the presence and absence of PGE_2 and the accumulation of PGE_2 metabolites in the supernatant was assessed by enzyme-linked immunosorbent assay. Experiments performed by E. Schönfeld and Y. Thabet. FOXP3, Forkhead box protein P3; HPGD, 15-Hydroxyprostaglandin dehydrogenase

E. Schönfeld could show in previously conducted experiments that the upregulation of HPGD in human T_{reg} cells occurs in a similar pattern to the regulation of the expression of FOXP3, the key transcription factor of T_{reg} cell development, across a variety of experimental conditions (Figure 3A). The T_{reg} cell specific expression and the coregulation with FOXP3 suggests that HPGD might play an important role in T_{reg} cells.

To determine whether HPGD is enzymatically active in human T_{reg} cells, we analyzed the production of PGE_2 metabolites when cultivating T_{reg} and T_{conv} cells in the presence or absence of PGE_2. We could detect a significant increase in PGE_2 metabolites in the supernatant of T_{reg} cells cultivated in the presence of PGE_2 compared to both T_{conv} cells cultivated in the presence of PGE_2 and to T_{reg} cells cultivated without PGE_2 (Figure 3 C). This indicates that PGE_2 is metabolized when cultivated with T_{reg} cells but not with T_{conv} cells and therefore leads to the conclusion that HPGD is enzymatically active. Thus, we could show that HPGD is both upregulated and enzymatically active in human T_{reg} cells.

4.2. Prostaglandin E_2 increases the suppressive capability of human T_{reg} cells

After confirming that HPGD is both present and enzymatically active in human T_{reg} cells, we assessed whether HPGD has an influence on human T_{reg} cell functionality *in vitro*. Thus, we measured the effect of T_{reg} cells on T_{conv} cell proliferation in the presence of different prostaglandins. Cell proliferation was measured by labeling T_{conv} cells with CFSE and then determining the dilution of CFSE on a flow cytometer after 72 hours.

As expected, when cultivating T_{conv} cells with increasing ratios of T_{reg} cells, a decrease in T_{conv} cell proliferation could be detected when compared to cultivating only T_{conv} cells. This effect could be increased significantly if PGE_2, the PG which is directly metabolized by HPGD, was added (Figure 4 A and B). None of the other PGs tested, including $PGF_{2\alpha}$, PGJ_2 and PGD_2 have any effect on the suppression of T_{conv} cell proliferation (Figure 4 C).

To confirm this finding, we performed a dose-titration of the different PGs on $CD4^+$ T cells. After three days of cultivation, we could not detect a significant decrease in proliferation caused by any of the other PGs, even when increasing the concentration up to 10 µM (Figure 4 D). Interestingly, the suppressive effect of PGE_2 seems to be dose dependent as $CD4^+$-cell proliferation was decreased with increasing amounts of PGE_2 added (Figure 4 D). Taken together, these results indicate that the suppressive effect, which was only observed

when PGE_2 was added but not when any of the other PGs were added to the culture, may be related to the enzymatic function of HPGD.

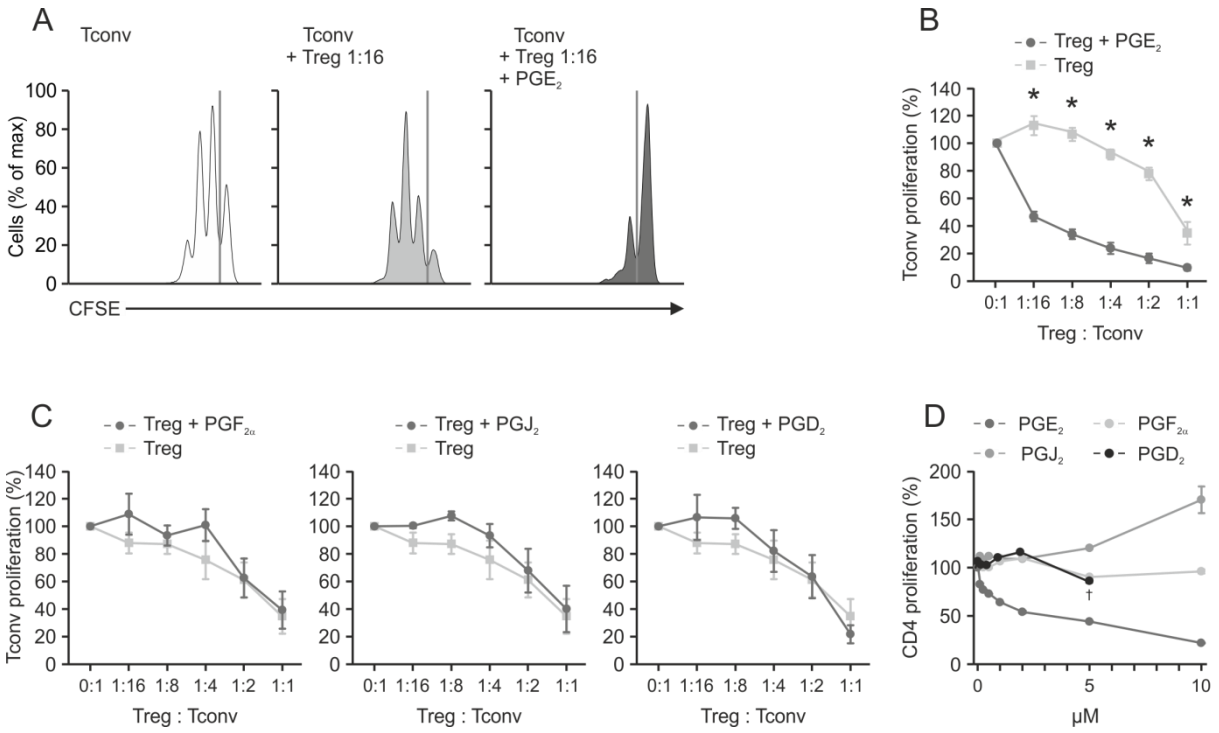

Figure 4: Only PGE_2 but not any of the other PGs have an effect on T_{conv} cell proliferation. **A)** T_{conv} cells were stained with CFSE and cultivated with CD3/CD28 coated beads either alone (left panel), with T_{reg} cells (middle panel) or with T_{reg} cells and 1 µM PGE_2 (right panel). After three days, proliferation was measured on a flow cytometer. **B)** Quantification of T_{conv} cell proliferation after three days cultivation in the presence of CD3/CD28 coated beads with or without 1 µM PGE_2 at different T_{conv} to T_{reg} cell ratios as a function of CFSE dilution. **C)** Quantification of T_{conv} cell proliferation after three days cultivation in the presence of CD3/CD28 coated beads with or without 1 µM different PGs at different T_{conv} to T_{reg} cell ratios as a function of CFSE dilution. **D)** Effect of dose titration of different PGs on the proliferation of $CD4^+$ T cells after three days of cultivation as a function of CFSE dilution. Experiments were partially carried out by Y. Thabet.

Previously, we analyzed the effect of the different PGs on T-cell proliferation only in the presence of T_{reg} cells. However, to determine whether T_{reg} cells are necessary to mediate the suppressive function of PGE_2, we analyzed the effect of PGE_2 on T_{conv} cells in the absence of T_{reg} cells. As expected, when PGE_2 was added to the entire $CD4^+$ T cell population, containing both T_{reg} and T_{conv} cells, proliferation was inhibited (Figure 5 A, top panel). However, when T_{reg} cells were removed from the population by magnetic depletion of CD25 expressing cells, PGE_2-mediated suppression of T_{conv} cell proliferation was greatly reduced (Figure 5 A, bottom panel, and B). This indicates that T_{reg} cells are clearly necessary for the PGE_2 dependent suppression mechanism.

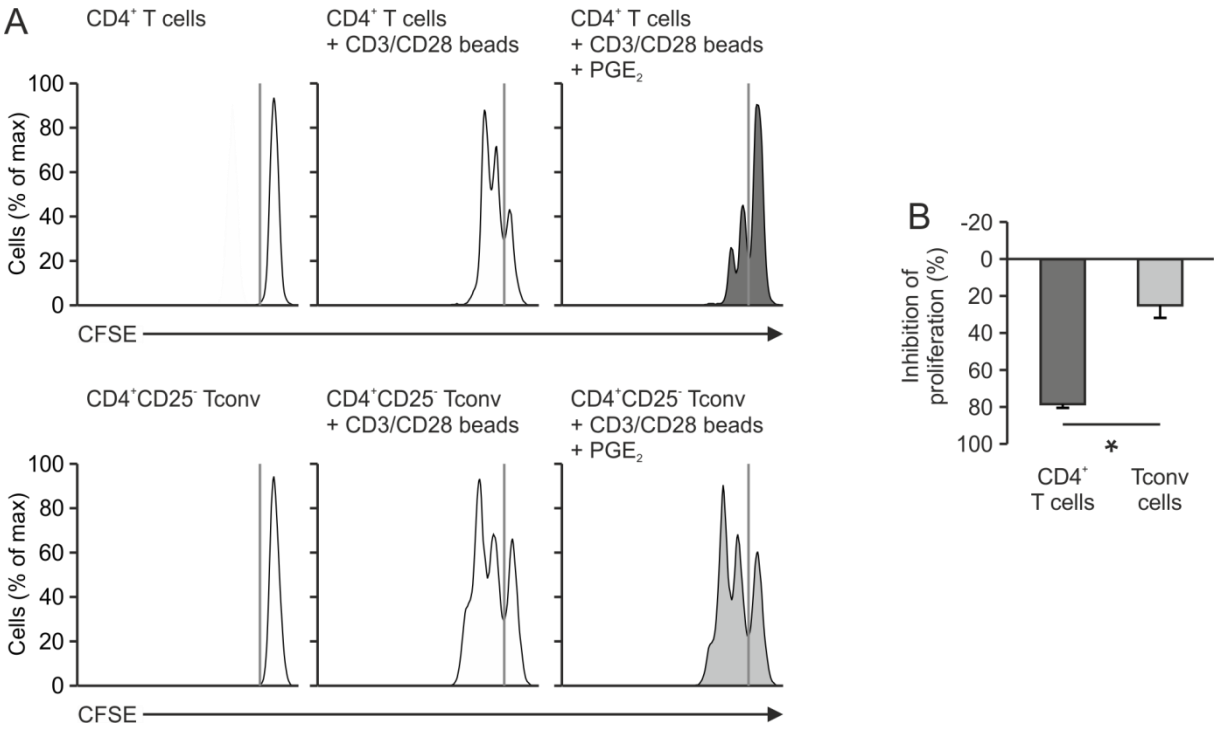

Figure 5: The presence of PGE_2 hampers T-cell proliferation in the presence of T_{reg} cells.
A) $CD4^+$ T cells (top panel) or T_{conv} cells (bottom panel) were stained with CFSE and cultivated with CD3/CD28 coated beads in the presence of absence of 1 µM PGE_2. CFSE dilution was measured on by flow cytometry. **B)** Quantification of the suppressive effect of 1 µM PGE_2 on the proliferation of $CD4^+$ cells vs. T_{conv} cells as a function of CFSE dilution. Experiments were partially performed by Y. Thabet.

In order to determine whether HPGD is directly involved in the decreased T_{conv} cell proliferation conferred by PGE_2, we analyzed the effect of the HPGD-generated PGE_2 metabolite 15-keto-PGE_2 on T_{conv} proliferation in the presence and absence of T_{reg} cells. Just like PGE_2, the metabolite suppresses the proliferation of $CD4^+$ T cells (Figure 6 A, top panel) in a dose dependent manner (Figure 6 B). However, unlike the effect propagated by PGE_2, 15-keto-PGE_2 can also hamper T_{conv} cell proliferation in the absence of T_{reg} cells (Figure 6 A, bottom panel, and B). When comparing the suppressive effect of PGE_2 and 15-keto-PGE_2 on the proliferation of T_{conv} cells in the presence of T_{reg} cells, no significant difference was observed (Figure 6 C). This indicates that the observed suppressive effect is not, in fact, caused directly by PGE_2 but rather by the metabolism of PGE_2 into 15-keto-PGE_2 by HPGD expressing T_{reg} cells.

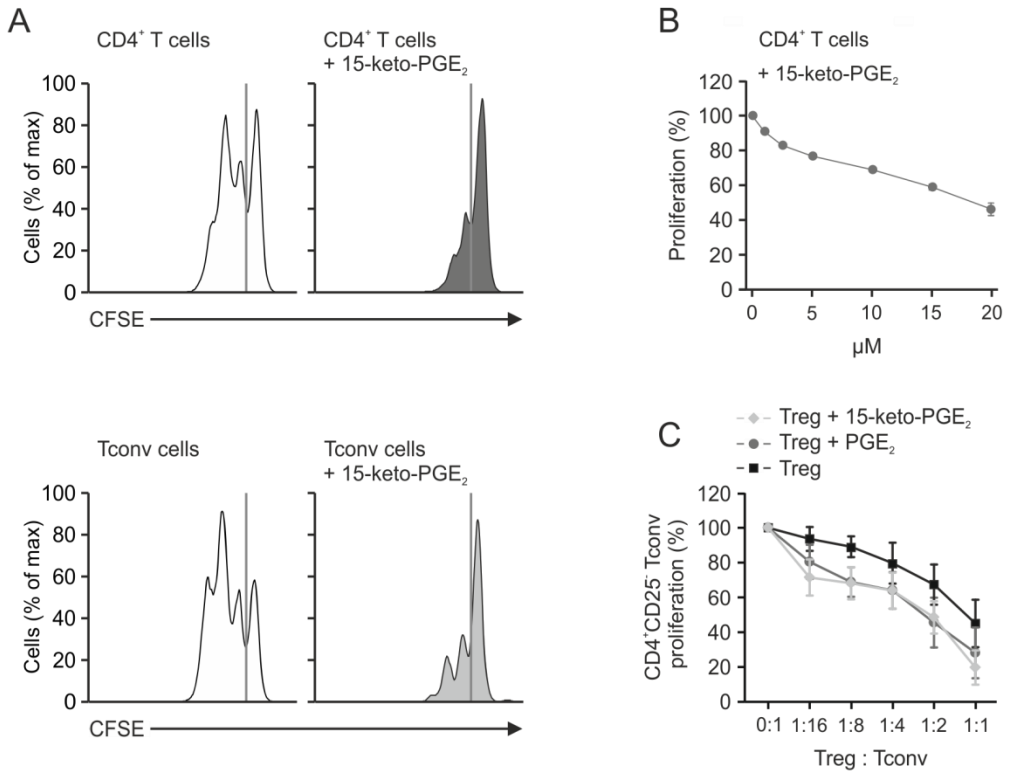

Figure 6: 15-keto-PGE_2 suppresses T_{conv} cell proliferation even in the absence of T_{reg} cells. **A)** $CD4^+$ T cells (top panel) or T_{conv} cells (bottom panel) were stained with CFSE and cultivated with CD3/CD28 coated beads in the presence or absence of 10 µM 15-keto-PGE_2 for three days. CFSE dilution was measured on a flow cytometer. **B)** Dose titration of the suppressive effect of 15-keto-PGE_2 on the proliferation of $CD4^+$ T cells as a function of CFSE dilution. **C)** Quantification of T_{conv} cell proliferation after three days of cultivation in the presence of CD3/CD28 coated beads with 1 µM PGE_2, with 10 µM 15-keto-PGE_2 or without PGs at different T_{conv} to T_{reg} cell ratios as a function of CFSE dilution. Experiments were partially performed by Y. Thabet.

To further support that 15-keto-PGE_2 is the metabolite which is responsible for the increased suppressive capability of T_{reg} cells in the presence of PGE_2, we analyzed the expression of the two main enzymes of 15-keto-PGE_2 metabolism: Prostaglandin reductase (PTGR) 1 and 2. While both enzymes could be detected in myeloid cells, we could not detect PTGR1 mRNA (Figure 7A) and only relatively low levels of PTGR2 (Figure 7B) in either the T_{reg} or the T_{conv} cell populations, suggesting that 15-keto-PGE_2 and not a further metabolite is responsible for the suppressive effect.

Thus, we could show that HPGD is involved in the suppressive function of human T_{reg} cells by metabolizing PGE_2 into 15-keto-PGE_2 and that the metabolite is sufficient to elicit the suppressive effect on T_{conv} cell proliferation. Furthermore, due to the absence of metabolizing enzymes, we hypothesize that 15-keto-PGE_2 directly acts on T_{conv} cells.

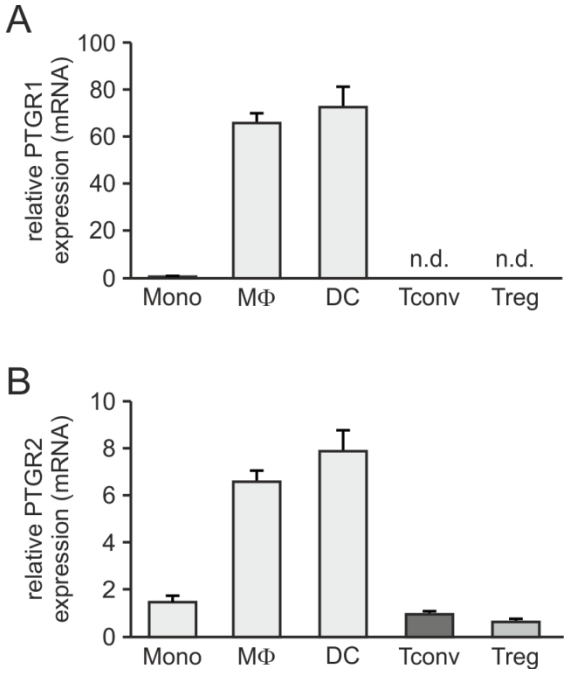

Figure 7: The 15-keto-PGE_2 metabolizing enzymes, PTGR1 and PTGR2, are only expressed at low levels in $CD4^+$ T cells compared to cells of the myeloid compartment.
Monocytes, macrophages, dendritic cells, T_{conv} and T_{reg} cells were isolated or differentiated from human blood. qRT-PCR was performed on **A)** PTGR1 and **B)** PTGR2. Mono, Monocytes; MΦ, Macrophages; DC, Dendritic cells; PTGR, Prostaglandin reductase; n.d., not detectable

4.3. Hpgd expression and functionality is conserved in the mouse

As a subsequent step, we wanted to analyze the role of HPGD in T_{reg} cells *in vivo* to better determine the systemic effect of HPGD for T_{reg} cell functionality, especially in the context of PGE_2-rich microenvironments, such as the VAT. To allow for this, we had to change from humans to the murine model system. To determine the suitability of the murine system for analyzing the role of Hpgd in T_{reg} cells, we first wanted to confirm that Hpgd is similarly upregulated in murine T_{reg} cells. Therefore, we isolated T cells from the spleen, the mesenteric lymph nodes (mLN), the peripheral lymph nodes (pLN), BM and peripheral blood (PB) and measured Hpgd mRNA expression by qRT-PCR. We could detect both a significant upregulation of Hpgd (Figure 8 A) and of Foxp3 (Figure 8 B) in T_{reg} cells compared to T_{conv} cells in all analyzed organs, similar to the upregulation of HPGD in human T_{reg} cells.

To further evaluate the role of Hpgd in T_{reg} cells, we crossed two previously published mouse lines: one with a loxP flanked exon 1 at the *Hpgd* locus (Roizen et al., 2008) and one with a YFP-Cre inserted into the 3' untranslated region of the *Foxp3* locus under the control of an IRES site (Rubtsov et al., 2008) (Appendix Figure 52 A and C). Crossing these two lines homozygously for the floxed *Hpgd* locus and homo- or hemizygously for the *Foxp3*

locus leads to the deletion of Hpgd selectively in T_{reg} cells and the expression of an YFP reporter in all T_{reg} cells. Littermates heterozygous for the floxed Hpgd allele were used as wildtype (WT) controls.

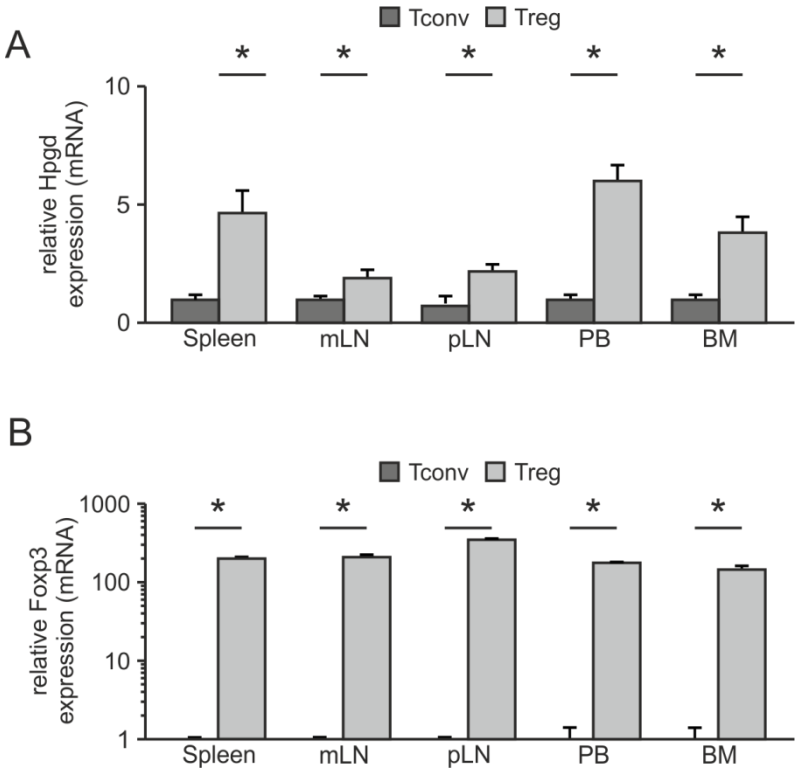

Figure 8: Hpgd and Foxp3 are significantly upregulated in murine T_{reg} cells compared to T_{conv} cells.
T_{reg} and T_{conv} cells were isolated from the spleen, mesenteric and peripheral lymph nodes (mLN and pLN), peripheral blood (PB) and bone marrow (BM). **A)** Hpgd and **B)** Foxp3 expression was determined by qRT-PCR.

Since it has been previously reported that the Foxp3-Cre line can exhibit some unspecific Cre-activity in cells outside of the T_{reg} cell lineage (Franckaert et al., 2015), we first analyzed the specificity of the deletion by PCR on genomic DNA isolated from T_{reg} and T_{conv} cells homozygous and heterozygous for the floxed Hpgd allele. Using a 3-primer PCR enabled us to differentiate between the wildtype, the conditional and the recombined allele (Figure 9 A). When analyzing $Hpgd^{FL/FL}$ Foxp3-Cre and $Hpgd^{FL/WT}$ Foxp3-Cre mice, we could clearly detect the wildtype allele only in mice heterozygous for the floxed Hpgd locus. Furthermore, the T_{conv} cell samples samples mainly expressed the conditional allele while T_{reg} cells mainly expressed the band for the recombined allele (Figure 9 B; quantified in C). This shows that even though we could detect some unspecific Cre-activity in T_{conv} cells, this activity is negligible especially when considering that T_{conv} cells do not express Hpgd at significant levels.

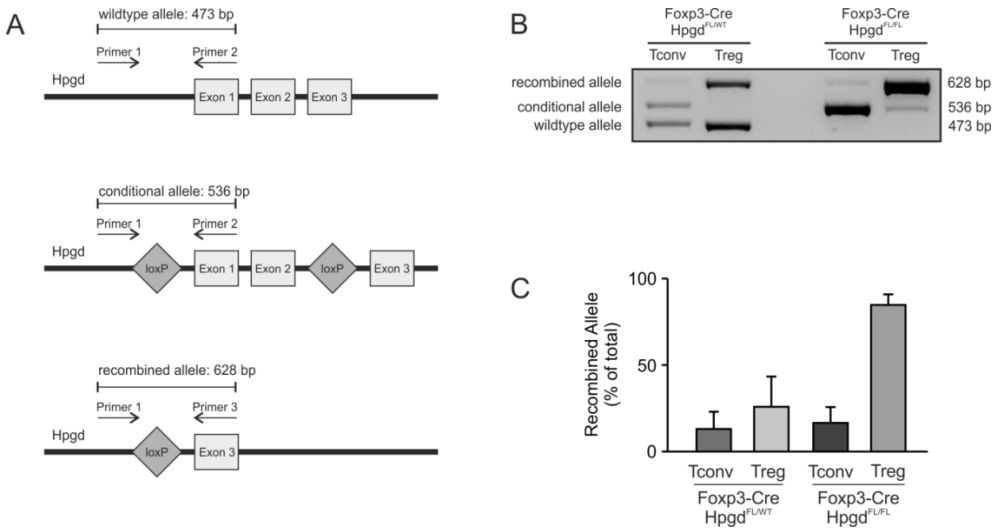

Figure 9: Genomic analysis of the *Hpgd* locus of Hpgd$^{FL/FL}$ Foxp3-Cre and Hpgd$^{FL/WT}$ Foxp3-Cre animals showed only limited recombination in T_{conv} cells.
A) Schematic illustration of the PCR of the genomic *Hpgd* locus for the wildtype (top), conditional (middle) and recombined (bottom) allele. **B)** Gel image and **C)** quantification of PCR data for the genomic *Hpgd* locus of T_{reg} and T_{conv} cells isolated from Hpgd$^{FL/FL}$ Foxp3-Cre and Hpgd$^{FL/WT}$ Foxp3-Cre mice. WT, wildtype; FL floxed.

To confirm that Hpgd functions in a similar manner in the mouse as in humans, we performed suppression assays with murine T_{reg} cells in the presence and absence of PGE_2. As in humans, the presence of PGE_2 augmented the suppressive capabilities of the murine T_{reg} cells (Figure 10 A). This effect cannot be observed, however, when Hpgd-deficient (KO) T_{reg} cells were used in the suppression assay (Figure 10 B). This indicates that the increased suppressive effect observed in the presence of PGE_2 is truly caused by the presence of Hpgd in T_{reg} cells and that the role of Hpgd for the suppressive capabilities of T_{reg} cells is conserved between mouse and man.

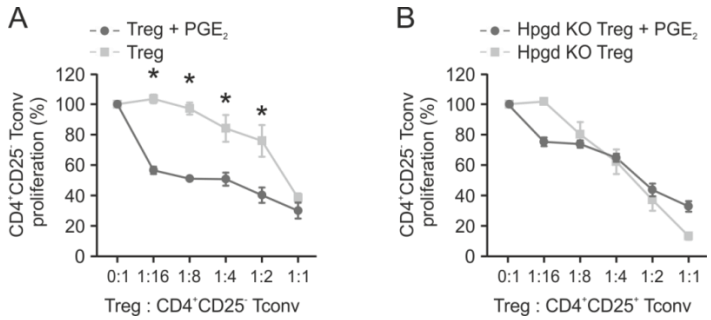

Figure 10: **PGE_2 only increases the suppressive effect of murine T_{reg} cells if they express Hpgd.**
Quantification of T_{conv} cell proliferation after three days of cultivation in the presence of CD3/CD28 coated beads with or without 1µM PGE_2 with increasing **A)** WT T_{reg} or **B)** Hpgd-deficient T_{reg} to T_{conv} ratios as a function of eFlour670 dilution. Experiments performed by Y. Thabet. KO, knock out

4.3.1. Analysis of T_{reg} cell functionality *in vivo*

Since we so far only analyzed the effect of Hpgd in *in vitro* assays, we assessed whether a loss of Hpgd in T_{reg} cells also influences the suppressive capabilities of T_{reg} cells *in vivo*. Therefore, we performed dextran sodium sulfate (DSS)-driven colitis experiments by administering DSS, a water soluble, negatively charged polysaccharide, to mice in drinking water. Within six days, this leads to the induction of colitis. Even though the exact mechanism of colitis induction is unclear, it is widely assumed that DSS damages the large intestine, causing proinflammatory intestinal content, such as bacteria, to enter the tissue and cause inflammation (Chassaing et al., 2014). Thus, disease severity can be linked to the ability of T_{reg} cells to suppress inflammation.

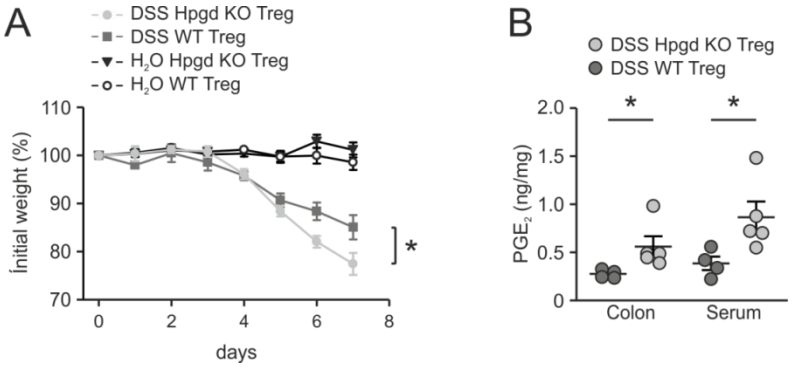

Figure 11: Hpgd-deficient T_{reg} cells are less efficient in attenuating DSS colitis.
A) Mice with wild type (WT) and Hpgd-deficient T_{reg} cells were given free access to either water or water supplemented with 5% (w/v) DSS for 6 days. Animals were weighed daily. **B)** PGE_2 content of colons and serum of diseased animals was measured by mass spectrometry, performed in the Institute of Clinical Pharmacology, Frankfurt by N. Ferreirós.

Colitis was induced both in WT and KO animals when DSS was administered, as measured by an increased weight loss compared to control groups which only received water (**Figure 11** A). However, we could detect a significantly higher weight loss in animals with Hpgd-deficient T_{reg} cells compared to WT littermate controls, indicating that T_{reg} cells which lack Hpgd are less efficient in attenuating the development of DSS colitis (**Figure 11** A). As expected, when measuring the PGE_2 concentrations by mass spectrometry in the colon and serum of animals with WT and KO T_{reg} cells subjected to DSS colitis by mass spectrometry, a significantly higher accumulation of PGE_2 could be observed in the KO animals compared to WT littermate controls (**Figure 11** B). This indicates that the increased development of colitis may be caused by the reduced metabolism of PGE_2 into 15-keto-PGE_2 caused by a loss of Hpgd, which leads to an accumulation of PGE_2 and a decrease in the suppressive capabilities of the T_{reg} cells, thus increasing disease severity.

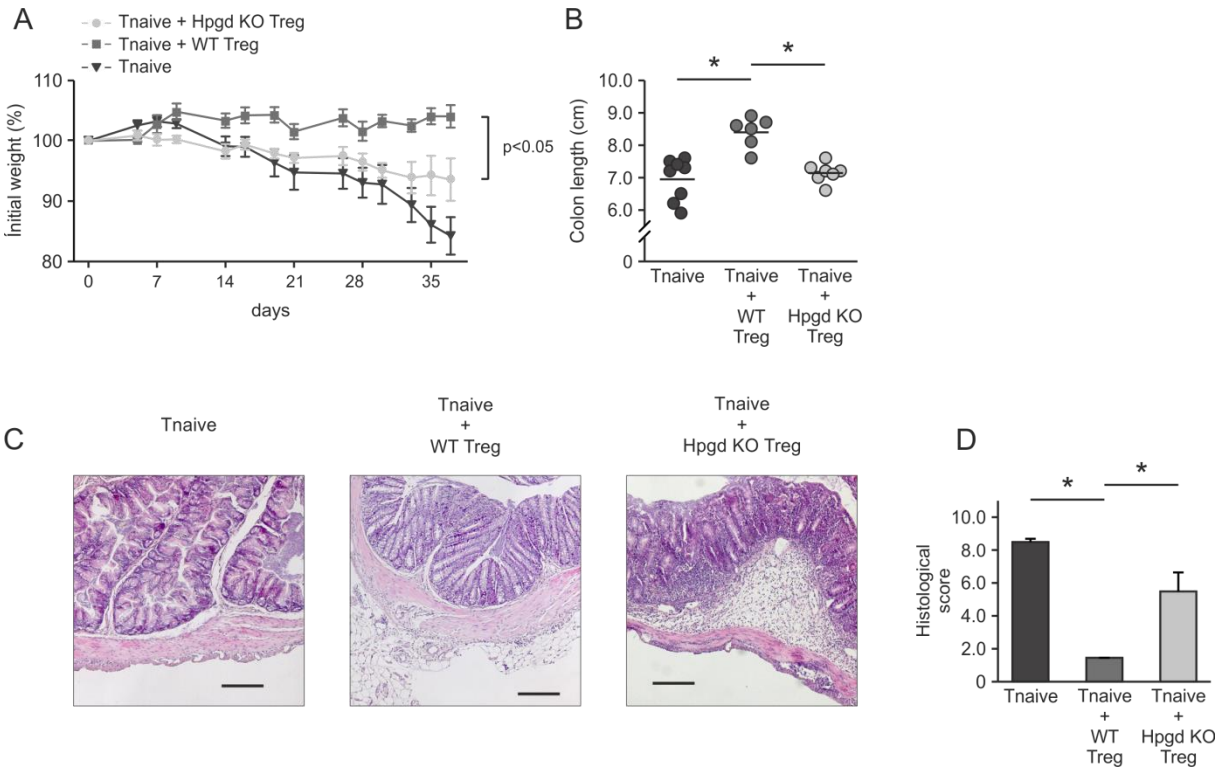

Figure 12: Hpgd-deficient T_{reg} cells are less efficient in preventing the development of adoptive transfer colitis.
A) Weight curve and **B)** colon length of Rag-$2^{-/-}$ animals injected with naïve T cells, naïve T cells and WT T_{reg} cells or naïve T cells and Hpgd-deficient T_{reg} cells. **C)** Hematoxylin and eosin stain of colons isolated from Rag-$2^{-/-}$ animals injected with naïve T cells, naïve T cells and WT T_{reg} cells or naïve T cells and Hpgd-deficient T_{reg} cells and **D)** histological score thereof. Histology was performed at the Institute for Pathology, University Hospital Halle by C. Wickenhauser. Tnaive, naïve T cells.

To analyze the role of T cells, more specifically T_{reg} cells, in the development of colitis more closely, we performed adoptive transfer colitis experiments. In classical adoptive transfer experiments, as pioneered by the lab of Fiona Powrie, naïve T cells are transferred into mice which lack B or T cells (Ostanin et al., 2009). For this, animals whose Rag-2 coding region was deleted (Rag-$2^{-/-}$) and who therefore can no longer produce B- or T-cells since they lack V(D)J recombination activity (Shinkai et al., 1992) are used as the recipient animals (Appendix, Figure 52 E). Due to the transfer of naïve T cells, the mice develop colitis, characterized by severe weight loss, infiltration of leukocytes in the colon, crypt abscesses and epithelial cell erosion (Coombes et al., 2005). One major advantage of this model is that it is ideal to study the effect of T_{reg} cells in an inflammatory setting by transferring T_{reg} cells in addition to naïve T cells and thus preventing or at least alleviating the onset of colitis (Izcue et al., 2006).

As expected, when we injected Rag-2$^{-/-}$ animals with naïve T cells, the animals developed colitis as characterized by severe weight loss. However, when WT T_{reg} cells were transferred in addition to naïve T cells, the animals no longer lost any weight, indicating that, as expected, T_{reg} cells could prevent the onset of colitis. When replacing the WT T_{reg} cells with KO T_{reg} cells, the animals still developed colitis (Figure 12 A). However, the disease severity was significantly reduced from Rag-2$^{-/-}$ animals which only received naïve T cells as determined by severity of weight loss (Figure 12 A), reduction of colon length (Figure 12 B) and histological score of colon tissue sections (Figure 12 C and D).

An analysis of absolute cell numbers of animals injected with naïve T cells, naïve T cells and WT T_{reg} cells or naïve T cells and Hpgd-deficient T_{reg} cells in spleen (Figure 13 A) and mLNs (Figure 13 B) showed that the number of T_{conv} cells was significantly reduced in both organs when T_{reg} cells were also injected compared to when only naïve T cells were introduced to the animals. However, this reduction is greatly reduced when Hpgd-deficient T_{reg} cells are introduced instead of WT T_{reg} cells, further indicating that Hpgd-deficient T_{reg} cells are less efficient in preventing T_{conv} cell proliferation also *in vivo*.

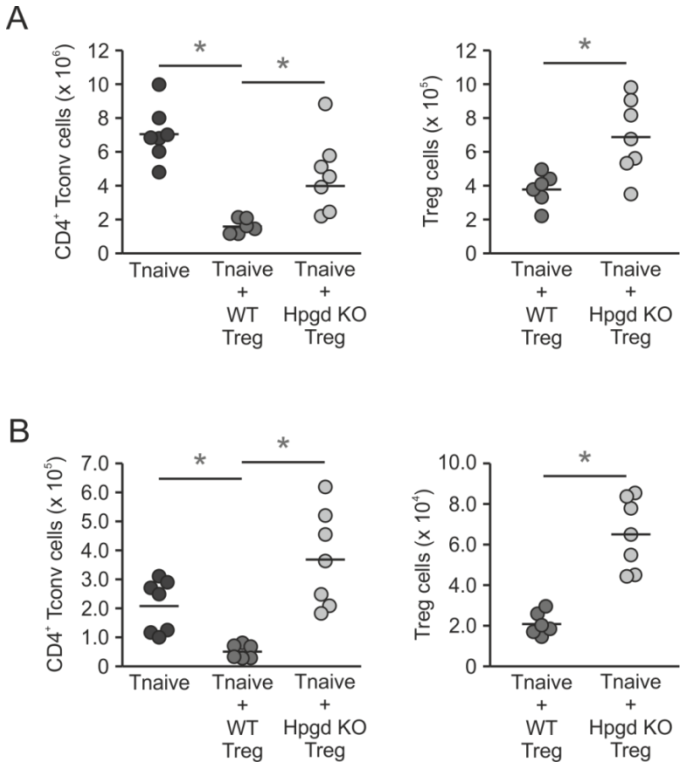

Figure 13: Hpgd-deficient T_{reg} cells are not as efficient in preventing T_{conv} cell proliferation in the adoptive transfer colitis model.
T_{conv} (left panel) or T_{reg} (right panel) cell numbers after induction of adoptive transfer colitis with naïve T cells, naïve T cells and WT T_{reg} cells or naïve T cells and Hpgd-deficient T_{reg} cells in **A)** spleen and **B)** mLN.

Next, we evaluated whether the loss of Hpgd in the animals led to decreased viability of the T_{reg} cells and whether the viability of the T_{reg} cells may influence the increased development of colitis. However, we found that the reduced ability of Hpgd-deficient T_{reg} cells to prevent the induction of colitis is not due to reduced viability or proliferation of the T_{reg} cells themselves as the number of T_{reg} cells is significantly increased in both the spleen and the mLNs when KO T_{reg} cells were injected instead of WT T_{reg} cells (Figure 13A and B, right panel). This accumulation of Hpgd-deficient T_{reg} cells may be a compensatory mechanism to make up for their reduced suppressive functionality.

Taken together these results indicate that Hpgd expression in T_{reg} cells is necessary for the effectual functionality of T_{reg} cells *in vivo* as a loss of Hpgd in T_{reg} cells leads to increased disease development both in DSS and adoptive transfer colitis.

4.3.2. 15-keto-PGE_2 suppresses T_{conv} cell proliferation via Ppar-γ signaling

In humans, we could show that the effect of PGE_2 on the proliferation of T_{conv} cells was mediated by the HPGD-dependent metabolism of PGE_2 into 15-keto-PGE_2 (Figure 6). To further analyze the role of 15-keto-PGE_2, we first evaluated whether the suppressive capability of the metabolite is conserved in the mouse. We observed that, just like in humans, 15-keto-PGE_2 can inhibit T_{conv} cell proliferation in a dose dependent manner even in the absence of T_{reg} cells (Figure 14 A and B).

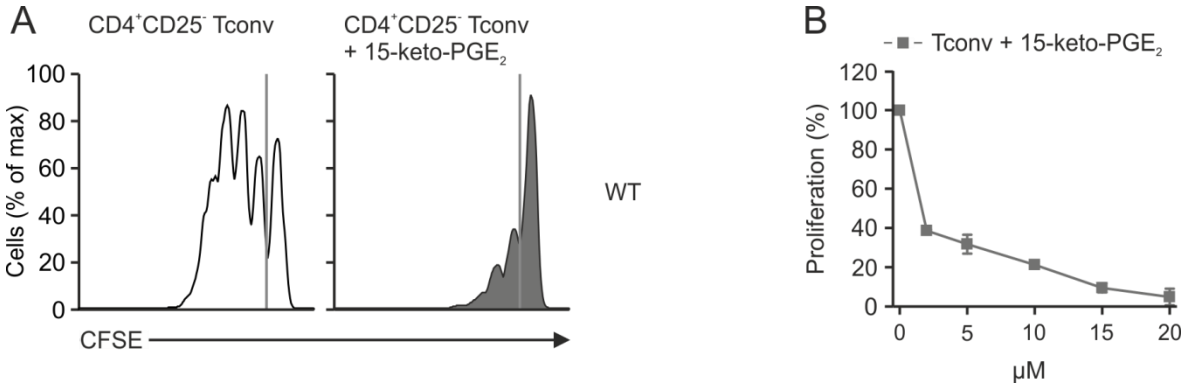

Figure 14: 15-keto-PGE_2 can inhibit murine T_{conv} cell proliferation even in the absence of T_{reg} cells.
A) T_{conv} cells were stained with CFSE and cultivated with CD3/CD28 coated beads in the presence of absence of 10 µM 15-keto-PGE_2 for three days. CFSE dilution was measured by flow cytometry. **B)** Effect of increasing amounts of 15-keto-PGE_2 on the proliferation of T_{conv} cells as a function of CFSE dilution. Experiments were conducted by Y. Thabet.

15-keto-PGE_2 has previously been implicated as a ligand of Ppar-γ (Chou et al., 2007). However, it has proven difficult to definitively identify receptor ligands, especially for nuclear receptors (Schupp and Lazar, 2010), since studies showing *in vitro* binding often cannot be confirmed *in vivo*. For instance, while 15-deoxy-$\Delta^{12,14}$-PGJ_2 has been shown to be a Ppar-γ ligand it has later been determined that endogenous levels of 15-deoxy-$\Delta^{12,14}$-PGJ_2 were too low to effectively act as a Ppar-γ ligand (Bell-Parikh et al., 2003; Forman et al., 1995). Furthermore, the ligand binding domain of Ppar-γ is relatively large (Nolte et al., 1998), thus allowing the binding of many, structurally distinct ligands and making effective ligand prediction difficult.

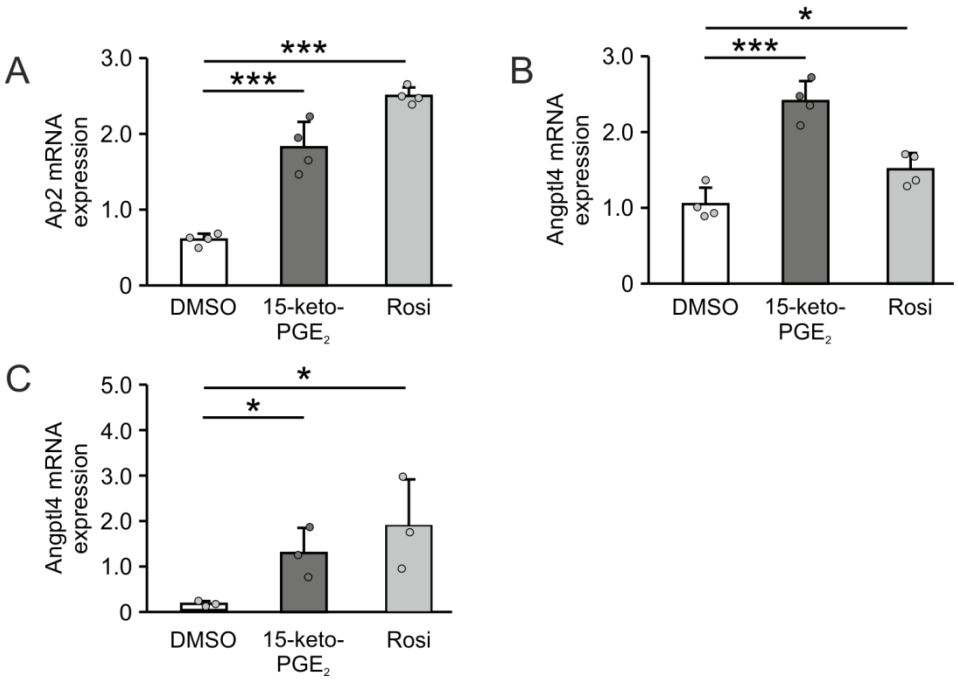

Figure 15: Stimulation with 15-keto-PGE_2 leads to an upregulation of genes downstream of Ppar-γ in differentiated 3T3-L1 cells and bone marrow-derived macrophages (BMDMs). 3T3-L1 cells were differentiated into adipocytes and stimulated overnight with 1 µM 15-keto-PGE_2, Rosiglitazone or DMSO as vehicle control. Ppar-γ activation was determined by measuring **A)** Ap2 and **B)** Angptl4 mRNA expression by qPCR. **C)** BMDMs were stimulated overnight with 15-keto-PGE_2, Rosiglitazone or DMSO as vehicle control. Ppar-γ activation was determined by measuring Angptl4 mRNA expression by qPCR. Angptl4, angiopoietin-like 4; Ap2, Adipocyte protein 2; Rosi, Rosiglitazone

Therefore, we attempted to confirm that 15-keto-PGE_2 is a Ppar-γ ligand by using the common 3T3-L1 assay for Ppar-γ ligand activation (Watanabe et al., 2003). 3T3-L1 cells were differentiated into adipocytes and then stimulated with the Ppar-γ ligand Rosiglitazone as a positive control, DMSO as vehicle control, as well as 15-keto-PGE_2. To assess ligand binding and Ppar-γ activation, the transcription of adipocyte protein 2(Ap2) and angiopoietin-

like protein 4 (Angptl4), two genes directly downstream of Ppar-γ, were assessed by qPCR. We could detect a significant upregulation of both Ap2 (Figure 15 A) and Angptl4 (Figure 15 B) after 15-keto-PGE_2 or Rosiglitazone stimulation in comparison to control samples treated only with DMSO.

However, this system is a very artificial method of measuring Ppar-γ activation. Therefore, we also analyzed the effect of DMSO, 15-keto-PGE_2 or Rosiglitazone stimulation on BMDMs and could detect a significant upregulation of Angptl4 in these cells in comparison to cells only stimulated with vehicle control (Figure 15 C), indicating that 15-keto-PGE_2, like Rosiglitazone, can activate the Ppar-γ-dependent transcriptional program.

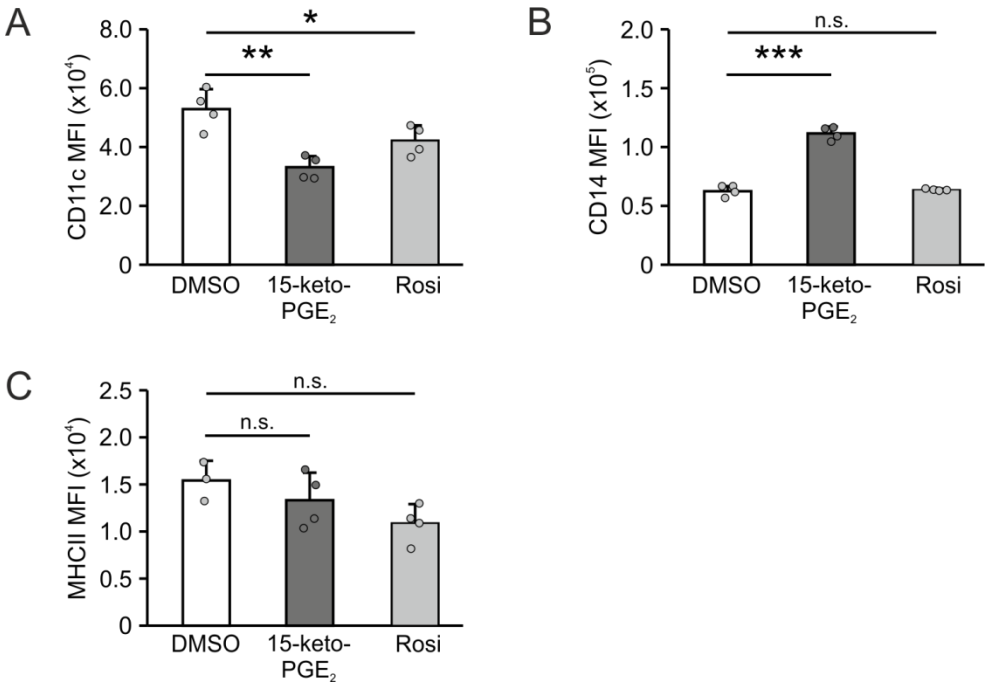

Figure 16: 15-keto-PGE_2 and Rosiglitazone inhibit the differentiation of bone marrow-derived dendritic cells (BMDCs) into mature DCs.
BMDCs were differentiated in the presence of 1 µM 15-keto-PGE_2, Rosiglitazone or DMSO as vehicle control. Differentiation of cells was assessed by determining the MFI of **A)** CD11c, **B)** CD14 or **C)** MHC-II by flow cytometry. MHCII, major histocompatibility complex II

In a subsequent step, we analyzed the effect of 15-keto-PGE_2 on the differentiation process of BMDCs since it has been previously shown that BMDCs cultivated in the presence of Rosiglitazone show a severe impairment in their ability to differentiate into mature BMDCs (Byun et al., 2016). To confirm that 15-keto-PGE_2 acts on BMDCs in a similar manner, we added either 15-keto-PGE_2, Rosiglitazone or DMSO to BMDC cultures and evaluated their ability to differentiate into mature BMDCs by flow cytometry. We could show that the

expression of CD11c, our surrogate marker for BMDC differentiation, was downregulated in cells stimulated with 15-keto-PGE_2 or Rosiglitazone compared to cells stimulated with DMSO as vehicle control (Figure 16 A). Further, we could detect an upregulation of the monocytic marker CD14 (Figure 16 B), while MHC-II expression levels remained constant, despite 15-keto-PGE_2 or Rosiglitazone stimulation (Figure 16 C), confirming once again that 15-keto-PGE_2 acts in a manner similar to the well-described Ppar-γ agonist Rosiglitazone and that, as previously published (Chou et al., 2007), 15-keto-PGE_2 can act as a Ppar-γ ligand.

Since we could show that 15-keto-PGE_2 can act in different immune cells via Ppar-γ signaling in a manner reminiscent of the Ppar-γ agonist Rosiglitazone, we analyzed whether the observed suppressive effect of 15-keto-PGE_2 on T_{conv} cell proliferation is also Ppar-γ dependent. Therefore, we generated mice whose $CD4^+$ T cells do not express Ppar-γ by crossing a mouse with a Cre-recombinase inserted after the CD4 promoter (Lee et al., 2001) to a mouse carrying a floxed *Pparg* allele (Akiyama et al., 2002) (Appendix Figure 52 B and D).

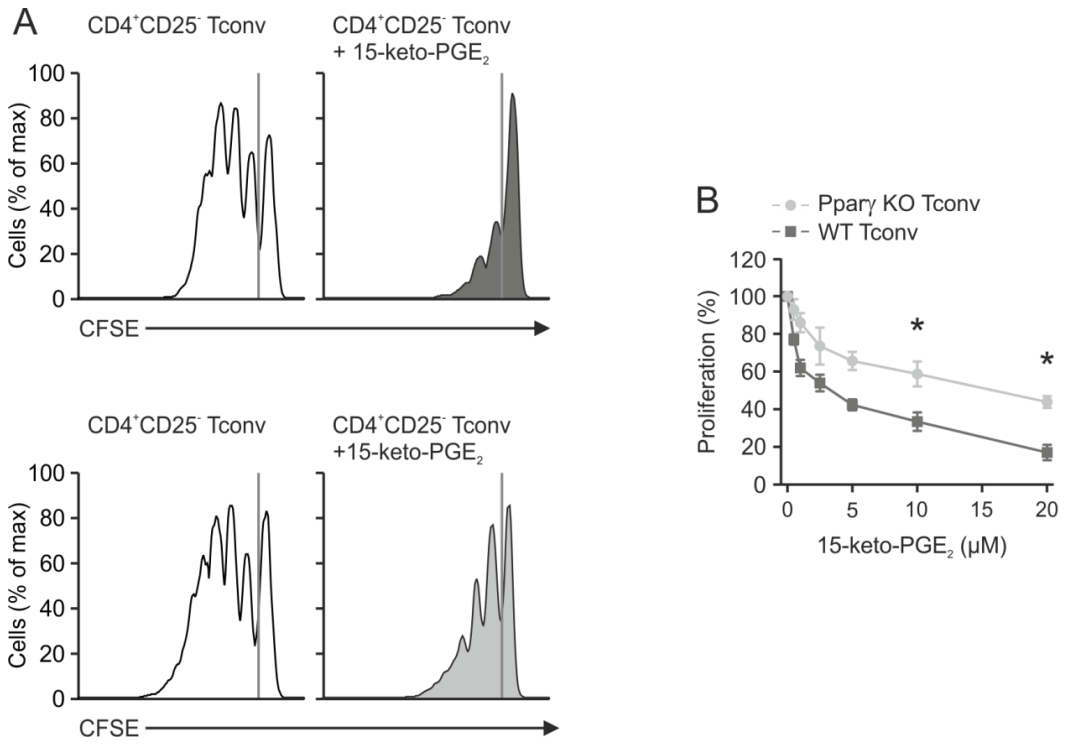

Figure 17: The suppressive effect of 15-keto-PGE_2 is partially dependent on Ppar-γ signaling.

A) Ppar-γ-sufficient (upper panel) and deficient (lower panel) T_{conv} cells were stained with CFSE and cultivated with CD3/CD28 coated beads in the presence of absence of 10 µM 15-keto-PGE_2 for three days. CFSE dilution was measured on by flow cytometry. **B)** Effect of increasing doses of 15-keto-PGE_2 on the proliferation of WT and Ppar-γ-deficient T_{conv} cells as a function of CFSE dilution. Experiments were conducted by Y. Thabet.

When adding 15-keto-PGE_2 to Ppar-γ-deficient T_{conv} cells, we could observe that the suppressive effect of the metabolite was significantly reduced (Figure 17 A and B). However, the effect was only partial as we could still observe a dose-dependent decrease in T_{conv} cell proliferation even in Ppar-γ-deficient T_{conv} cells (Figure 17 B). This indicates that while 15-keto-PGE_2 seems to at least partially act through Ppar-γ signaling, this is not the only manner in which 15-keto-PGE_2 suppresses T_{conv} cell proliferation.

4.3.3. Hpgd expression in T_{reg} cells is important for immune cell homeostasis in VAT of aged mice.

Since Ppar-γ has been shown to be vital to maintain healthy metabolic signaling and homeostasis and is further clearly associated with the VAT-associated transcriptional program of T_{reg} cells, we hypothesized that Hpgd might also be involved in the governance of metabolic processes. Further evidence that PGE_2, and therefore also the PGE_2 metabolizing enzyme, Hpgd, might play an important role in the VAT is the high expression of COX-1, a central enzyme in the metabolic pathway of PGE_2 (Figure 1), in VAT (Hétu et al., 2007). Therefore, we studied the role of Hpgd expressing T_{reg} cells in the VAT as well as their role in immune and metabolic homeostasis.

When analyzing Hpgd levels in VAT in comparison to other tissue resident T_{reg} cells, we could clearly show that, while Hpgd is upregulated in all tissue T_{reg} cells, its expression is about 20-fold elevated in VAT T_{reg} cells compared to T_{conv} cells while in all other organs the Hpgd expression in T_{reg} cells is only elevated between 0.5 – 3-fold (Figure 18).

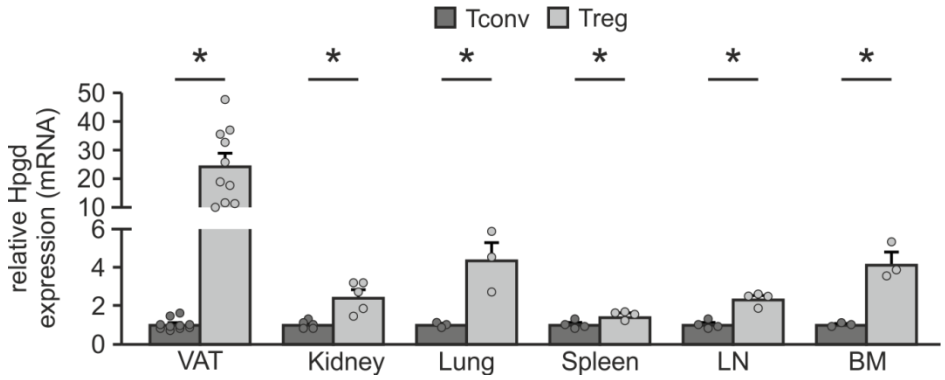

Figure 18: Hpgd is highly expressed in VAT T_{reg} cells.
T_{reg} and T_{conv} cells were isolated from the VAT, kidney, lung, spleen, mesenteric lymph nodes and bone marrow of WT animals and Hpgd mRNA expression was determined by qRT-PCR. Mean T_{conv} expression was normalized to 1.

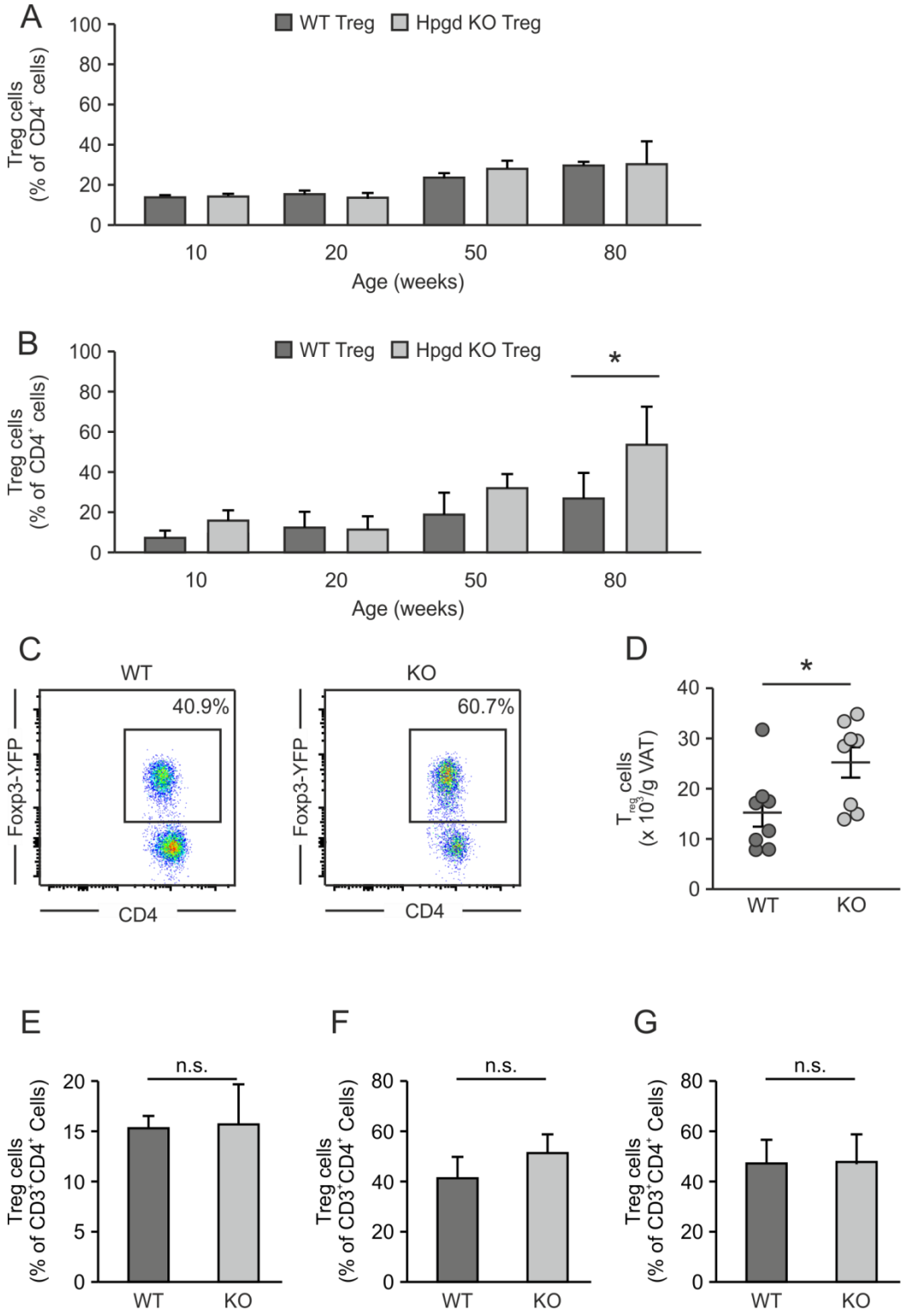

Figure 19: T_{reg} cell fractions are significantly increased in aged animals with Hpgd-deficient Treg cells.

Analysis of the $CD4^+$ $Foxp3^+$ T_{reg} cell fraction by flow cytometry in **A)** spleen and **B)** VAT of animals with Hpgd-deficient and WT T_{reg} cells. **C)** Representative dot plots of VAT T_{reg} cell populations in 80-week old animals with Hpgd-deficient (right) and WT T_{reg} cells. **D)** Analysis of absolute numbers of T_{reg} cell populations in VAT of 80-week old animals with WT and Hpgd-deficient T_{reg} cells. Analysis of the $CD4^+$ $Foxp3^+$ T_{reg} cell fraction in aged animals with Hpgd-deficient and WT T_{reg} cells in **E)** the lung, **F)** the skin and **G)** the colon.

As has been previously described, deficiencies in T_{reg} cell function either take effect immediately in the so-called scurfy phenotype, a fatal and systemic autoimmune disease (Godfrey et al., 1991; Sharma et al., 2009), or only develop as the animal ages (Fessler et al., 2013; Huynh et al., 2015; Raynor et al., 2012; Shrestha et al., 2015). Therefore, we analyzed T_{reg} cell populations in young and aged mice. As expected, we could detect an age-related increase in the T_{reg} cell population both in the spleen (Lages et al., 2008) and in the VAT (Cipolletta et al., 2015) (Figure 19 A and B). This age-related increase was much more pronounced in Hpgd-deficient T_{reg} cells of the VAT, leading to a significant increase in VAT-resident T_{reg} cells in 80 week old animals with Hpgd-deficient T_{reg} cells when compared to WT littermates (Figure 19 B and C). This difference remains significant both when analyzing relative and absolute T_{reg} cell numbers (Figure 19 C and D). This observation is VAT specific, as we could not observe such an increase in any other lymphoid or non-lymphoid organ we analyzed, including the spleen (Figure 19 A), the lung (Figure 19 E), the skin (Figure 19 F) and the colon (Figure 19 G). Furthermore, we could not detect a difference in T_{reg} cell accumulation in female animals of the same age (data not shown).

Since we could observe a significant increase in T_{reg} cells in the VAT of animals with Hpgd-deficient T_{reg} cells, we wanted to analyze whether this increase is caused by enhanced proliferation. Therefore, we analyzed the expression of the proliferation marker Ki-67 by flow cytometry and could observe a significant upregulation of Ki-67 in Hpgd-deficient VAT-T_{reg} cells compared to their WT counterparts (Figure 20 A and B). Such an increase has previously been associated with increased inflammation in VAT (Kolodin et al., 2015). Next, we analyzed Ki-67 expression in splenic T_{reg} cells deficient for Hpgd (Figure 20 C) and could not detect a significant increase in Ki-67 expression of splenic T_{reg} cells, even though we could detect a trend towards increased Ki-67 expression in Hpgd-deficient T_{reg} cells. This indicates that the observed increase in the VAT-resident Hpgd-deficient T_{reg} cell population is most likely caused by local proliferation of T_{reg} cells and not by a generally increased proliferation of T_{reg} cells in secondary lymphoid organs.

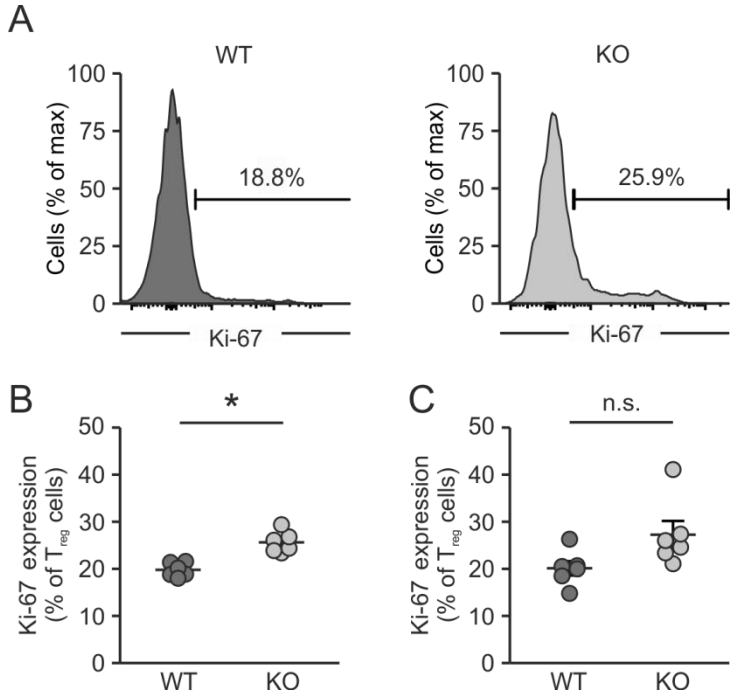

Figure 20: Ki-67 is significantly upregulated in Hpgd-deficient VAT-resident T_{reg} cells of aged animals.
A) Histograms of Ki-67 expression in VAT-resident WT and Hpgd-deficient T_{reg} cells and **B)** quantification thereof. **C)** Quantification of Ki-67 expression in splenic WT and Hpgd-deficient T_{reg} cells.

Subsequently, we analyzed whether the observed increase in VAT-T_{reg} cells in animals with Hpgd-deficient T_{reg} cells correlates with an increase in absolute VAT mass. However, when analyzing the weight of the VAT in these animals, we could not detect any difference (Figure 21 A). Further, no difference in splenic weight or overall bodyweight (Figure 21 B and C) could be detected, indicating that the observed increase in the T_{reg} cell population in the VAT is an absolute increase and not caused by increased body or organ weight.

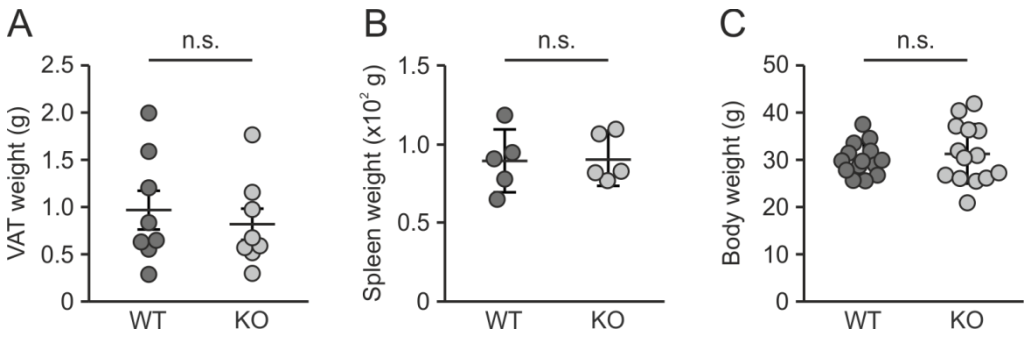

Figure 21: No significant difference in VAT, splenic or body weight between aged animals with Hpgd-deficient T_{reg} cells and age-matched littermate controls.
A) VAT, **B)** splenic and **C)** body weight of aged animals with Hpgd-deficient T_{reg} cells and WT littermate controls.

To analyze how the loss of Hpgd in T_{reg} cells would impact the phenotype and transcriptional identity of T_{reg} cells, we analyzed several typical T_{reg} cell markers such as CTLA-4, GITR, and Helios in both the WT and KO T_{reg} cell populations of the spleen (Figure 22 A) or the VAT (Figure 22 B) and observed no differences. Moreover, when analyzing the VAT-specific T_{reg} marker ST2, we also could not detect any difference (Figure 22 B).

Since we could observe a decrease in suppressive T_{reg} cell function coupled with an increase in the VAT-resident T_{reg} cell population of aged KO animals, we hypothesized that this increase in the T_{reg} cell population may be caused by a compensatory effect and be linked to increased VAT inflammation. Therefore, we analyzed the VAT-resident myeloid population of these animals.

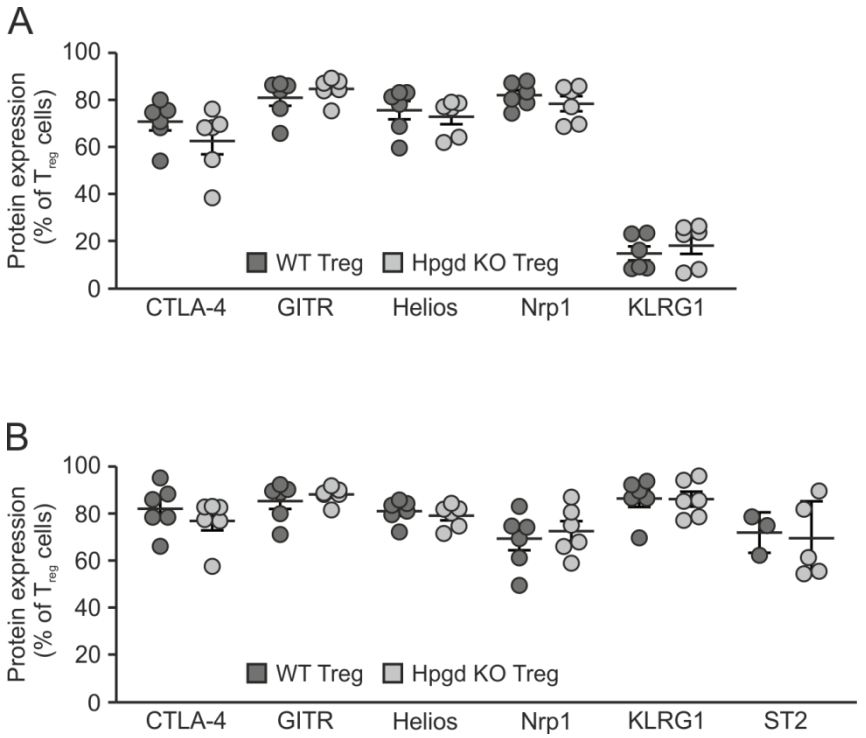

Figure 22: Phenotypic characterization of splenic and VAT-resident, Hpgd-deficient or WT T_{reg} cells of aged animals.
Quantification of classical T_{reg} cell associated marker protein in **A)** splenic and **B)** VAT-resident T_{reg} cells isolated from aged animals with WT and Hpgd-deficient T_{reg} cells. CTLA-4, cytotoxic T-lymphocyte-associated Protein 4; GITR, glucocorticoid-induced TNFR family related gene; Nrp1, Neuropilin-1; KLRG1, killer-cell lectin like receptor G1.

We could detect an increased infiltration of macrophages in the VAT of aged animals with KO T_{reg} cells by flow cytometry (Figure 23 A and B). Further analysis of the macrophage population showed that the macrophages are mainly pro-inflammatory in nature, as characterized by the increased expression of the marker CD11c (Figure 23 C).

Furthermore, we analyzed the infiltrating granulocytes in the VAT of aged KO animals, since an increase in granuolcytes has been linked to obesity, metabolic dysregulation and increased adipose tissue inflammation (Huh et al., 2014; Talukdar et al., 2012). However, we could not detect a difference in the VAT-resident granulocyte population of aged KO compared to WT animals.

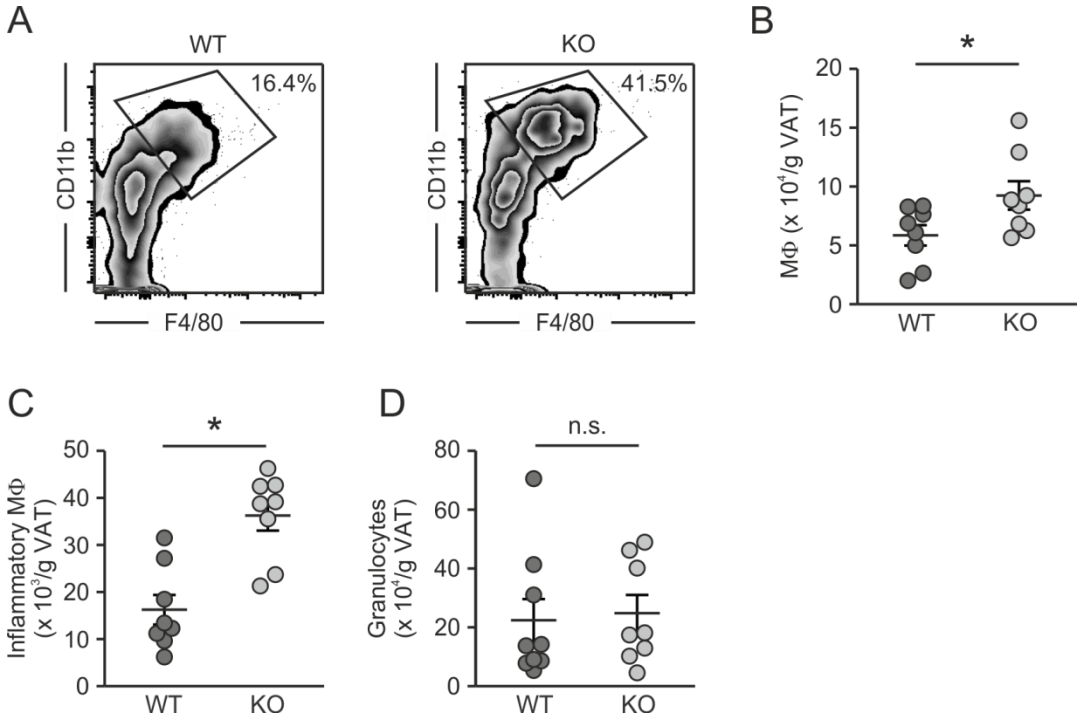

Figure 23: Aged animals harboring Hpgd-deficient T_{reg} cells show increased infiltration of proinflammatory macrophages in the VAT.
A) Representative dot plot and **B)** quantitative analysis of macrophage population in the VAT of aged animals with KO T_{reg} cells or WT littermate controls. Quantitative analysis of **C)** the proinflammatory macrophage population and **D)** the granulocyte population in the VAT of these animals.

To confirm this increased infiltration of myeloid cells, histological analyses of the VAT of aged animals with KO T_{reg} cells and of age matched littermate controls were performed by the laboratory of C. Wickenhauser. We could confirm the previously observed significant increase in macrophage infiltration in the VAT of aged animals with KO T_{reg} cells as compared to WT littermate controls (Figure 24 A and B). Furthermore, we detected a striking increase in adipocyte size in these animals (Figure 24 A and C). These observations are further indicative of increased inflammation in the VAT of aged animals with KO T_{reg} cells.

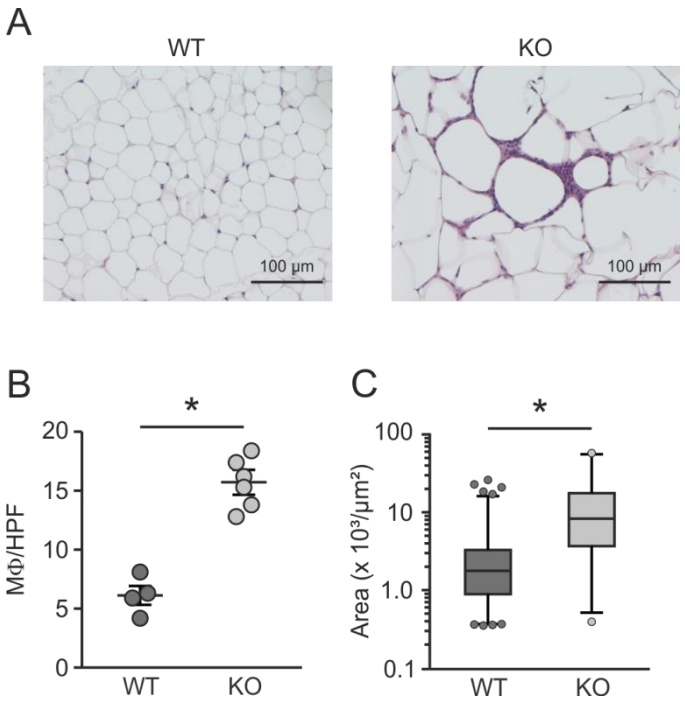

Figure 24: Aged animals with Hpgd-deficient T_{reg} cells show an increased infiltration of macrophages and adipocyte size in VAT.
A) Histological analysis of VAT of aged animals with KO T_{reg} cells and WT littermate control animals stained for F4/80 (purple). Quantitative analysis of **B)** macrophages per high power field and **C)** size of adipocytes in VAT of aged animals with Hpgd-deficient T_{reg} cells and WT littermate control animals. Histology was performed in the Institute for Pathology in Halle by C. Wickenhauser.

In contrast, in aged female mice, we could not detect any differences in the VAT-resident immune cell compartment (Figure 25 A-C), a not unexpected observation as it has been previously described that the makeup of the VAT-resident immune cell compartment of female mice differs from that of male animals (Ahnstedt et al., 2018).

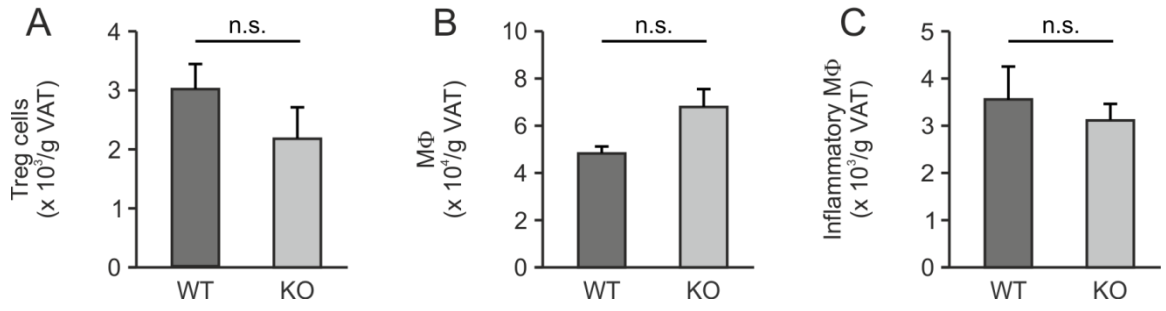

Figure 25: No difference in the VAT-resident T_{reg} or macrophage population could be detected between aged female mice with Hpgd-competent or deficient T_{reg} cells.
Quantitative analysis of the **A)** T_{reg} cell **B)** macrophage and **C)** inflammatory macrophage population in the VAT of aged female animals with Hpgd-deficient T_{reg} cells or WT littermate controls.

All in all, we could observe an age-related increase of T_{reg} cells in the VAT of male animals with a T_{reg} cell specific deletion of Hpgd. Despite being unable to detect a phenotypic change in these T_{reg} cells, we could observe an increase in inflammation in the VAT of animals with Hpgd-deficient T_{reg} cells as shown, for instance, by an increased proinflammatory macrophage accumulation.

4.3.4. Hpgd expression in T_{reg} cells is dependent on Ppar-γ signaling

Since we could observe that the suppressive effect of Hpgd is at least partially mediated by the Ppar-γ ligand 15-keto-PGE_2, we subsequently analyzed the effect of Ppar-γ signaling on T_{reg} cell biology by selectively deleting Ppar-γ only in T_{reg} cells. This was achieved by crossing animals with floxed Ppar-γ (Akiyama et al., 2002) to animals expressing the Cre-recombinase in a Foxp3 dependent manner (Rubtsov et al., 2008) (Appendix Figure 52 B and C) and analyzing Hpgd expression in T_{reg} cells isolated from these animals. While we could observe Hpgd expression in T_{reg} cells isolated from WT control animals, Hpgd levels were decreased in T_{reg} cells deficient for Ppar-γ independent on whether the T_{reg} cells were isolated from LNs (Figure 26 A), the spleen (Figure 26 B) or from VAT (Figure 26 C). This seems to indicate that Ppar-γ signaling is necessary for Hpgd expression and thus that Hpgd is downstream of Ppar-γ.

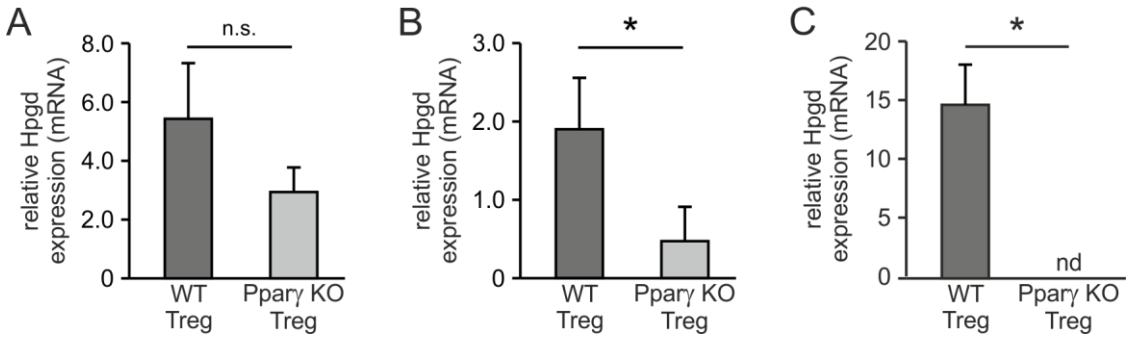

Figure 26: Ppar-γ dependent expression of Hpgd
T_{reg} cells were isolated from **A)** mLN, **B)** spleen and **C)** VAT of WT animals and animals with Ppar-γ-deficient T_{reg} cells and Hpgd mRNA levels were determined by qRT-PCR.

4.3.5. Loss of Hpgd leads to mainly extrinsic effects in T_{reg} cells

To further analyze potential differences between WT and KO Treg cells, we performed transcriptome analysis of Treg and Tconv cells isolated from both the spleen and the VAT to determine whether the deletion of Hpgd in Treg cells affects the general or VAT-resident T_{reg} cell signature.

Therefore, we performed RNA-seq of splenic T_{reg} cells of aged WT and KO animals. We could not detect any major differences between the KO and WT T_{reg} cells when performing t-SNE analysis of variable genes (Figure 27 A). Furthermore, when comparing expression against the murine T_{reg} cell signature (Hill et al., 2007), we could not detect any major differences in the expression of core-T_{reg} genes between Hpgd-competent and deficient T_{reg} cells (Figure 27 B).

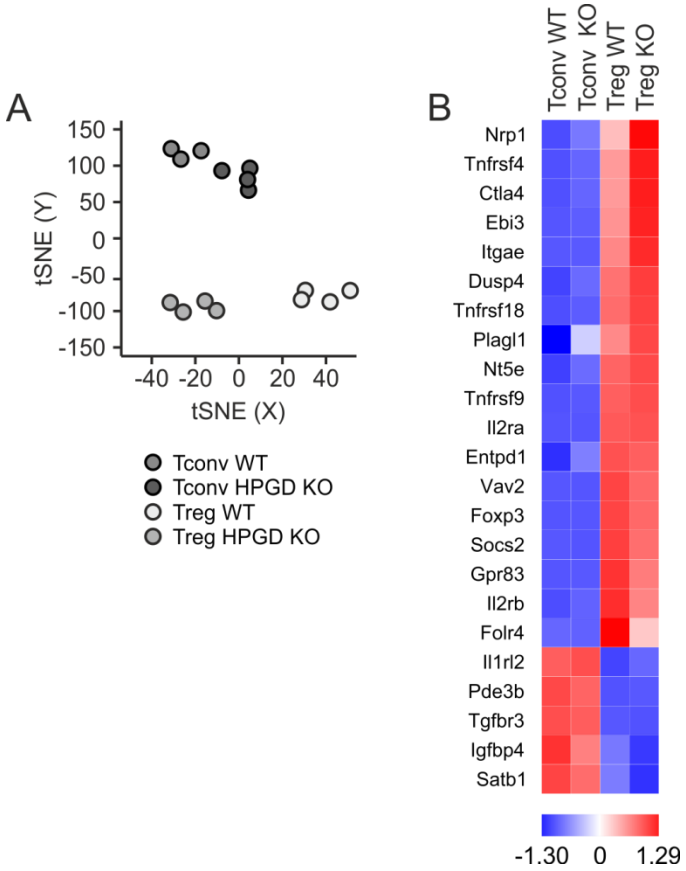

Figure 27: No major transcriptomic differences between splenic WT and Hpgd-deficient T_{reg} cells could be detected.
Transcriptome analysis of T_{reg} and T_{conv} cells isolated from the spleen of least three animals harboring Hpgd-deficient or WT T_{reg} cells. **A)** t-SNE analysis based on variably expressed genes and **B)** heat map of selected genes from the murine T_{reg} cell signature (Hill et al., 2007).

Similarly, when analyzing VAT-resident T_{reg} cells, we could not detect any overt differences in gene expression between VAT-resident WT and KO T_{reg} cells, as evidenced by close proximity of WT and KO Treg cells in a t-SNE analysis (Figure 28 A) or in their expression of VAT T_{reg} cell signature genes (Figure 28 B), thus further supporting that the core program of these cells is not disturbed by the deletion of Hpgd. In summary, this

indicates that the observed effects of a T_{reg} specific deletion of Hpgd are not of an intrinsic nature but rather caused by the loss of the enzymatic action of Hpgd.

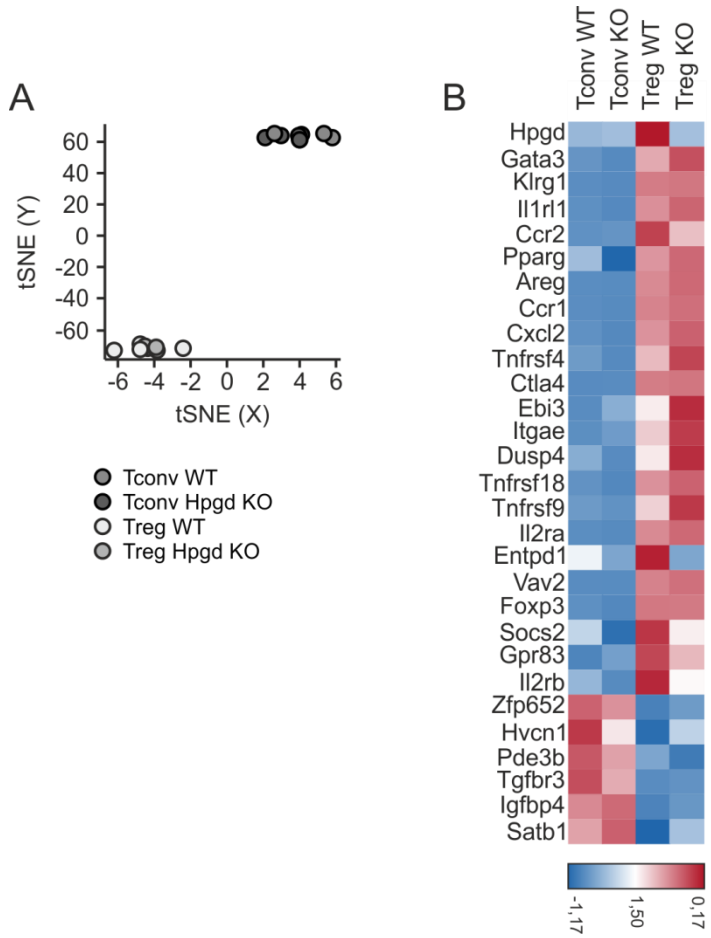

Figure 28: No difference in the transcriptome between VAT WT and Hpgd-deficient T_{reg} cells could be detected.
Transcriptome analysis of T_{reg} and T_{conv} cells isolated from the spleen of least three animals harboring Hpgd-deficient or WT T_{reg} cells. **A)** t-SNE based on variably expressed genes and **B)** heat map of selected genes from the murine VAT T_{reg} cell signature.

To further validate our hypothesis, we performed adoptive colitis experiments where we transferred Hpgd-deficient or sufficient T_{reg} cells in combination with WT naïve T cells into Rag-$2^{-/-}$ animals. We co-transferred RFP-expressing WT T_{reg} cells to prevent the onset of colitis, which cannot be completely ablated by the transfer of KO T_{reg} cells (See Figure 12) This enabled us to analyze differences between WT and Hpgd-deficient T_{reg} cells independently of any effects caused by any functional differences caused by the loss of Hpgd resulting in the onset of disease (Figure 29 A). We observed the animals for 8 weeks after injection and could detect no development of colitis in animals transfected with T_{reg} cells while animals injected only with naïve T cells experienced colitis (Figure 29 B). We

sacrificed the animals 8 weeks after injection and isolated T_{reg} cells from the mLN and could not detect a difference in the number of T_{reg} cells recovered between animals injected with WT and KO T_{reg} cells (Figure 29 C) or in the ratio of YFP to RFP positive T_{reg} cells (Figure 29 D). Furthermore, transcriptome analysis of these cells did not reveal any significant differences in their gene expression profile (Figure 29 E). Taken together, these data seem to indicate that the T_{reg} cell specific deletion of Hpgd indeed has mainly extrinsic effects and does not affect the general phenotype or the transcriptional program of these cells.

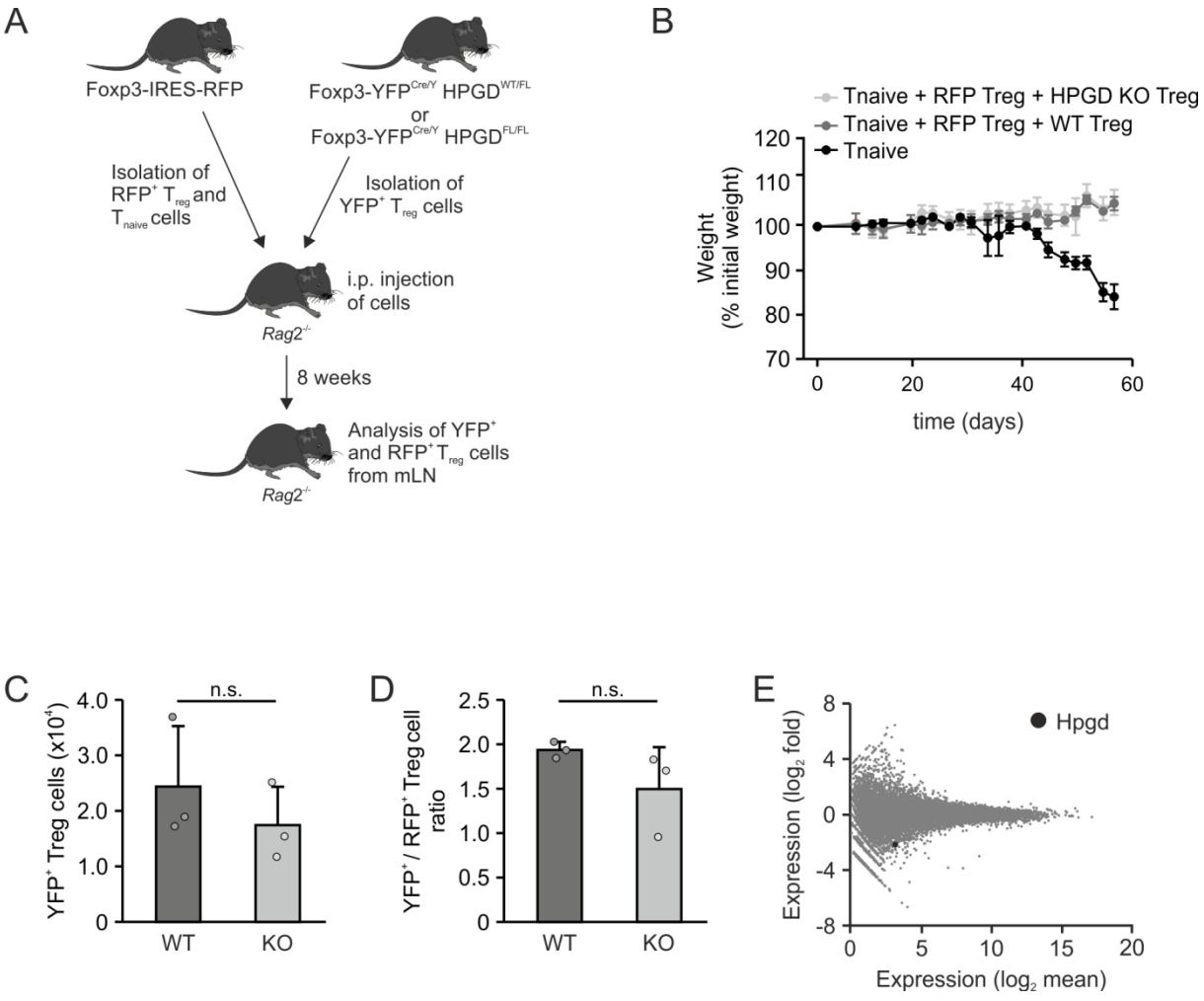

Figure 29: Co-transfer of Hpgd-deficient or competent T_{reg} cells with WT T_{reg} cells into Rag-$2^{-/-}$ animals showed no intrinsic defects in Hpgd-deficient T_{reg} cells

A) Scheme of the experimental set-up. Hpgd-deficient or competent T_{reg} cells were injected into Rag-$2^{-/-}$ animals with WT naïve T cells and WT T_{reg} cells. Animals were sacrificed after 8 weeks and T_{reg} cells from mLN were analyzed. **B)** Weight curve of animals from **(A)** as an indication of colitis development. Recovered T_{reg} cells from mLN as **C)** absolute number of YFP^+ T_{reg} cells and **D)** ratio of YFP^+ to RFP^+ T_{reg} cells. **E)** MA plot of gene expression of YFP^+ Hpgd-competent vs. Hpgd-deficient T_{reg} cells isolated from **(A)**.

4.3.6. Expression of Hpgd in T_{reg} cells is important for metabolic homeostasis in aged mice

Fat tissue is an important metabolic organ. Not only does it fulfill an important role in both lipid production and the regulation thereof (Summers, 2006) as well as in the metabolism of amino acids (Frayn et al., 1991), but it also fulfills important endocrine functions. Adipose tissue produces a variety of different hormones, cytokines and complement factors (Summers, 2006). In response to these signals, immune cells in the VAT are activated, utilizing the adipose tissue as an important nutrient source, thus further increasing immune cell activation. Under obese conditions, immune cells in the VAT exhibit continuous low-grade activation, leading to systematic inflammation while during malnutrition immune cell activation is inhibited (Wensveen et al., 2015a). Thus, fat tissue plays a vital role in linking the metabolism with the immune system. Furthermore, fat tissue can be divided into two, functionally distinct subtypes: white adipose tissue (WAT), such as the VAT, which consists mainly of white adipocytes and confers largely negative effects on adiposity and insulin sensitivity, and brown adipose tissue (BAT), which consist mainly of brown adipocytes and has been shown to improve adiposity, insulin resistance and hyperlipidemia (Bartelt and Heeren, 2014).

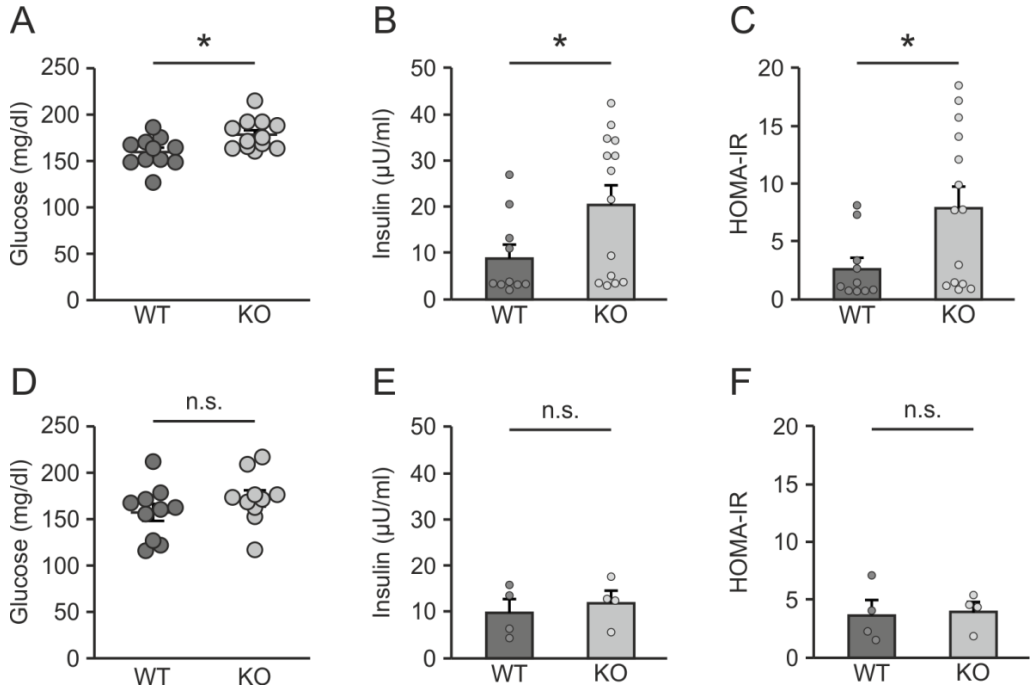

Figure 30: Metabolic parameters are worsened in aged animals with Hpgd-deficient T_{reg} cells compared to WT littermate controls.
Blood glucose levels after overnight fasting in **A)** aged and **D)** young animals with Hpgd-deficient T_{reg} cells or WT littermate controls. Insulin levels after overnight fasting in **B)** aged and **E)** young animals with Hpgd-deficient T_{reg} cells or WT littermate controls. HOMA-IR of **C)** aged and **F)** young animals with Hpgd-deficient T_{reg} cells or WT littermate controls.

Since a loss of Hpgd in T_{reg} cells seems to lead to a dysregulation of immune cell populations in the VAT of aged animals resulting in local inflammation, we analyzed whether this perturbation of the immune cell compartment in the VAT also affects the metabolism of these animals.

We performed all metabolic studies in male mice since it has been published that female mice are protected against metabolic syndrome under certain conditions (Pettersson et al., 2012), such as when challenged with HFD. Furthermore, we could not observe any differences in VAT-resident immune cell populations in female animals with Hpgd-deficient T_{reg} cells (Figure 25).

Since we could not observe a difference in bodyweight or VAT weight, but could detect a change in adipocyte size, we next analyzed the insulin signaling of aged animals with Hpgd-deficient T_{reg} cells and their WT littermates. We measured the fasting glucose of these animals and could detect a significant increase in fasting glucose (Figure 30 A) and insulin levels after overnight fasting (Figure 30 B) in animals with Hpgd-deficient T_{reg} cells. Therefore, these animals also had a higher Homeostatic Model Assessment for Insulin Resistance (HOMA-IR) score, a factor used to quantify insulin resistance, than the WT control animals (Figure 30 C). This seems indicative for the development of a metabolic dysregulation in aged animals when Hpgd is deleted in T_{reg} cells. When analyzing these parameters in young animals, these differences could no longer be observed (Figure 30 D-F), showing that, like the expansion of T_{reg} cells in the VAT, the metabolism of animals with a T_{reg} cell specific Hpgd deletion is only disturbed in aged animals. To further confirm these observations, glucose and insulin tolerance tests were performed to assess the ability of the animals to appropriately react to the presence of glucose or insulin. For this, animals were fasted overnight or for four hours and then injected with glucose or insulin, respectively. To evaluate the metabolic state of these animals, blood glucose levels were measured at fixed intervals after injection.

We could observe that aged animals with Hpgd-deficient T_{reg} cells responded significantly less to both insulin (Figure 31 A) and glucose stimulation (Figure 31 B) than their WT counterparts. In young animals, however, no such difference could be measured (Figure 31 C and D), again indicating that the observed effect of Hpgd on the metabolism of the animals is age dependent.

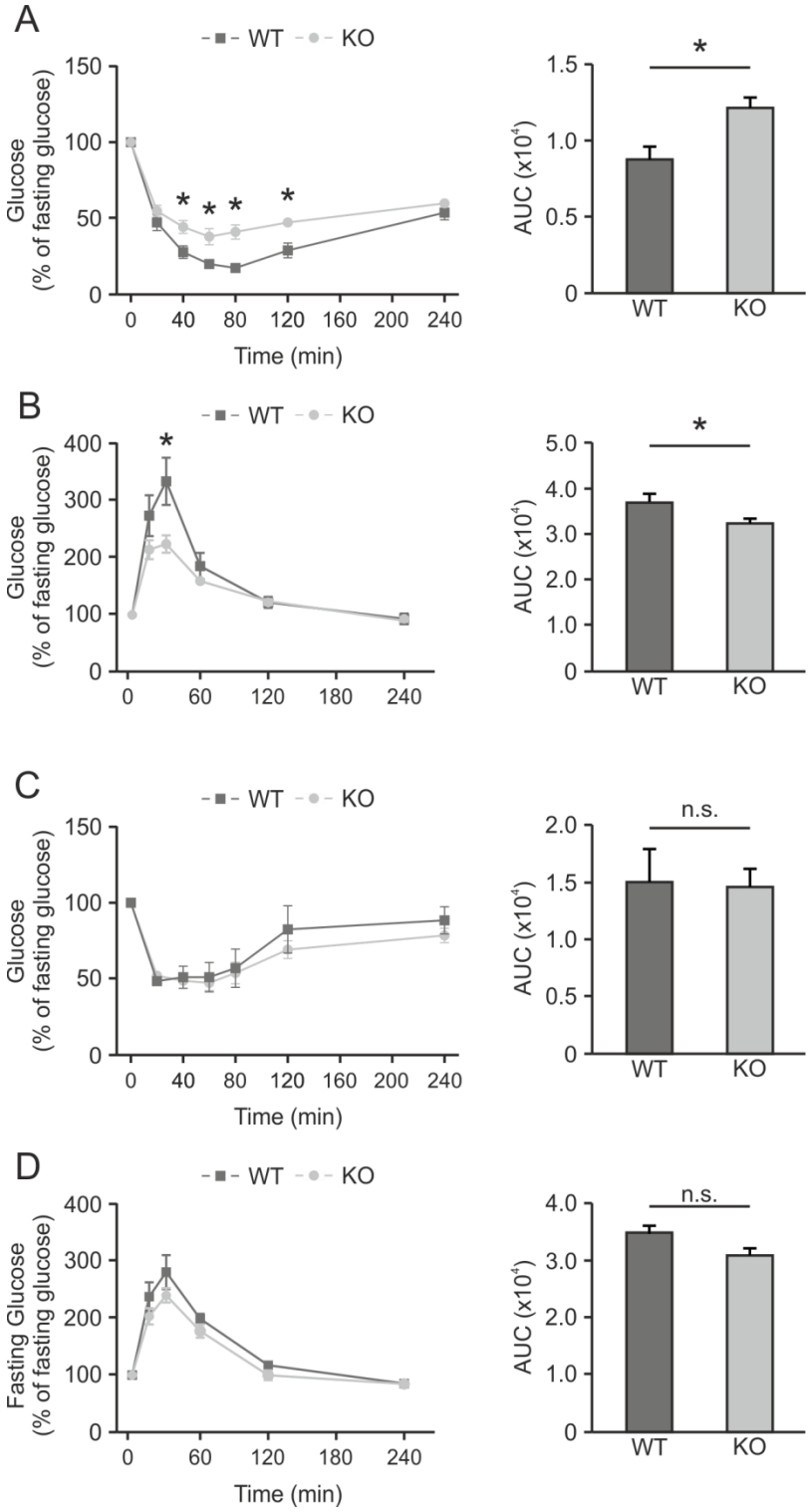

Figure 31: The metabolism of aged animals with Hpgd-deficient T_{reg} cells is less responsive to insulin and glucose.

A) Insulin tolerance test of aged animals with WT or Hpgd-deficient T_{reg} cells (left) and calculated AUC (right). **B)** Glucose tolerance test of aged animals with WT or Hpgd-deficient T_{reg} cells (left) and calculated AUC (right). **C)** Insulin tolerance test of young animals with WT or Hpgd-deficient T_{reg} cells (left) and calculated AUC (right). **D)** Glucose tolerance test of young animals with WT or Hpgd-deficient T_{reg} cells (left) and calculated AUC (right). AUC, area under the curve

Since we could observe a clear decrease in the response to insulin and glucose in old KO animals, we analyzed these animals in metabolic cages for 48 hours in collaboration with A. Pfeifer, University Hospital Bonn, to assess whether this is caused by alterations in their baseline activity, food intake or homeostatic metabolism. We could detect no difference in food intake (Figure 32 A), water intake (Figure 32 B), body composition (Figure 32 C) or motility (Figure 32 D). Furthermore, no difference in their respiration could be detected (Oxygen consumption, Figure 32 E, carbon dioxide consumption Figure 32 F, or respiratory exchange rate Figure 32 G), thus indicating that the animals show no difference in their homeostatic metabolism.

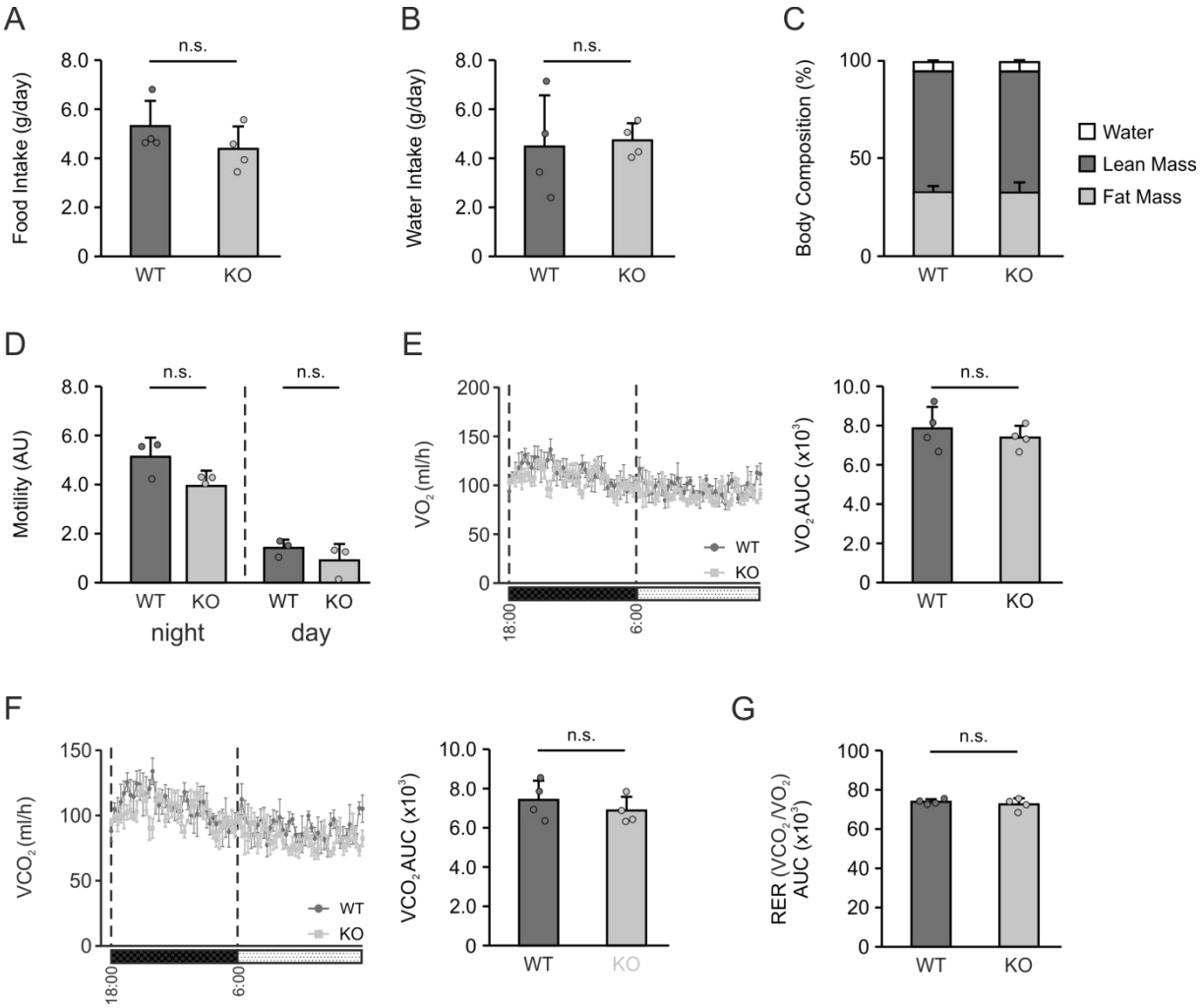

Figure 32: No difference in the metabolism of aged mice with Hpgd-deficient or competent T_{reg} cells could be detected under homeostatic conditions.

Aged animals with Hpgd-deficient T_{reg} cells and age-matched WT control animals were placed in metabolic cages and their **A)** food intake, **B)** water intake, **C)** body composition, **D)** motility, **E)** oxygen consumption, **F)** carbon dioxide consumption and **G)** respiratory exchange rate were recorded over a period of 48 hours. O_2, oxygen; CO_2, carbon dioxide; RER, respiratory exchange rate. Measurements performed by F. Copperi

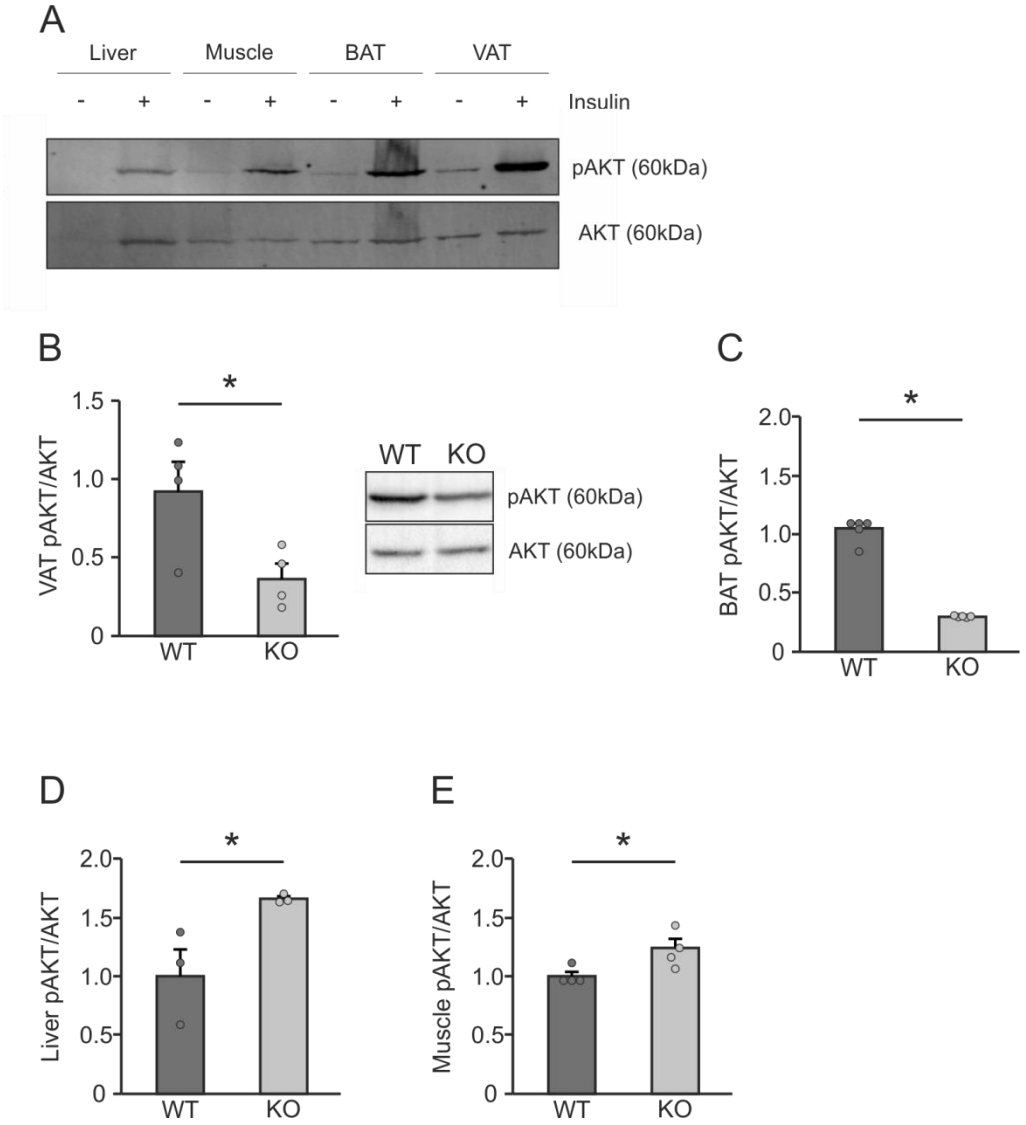

Figure 33: pAKT signaling is reduced in the fat tissue of aged animals with Hpgd-deficient T_{reg} cells.
A) Immunoblot of liver, muscle, brown adipose tissue (BAT) and VAT of WT animals against pAKT (top) and AKT (bottom). Organs were harvested 3 min after i.p. injection of 0.5 U/kg bodyweight insulin or 200 µl PBS. pAKT to AKT ratio of aged animals with WT and Hpgd-deficient T_{reg} cells (after insulin challenge as described in A) from **B)** VAT, **C)** BAT, **D)** liver and **E)** skeletal muscle samples. pAKT, phosphorylated AKT.

Subsequently, we analyzed the ratio of phosphorylated to unphosphorylated AKT in aged animals with Hpgd-deficient and Hpgd-competent T_{reg} cells in the VAT, BAT, liver and skeletal muscle harvested three min after challenging the animals with 0.5 U/kg bodyweight of insulin. The ratio of pAKT/AKT after insulin challenge in animals with Hpgd-deficient T_{reg} cells in the VAT and BAT is skewed towards AKT (Figure 33 B and C), indicating that insulin signaling in the fat tissue is reduced in these animals. Conversely, the pAKT/AKT ratio is skewed towards pAKT in both the liver and the skeletal muscle samples (Figure 33 D

and E), indicating that insulin signaling in these organs is increased, potentially due to a compensatory effect.

In an effort to more closely analyze the effect of Hpgd-deficient T_{reg} cells on insulin signaling in the VAT, we went further upstream in the insulin signaling cascade and investigated the mRNA expression of INSR1, IRS1 and IRS2 in the VAT of aged animals with Hpgd-deficient and competent T_{reg} cells, sacrificed three min after insulin challenge.

We could detect a significant decrease in mRNA levels of INSR1 in the VAT of aged animals with Hpgd-deficient T_{reg} cells compared to age-matched WT control animals (Figure 34). However, we could not detect a difference in either IRS1 or IRS2 mRNA expression in these samples (Figure 34), suggesting that the decrease in insulin signaling might be caused by a downregulation of the receptor INSR1.

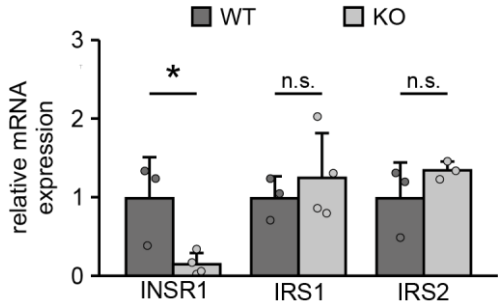

Figure 34: INSR1 mRNA is expressed at lower levels in VAT of aged animals with Hpgd-deficient T_{reg} cells after insulin challenge.
Aged animals were challenged with 0.5 U/ml insulin for three min prior to sacrifice. VAT was excised and mRNA was isolated from the whole organ and mRNA expression of the insulin receptor 1 (INSR1) and of the insulin receptor substrates (IRS) 1 and 2 was determined. Mean expression of WT animals was normalized to 1.

To analyze the composition and functionality of the VAT and BAT of aged animals with Hpgd-deficient T_{reg} cells, we performed protein analysis by immunoblotting.

As expected, we could not detect any uncoupling protein 1 (Ucp1), a marker for brown adipocytes, in the VAT (Figure 35 A). However, we could observe a significant increase in Ap2 in VAT of mice with KO T_{reg} cells (Figure 35 A, quantified in Figure 35 B). Ap2 is a fatty acid binding protein directly downstream of Ppar-γ, whose deletion has been implicated in the improvement of multiple different pathologies associated with the development of a metabolic syndrome. Similarly, deletion of Ap2 leads to protection against obesity, (Hotamisligil et al., 1996; Uysal et al., 2000), improved insulin signaling (Maeda et al., 2005)

and protection against atherosclerosis (Boord et al., 2002; Makowski et al., 2001). Furthermore, it has been suggested that inhibiting Ap2 might be a treatment option for different metabolic diseases (Furuhashi et al., 2007). Thus, the observed upregulation of Ap2 in VAT is further indicative of a worsened metabolic state in aged animals with Hpgd-deficient T_{reg} cells.

Meanwhile, in the BAT we could observe a downregulation of Ap2 in aged animals with Hpgd-deficient T_{reg} cells compared to age-matched littermate control animals (Figure 35 C, quantified in Figure 35 D). This might suggest a compensatory effect in the BAT. Furthermore, we could not detect a difference in Ucp1 expression between aged animals with Hpgd-competent and deficient-T_{reg} cells (Figure 35 C, quantified in Figure 35 E), suggesting that the functionality of the BAT is not negatively influenced by a lack of Hpgd in T_{reg} cells.

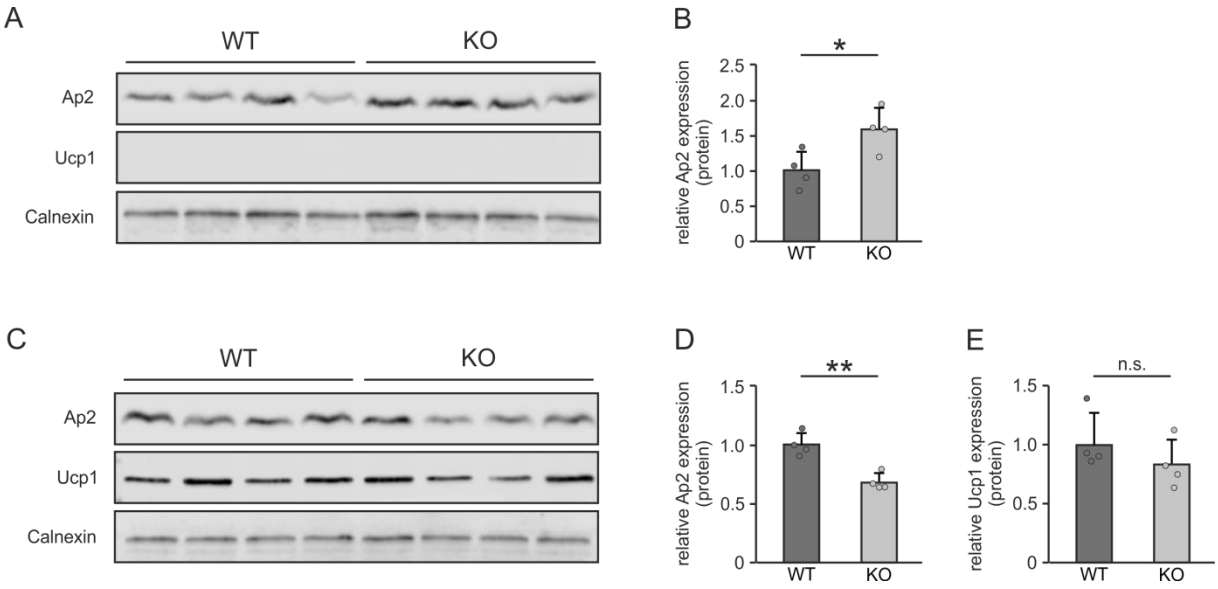

Figure 35: Ap2 is upregulated in VAT of aged animals with Hpgd-deficient T_{reg} cells compared to WT control animals.
Immunoblot of **A)** VAT and **C)** BAT of aged animals with Hpgd-deficient or competent T_{reg} cells of Ap2, Ucp1 and Calnexin. Quantification of Ap2 in **B)** VAT and **D)** BAT and **E)** Ucp1 in BAT. Ucp1, uncoupling protein 1

It has been previously described that metabolic dysregulation and the VAT-resident immune cell population are linked (Andersen et al., 2016). Besides alterations in the myeloid cell compartment, it has also been described that natural killer (NK) cell numbers are increased in high fat diet (HFD) models. This increase in NK cell numbers goes hand in hand with an increase in insulin resistance (Lee et al., 2016). Additionally, it has been shown that obesity leads to the upregulation of receptors on adipocytes which activate NK cells on

adipocytes, thus resulting in the production of pro-inflammatory cytokines by NK cells. These cytokines consequently lead to the recruitment and polarization towards a more pro-inflammatory state of macrophages in the VAT (Wensveen et al., 2015b). Since we observed an increase in the T_{reg} cell and proinflammatory macrophage compartments in animals with a T_{reg} cell specific deletion of Hpgd in aged animals (see chapter 4.3.3), we analyzed the NK-cell population in the VAT of these animals.

In accordance with these published data, we could observe an increase in the NK cell population in the VAT of aged animals with Hpgd-deficient T_{reg} cells compared to WT littermate controls (Figure 36 A). However, we could not detect a difference in the NKT-cell population of VAT in these animals (Figure 36 C) or a difference in the NK or NKT-cell population in the spleen (Figure 36 B and D). These observations, linked with the increased infiltration of pro-inflammatory macrophages and decreased Ap2 levels in the VAT as well as decreased insulin sensitivity in aged animals with Hpgd-deficient T_{reg} cells, are similar to previously published data of animals fed a HFD and might indicate that Hpgd in T_{reg} cells plays a role in obesity.

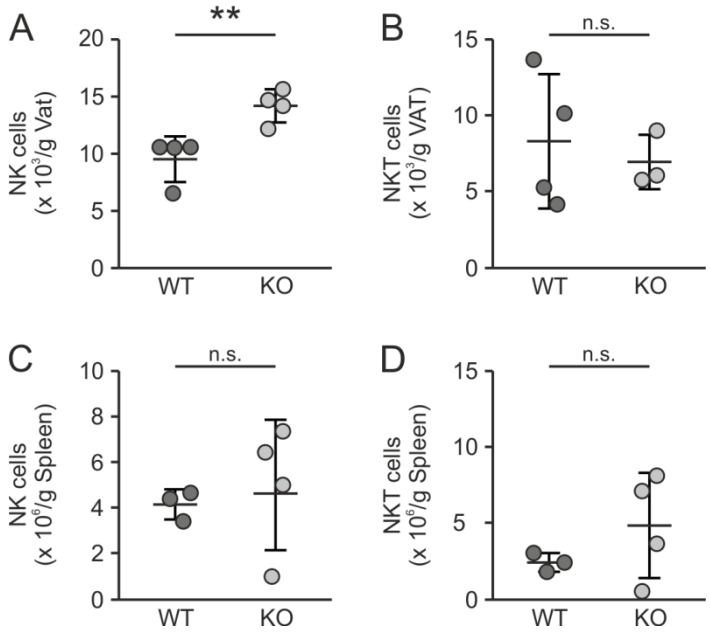

Figure 36: Aged animals with Hpgd-deficient T_{reg} cells have an increased NK-cell population in the VAT.

Absolute **A)** NK and **B)** NKT cell numbers in WT animals and animals with Hpgd-deficient T_{reg} cells isolated from the VAT. Absolute **C)** NK and **D)** NKT cell numbers in WT animals and animals with Hpgd-deficient T_{reg} cells isolated from the spleen.

4.3.7. Loss of Hpgd in T_{reg} cells leads to reduced insulin sensitivity during high fat diet

Since we could show that a T_{reg} cell specific deletion of Hpgd affects both the immune homeostasis of the VAT as well as the metabolism of aged animals, we attempted to exacerbate the observed effects by challenging these animals by inducing obesity. To this end, we subjected young animals to HFD for 15 weeks. However, even though the animals gained significantly more weight than the littermate control animals on normal diet (ND) (Figure 37 A), there was no significant difference in the weight between animals with Hpgd-deficient T_{reg} cells and WT littermate controls after 15 weeks of HFD feeding (Figure 37 A and B).

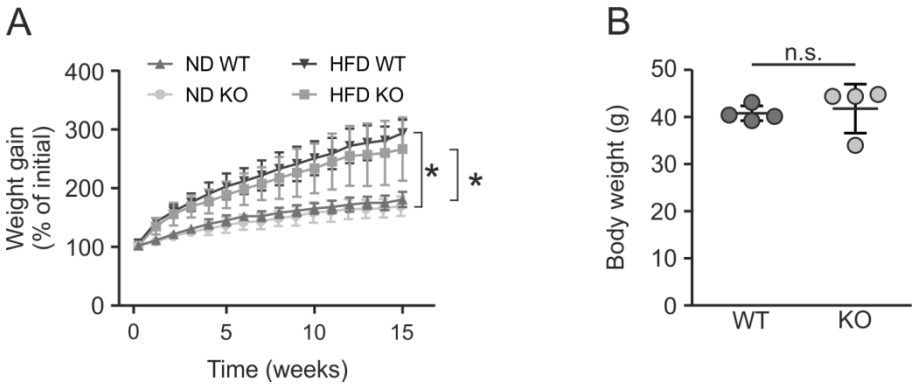

Figure 37: No difference in weight gain between animals with Hpgd-deficient T_{reg} cells and WT littermate control animals after 15 weeks of HFD.
A) Weight curve of animals with Hpgd-deficient or WT T_{reg} cells after 15 weeks on HFD or ND. **B)** Final weight of animals with Hpgd-deficient T_{reg} cells after 15 weeks on HFD and of WT littermate control animals. HFD, high fat diet; ND normal diet.

After fasting these animals for 16 hours and measuring fasting glucose levels, we could not detect a difference between the animals with Hpgd-deficient and Hpgd-competent T_{reg} cells, either on ND or on HFD (Figure 38 A). However, we could detect a clear increase in fasting glucose between animals subjected to ND vs. HFD diet. This, in conjunction with the decrease in insulin sensitivity in HFD-fed animals (Figure 38 B and C), demonstrated that the induction of obesity successfully reduced the metabolic responsiveness of these animals.

When comparing the effect of insulin on animals with a T_{reg} cell specific deletion of Hpgd to WT littermate controls after 15 weeks of HFD, we could observe that the animals with deficient T_{reg} cells respond less (Figure 38 B and C), resembling what we observed previously with aged animals under homeostatic conditions (Figure 31 A). However, the difference in insulin sensitivity in these obese animals is not as pronounced as in the aged animals.

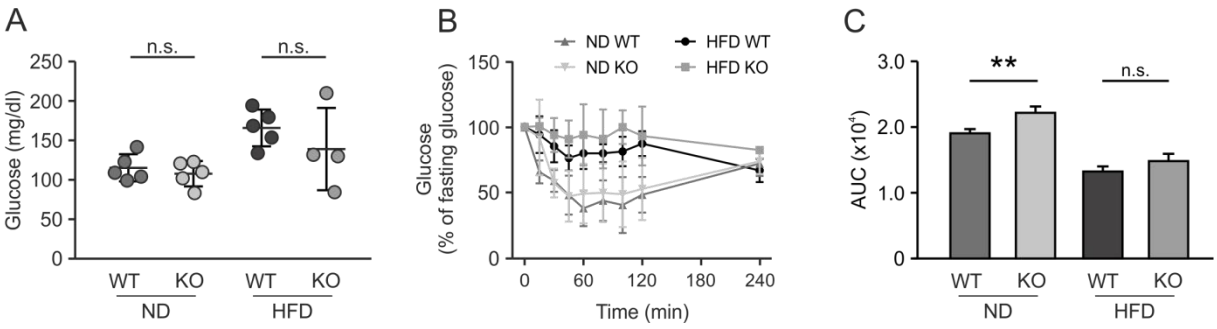

Figure 38: Animals with Hpgd-deficient T_{reg} cells show reduced insulin sensitivity after 15 weeks of HFD feeding.
A) Blood glucose levels after overnight fasting of animals with Hpgd-deficient or WT T_{reg} cells after 15 weeks on HFD or ND. **B)** Insulin tolerance test and **C)** corresponding AUC of animals with Hpgd-deficient or WT T_{reg} cells 15 weeks on HFD or ND.

Subsequently, we analyzed the VAT of these animals and could observe that the VAT of animals with Hpgd-deficient T_{reg} cells weighed less than that of WT littermate control animals after 15 weeks of HFD feeding (Figure 39 A). Further, similar to our observations in aged animals, we could detect an increase in the number of T_{reg} cells per gram VAT in these animals (Figure 39 B). However, we could not detect a difference in the percentage or the absolute size of the population (data not shown), indicating that the observed difference in T_{reg} cells may be caused by the decreased amount of VAT in the animals with Hpgd-deficient T_{reg} cells.

In addition, unlike in aged animals, we could not detect an increase in the macrophage population in the VAT of animals with Hpgd-deficient T_{reg} cells compared to WT littermate control animals after 15 weeks of HFD feeding (Figure 39 C).

Thus, subjecting animals to HFD does not seem to completely recapitulate the phenotype observed in aged animals – apart from a slight decrease in insulin sensitivity in animals with Hpgd-deficient T_{reg} cells compared to WT littermate control animals on HFD diet. This indicates that the HFD model is not the optimal model to study the effect of a T_{reg} cell specific loss of Hpgd, possibly due to the obesity caused increase of basal inflammation which no longer enables us to detect the increase in inflammation in the KO animals in comparison to WT animals.

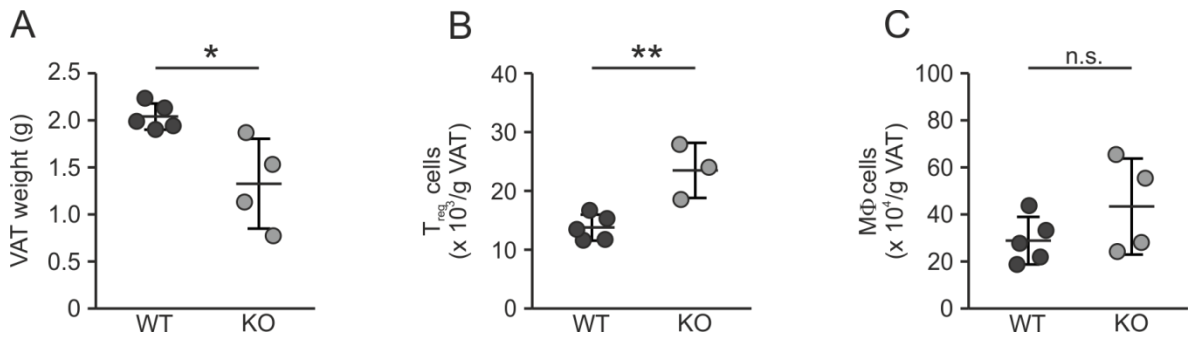

Figure 39: Analysis of VAT of animals with Hpgd-deficient or Hpgd-competent T_{reg} cells after 15 weeks of HFD.
A) Weight of VAT of animals with Hpgd-deficient T_{reg} cells and WT littermate control animals after 15 weeks of HFD. **B)** T_{reg} and **C)** $F4/80^+$ Macrophage population of the VAT of animals with and without Hpgd-deficient T_{reg} cells after 15 weeks of HFD feeding in cells/g VAT.

4.4. HPGD in human T2D

Controlling inflammation is crucial for limiting T2D pathogenesis, as increased levels of pro-inflammatory cytokines have been linked to decreased insulin sensitivity and several of the secondary associated effect (Bruun et al., 2003). Furthermore, T_{reg} cells have been shown to be vital in suppressing inflammation at primary and secondary sites of T2D pathogenesis, including in VAT and the kidneys (Eller et al., 2011; Kornete et al., 2013). Thus, a correlation between T2D and T_{reg} cell functionality exists. Since the phenotype we observed in aged animals with KO T_{reg} cells is reminiscent of non-obese T2D, i.e. no significant weight gain coupled with a dysregulation of the immune cell population in the fat tissue and decreased insulin sensitivity, we analyzed PB of lean T2D patients compared to healthy control patients. Thus, we applied linear support vector regression (SVR), which infers the contribution of various gene expression signatures in one dataset to a publicly available microarray dataset.

This allowed us to estimate the distribution of different immune cell populations in the cohort (Newman et al., 2015). When analyzing these data, we could observe a significant change in the makeup of the leukocyte population of PB samples isolated from T2D patients compared to healthy controls (Figure 40 A). The granulocyte and monocyte population of T2D patients is expanded, reminiscent of the increase of the myeloid population in the VAT of aged animals with a T_{reg} cell specific deletion of Hpgd. When further analyzing the T_{reg} cells of this dataset, we could detect a significant decrease in the frequency of T_{reg} cells in the PB of T2D patients compared to healthy individuals (Figure 40 B).

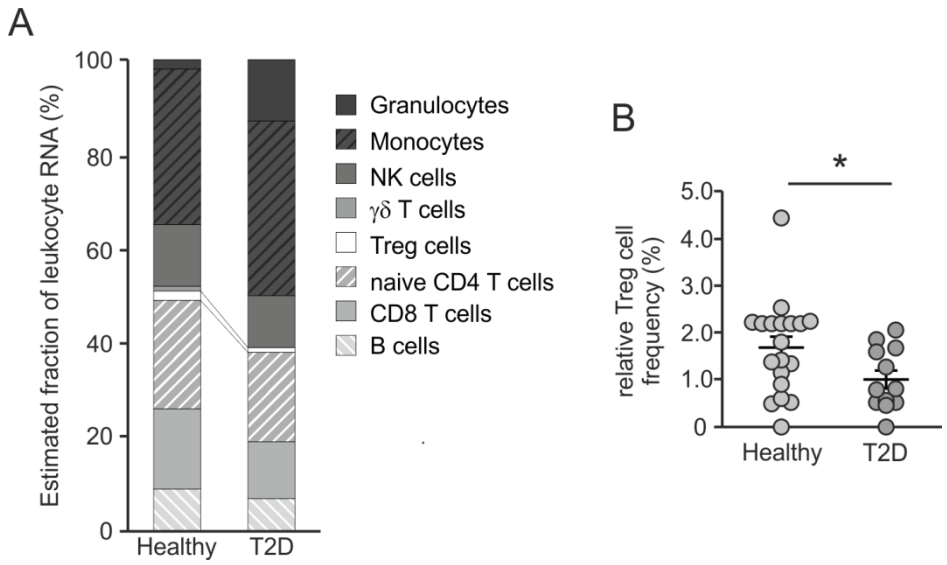

Figure 40: Human T2D patients have a smaller T_{reg} cell fraction compared to healthy individuals.
A) Relative quantification of leukocyte populations of microarray data of PB isolated from healthy controls and patients with type II diabetes (T2D) as determined by linear support vector regression. **B)** Relative quantification of T_{reg} cells in microarray samples of PB of T2D patients and healthy controls as determined by linear support vector regression. Analysis performed by K. Baßler.

In a separate microarray dataset, consisting of T_{reg} and T_{conv} cells isolated from the PB of T2D patients and healthy individuals, we more closely analyzed gene expression in T_{reg} cells of T2D patients. We could not detect a difference in FOXP3 levels between T_{reg} cells isolated from healthy individuals and T2D patients (Figure 41 A).

In a subsequent step, we analyzed HPGD expression levels in this dataset. As expected, the level of HPGD expression is significantly higher in T_{reg} cells than in T_{conv} cells, both in T2D and in healthy control samples. However, the observed increase in HPGD levels is significantly lower in T2D patients than in healthy individuals (Figure 41 B).

To confirm these bioinformatic analyses with our own experimental data, we sorted $CD3^+CD4^+CD25^+CD127^-$ T_{reg} and $CD3^+CD4^+CD25^-CD127^+$ T_{conv} cells from PB of T2D patients and healthy, age-matched individuals and analyzed both FOXP3 and HPGD expression. Using qRT-PCR, we could confirm that, as anticipated, the T_{reg} cells of both healthy and T2D patients express significantly more FOXP3 than the T_{conv} cells, with no detectable difference between T2D and healthy control T_{reg} cells (Figure 42 A).

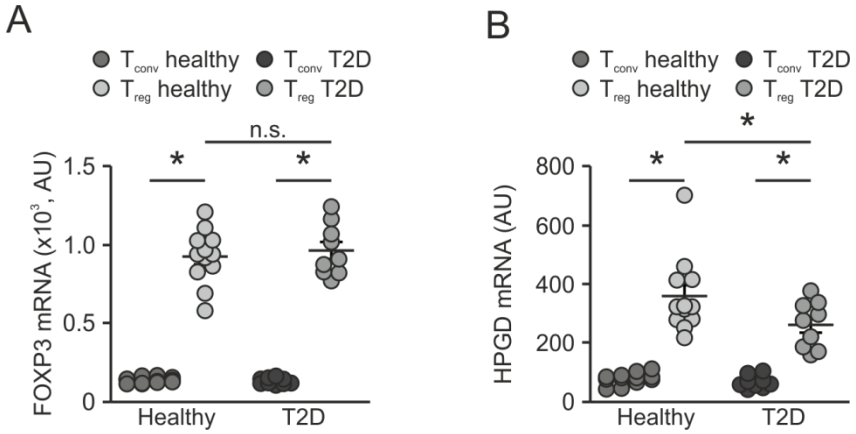

Figure 41: T2D patients express significantly lower amounts of HPGD in PB T_{reg} cells than healthy individuals.
Relative **A)** FOXP3 and **B)** HPGD mRNA levels of T_{reg} and T_{conv} cells isolated from the pB of T2D patients and healthy controls.

When analyzing HPGD expression in these cells, we could detect a significant increase in both T2D and healthy control T_{reg} cells compared to T_{conv} cells. Additionally, as observed in the microarray dataset, we could measure a significant decrease in HPGD expression in T_{reg} cells of T2D patient samples compared to healthy control T_{reg} cells (Figure 42 B). Thus our data confirm the microarray data analysis.

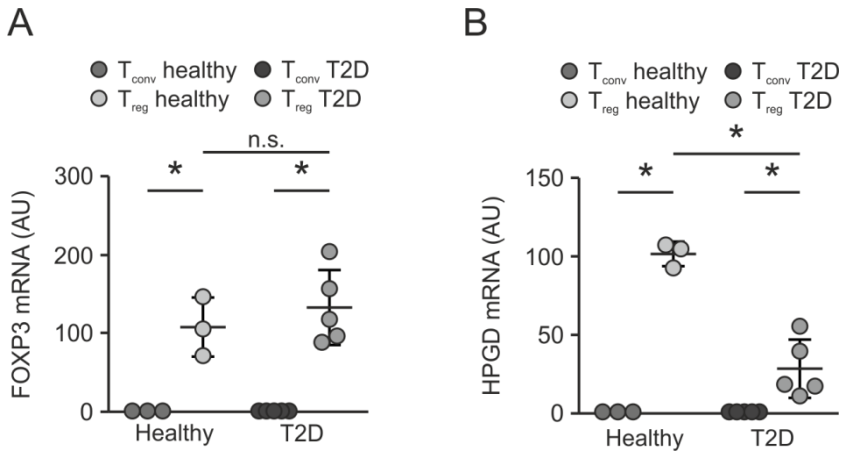

Figure 42: T2D patients exhibit significantly lower HPGD in T_{reg} cells isolated from PB than healthy individuals.
Relative **A)** FOXP3 and **B)** HPGD levels of T_{reg} and T_{conv} cells isolated from the PB of T2D patients and healthy individuals. Expression of T_{conv} cells was normalized to 1.

Furthermore, when analyzing the PB T_{reg} cell population in T2D patients compared to healthy individuals, we could detect a significant increase in the relative size of the population in T2D patients (Figure 43 A and B), however, this increase was based on a shift of the T_{reg}/T_{conv} ratio in these T2D patients. This increase is reminiscent of the increase in the T_{reg} cell population of the VAT of aged animals with Hpgd-deficient T_{reg} cells (Figure 19 B and

C). Taken together, these data seem to indicate that HPGD expression in T_{reg} cells might play a role in human T2D. However, it remains unclear whether a decrease of HPGD-levels and the accompanying decrease in T_{reg} cell functionality is a cause or an effect of T2D.

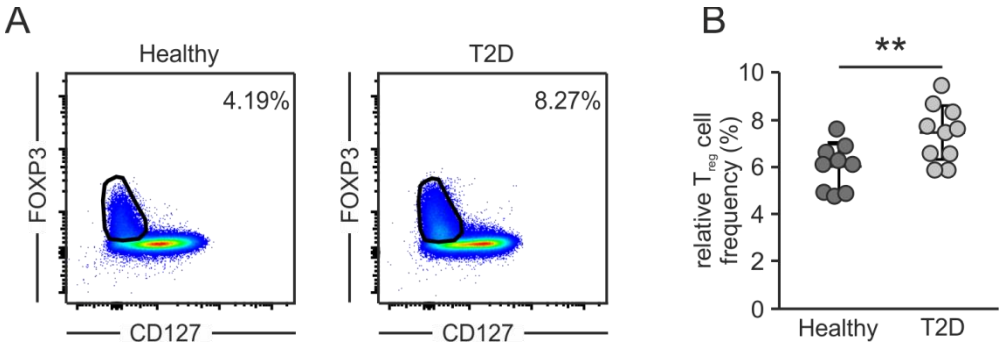

Figure 43: T2D patients exhibit a significantly higher T_{reg} cell population than healthy age matched individuals.
Cells were isolated from PB of T2D patients and age-matched healthy controls and stained for protein measurements. **A)** Representative plots and **B)** quantification.

All in all, in this work we could show that Hpgd is an important mediator of both human and murine T_{reg} cell suppression through the metabolism of PGE_2 into 15-keto-PGE_2 in an at least partially Ppar-γ-dependent manner. A T_{reg} cell specific loss of Hpgd led to a decrease in suppression in PGE_2-rich environment accompanied by an increase in the VAT-resident T_{reg} and proinflammatory macrophage population coupled with a decrease in metabolic function. Further, we could correlate decreased HPGD levels in human T_{reg} cells to T2D.

4.5. MEOX1 is upregulated in human T_{reg} cells

To further analyze the regulation of gene expression in T_{reg} cells and identify key components of the T_{reg} cell transcriptome, an extensive bioinformatic analysis of different T_{reg} and T_{conv} cell populations was performed by K. Baßler during his master thesis. This led to the identification of the transcription factor MEOX1 as highly upregulated in stimulated human T_{reg} cells. When analyzing the expression of MEOX1 and FOXP3 in the previously published microarray dataset used to identify HPGD as key T_{reg} cell molecule (Beyer et al., 2011), MEOX1 was found to be upregulated in most T_{reg} cell conditions, and most highly upregulated in conditions 27 and 28, the two conditions in which T_{reg} cells were activated with CD3 and IL-2 (Figure 44 B) whilst FOXP3 was upregulated across all T_{reg} cell conditions (Figure 44 A).

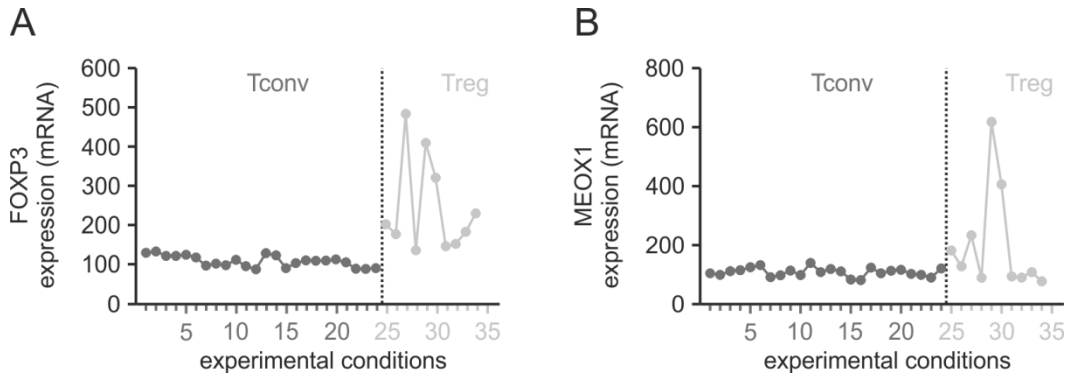

Figure 44: MEOX1 is upregulated in human T_{reg} cells.
A) FOXP3 and **B)** MEOX1 mRNA levels in $CD4^+$ T_{conv} and T_{reg} cells under different stimulation conditions (available under GEO accession number GSE15390). Analysis performed by K. Baßler.

To validate the bioinformatics analyses, T_{reg} and T_{conv} cells were sorted from human blood and MEOX1 mRNA expression was analyzed. As expected, we could detect significantly elevated FOXP3 levels in T_{reg} cells compared to T_{conv} cells (Figure 45 A). Moreover, we could also detect increased MEOX1 levels in these cells (Figure 45 B). This increase in MEOX1 expression could be increased by stimulating the cells overnight with IL-2 (Figure 45 C), thus further confirming the results of the microarray analysis (Figure 44B).

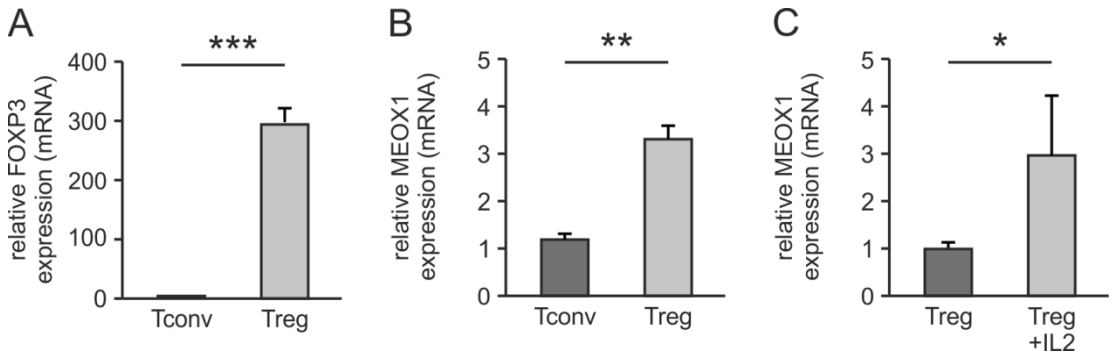

Figure 45: MEOX1 is upregulated in human T_{reg} cells.
A) FOXP3 and **B)** MEOX1 mRNA expression of sorted human T_{reg} and T_{conv} cells. **C)** Sorted human T_{reg} cells were cultivated overnight either with or without 100 U IL-2 per ml and MEOX1 mRNA expression was measured by qRT-PCR. Mean expression of T_{conv} cells (panel A and B) or unstimulated T_{reg} cells (panel C) was normalized to 1.

In an effort to further explore the role of IL-2 for MEOX1 expression, T_{reg} cells were isolated by positive magnetic bead sorting and stimulated with different levels of IL-2, ranging from 10 U/ml (Figure 46 A) and 100 U/ml (Figure 46 B) to 1000 U/ml (Figure 46 C) and MEOX1 levels were determined at defined intervals between 12 and 72 hours after stimulation.

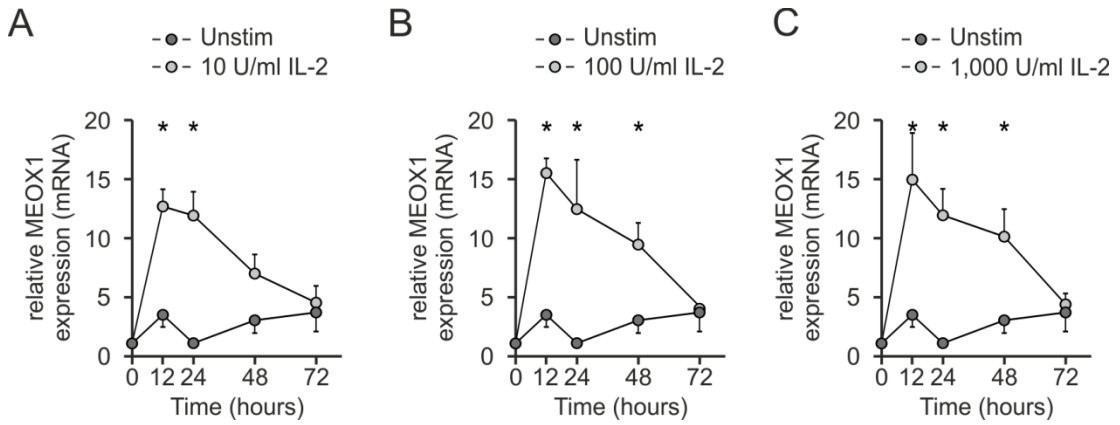

Figure 46: MEOX1 expression is upregulated in human T_{reg} cells in the presence of IL-2.
Human T_{reg} cells were cultivated in the presence of **A)** 10 **B)** 100 and **C)** 1000 U/mL IL-2 for 72 hours and MEOX1 mRNA levels were determined before stimulation and 12, 24, 48 and 72 hours after stimulation. As control, unstimulated T_{reg} cells were used. MEOX1 expression at 0 hrs was normalized to 1.

Already after 12 hours, we could observe a more than 10-fold increase in MEOX1 levels which then continuously decreased again until after 72 hours of stimulation MEOX1 levels returned to unstimulated levels. This increase was dose-independent as there seems to be no difference between stimulating with 10, 100 or 1,000 U/ml of IL-2 (Figure 46 A-C).

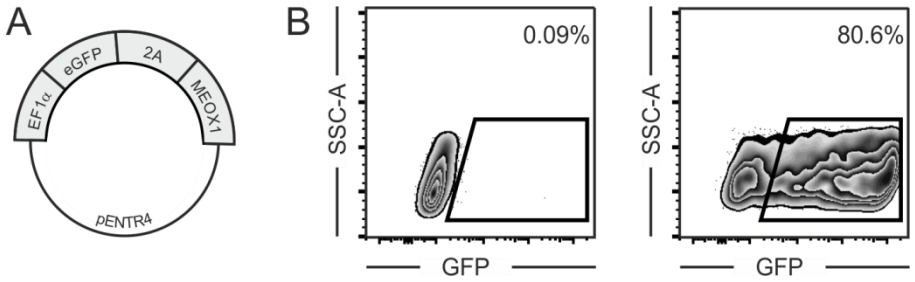

Figure 47: Transfection of a MEOX1 expression plasmid into HEK293T cells.
A) Construct used for transfection into HEK293T cells. eGFP linked with a 2A peptide to MEOX1 under the control of the constitutive EF1-α promoter in a pENTR4 backbone. **B)** Transfection efficacies of HEK293T cells with an empty pENTR4 plasmid (left) and the pENTR4-eGFP-2A-MEOX1 construct (right).

In a subsequent step, the protein expression of MEOX1 in human T_{reg} and T_{conv} cells was examined. Due to the limited availability of human T_{reg} cell protein samples, the WES system, a capillary system with a theoretical detection limit of 0.3 µg of protein was used. To test the WES system and the MEOX1 antibodies, a positive control for protein analyses was generated by transfecting a plasmid containing MEOX1 under the control of an EF1-α promoter, a constitutive promoter of human origin (Figure 47 A) into HEK293T cells. Only

samples with transfection efficiencies of 70% or higher were used for subsequent protein analysis (Figure 47 B).

When applying protein lysates of HEK293T cells and HEK293T cells containing the MEOX1 overexpression plasmid to a traditional immunoblot, a specific band of approximately 36 kDa was detected only in the sample overexpressing MEOX1 (Figure 48 A), even though MEOX1 is predicted to run at 28 kDa. However, since MEOX1 expression was artificially induced in HEK293T cells by transfection and could not be detected in normal HEK cell lysates, we conclude that this is the specific MEOX1 band, running slightly higher due to possible posttranslational modifications. When applying these samples to the more sensitive WES system, we could detect a peak at 38 kDa in the samples overexpressing MEOX1 but not in the HEK293T cell protein lysate (Figure 48 B). Due to the similar size and expression, we assume that this is the same peak that we already observed on the traditional immunoblot.

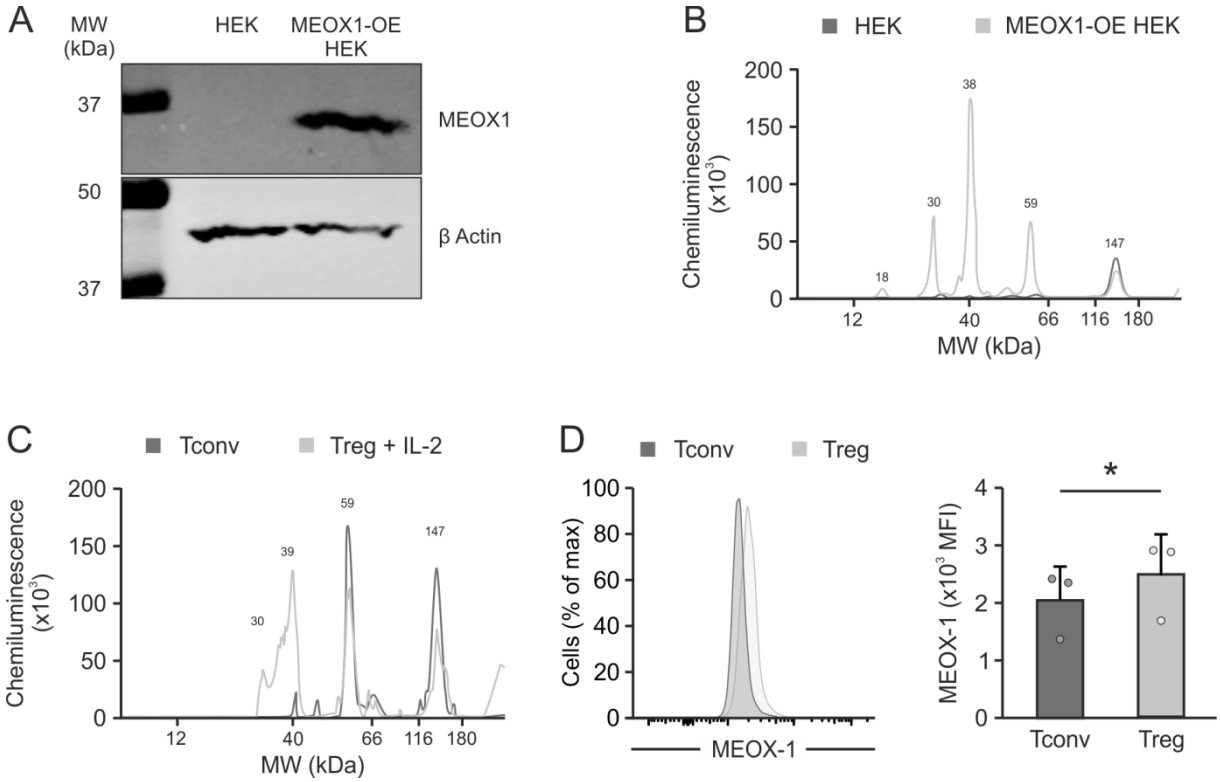

Figure 48: MEOX1 is upregulated on protein level in stimulated human T_{reg} cells compared to T_{conv} cells.
A) Traditional western and **B)** WES of HEK cells and HEK cells overexpressing MEOX1. **C)** WES of human T_{conv} cells and T_{reg} cells stimulated overnight with 100 U/mL IL-2. **D)** Representative (left) and cumulative (right) flow cytometric analysis of MEOX-1 expression in IL-2 stimulated T_{reg} and T_{conv} cells. OE, overexpression

After confirming that the antibody is capable of specifically detecting MEOX1 using the WES system, we then compared the MEOX1 expression between sorted human T_{conv} and T_{reg} cells after stimulating the cells with 100 U/ml IL-2 for 16 hours and could detect a peak at 39 kDa in the T_{reg} cell lysate but not in the T_{conv} cell sample (Figure 48 B). We could confirm these data in flow cytometric analyses, where we could show that MEOX1 is expressed at significantly higher levels in IL-2 stimulated T_{reg} cells compared to IL-2 stimulated T_{conv} cells (Figure 48 D). Thus, we could clearly show that MEOX1 is present not only on mRNA but also on protein level in T_{reg} cells but not in T_{conv} cells after IL-2 stimulation.

4.5.1. MEOX1 is regulated by FOXP3 but does not control the expression of HPGD

Next, we were interested in the mechanisms through which expression of MEOX1 is regulated. As E. Schönfeld could show in her PhD thesis that HPGD, similar to MEOX1, is also upregulated after IL-2 stimulation (Schönfeld, 2011), we decided to more closely analyze whether there might be a connection between the regulation of MEOX1 and HPGD.

K. Baßler found that HPGD and MEOX1 both appear in the same WGCNA module, thus indicating that a similar mechanism of gene expression is likely. We hypothesized that the most likely common mechanism of regulation is by the T_{reg} cell defining transcription factor FOXP3, which we have previously shown binds to the *HPGD* locus and governs HPGD expression (data not shown). Indeed, when K. Baßler perfomed a binding motive analysis of T_{reg} cells stimulated with IL-2 using iRegulon, he found that MEOX1 contains a FOXP3 binding site. This implies that MEOX1 expression might be regulated by FOXP3 binding. Therefore, we analyzed the effect of silencing FOXP3 in human T_{reg} cells by introducing small, interfering RNAs (siRNAs) against FOXP3 and subsequently analyzing MEOX1 expression.

In order to confirm the knockdown efficiency, we analyzed FOXP3 expression and could detect a decrease in FOXP3 expression of more than 50% in cells transfected with FOXP3 siRNAs compared to control cells transfected with scrambled siRNAs (Figure 49 A).

When analyzing MEOX1 expression in these cells, we could detect a significant decrease in MEOX1 expression in cells transfected with siRNAs specific for FOXP3 compared to the control cells. This indicates that FOXP3 is upstream of MEOX1 and that the presence of FOXP3 promotes the expression of MEOX1 (Figure 49 B).

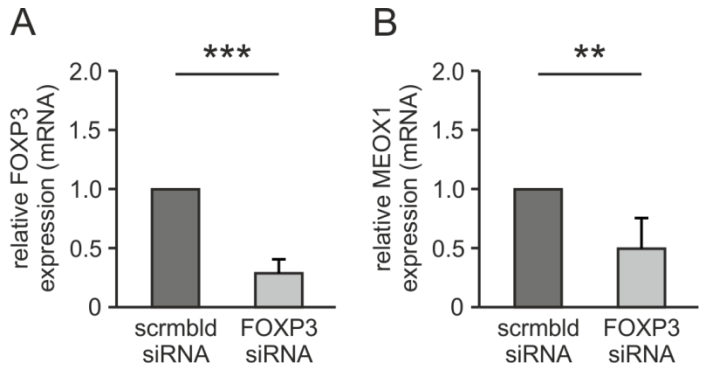

Figure 49: A knockdown of FOXP3 in human T_{reg} cells leads to a reduction of MEOX1 expression

Relative **A)** MEOX1 and **B)** FOXP3 levels in human T_{reg} cells, 48 hours after transfection with either scrambled or FOXP3 siRNA. Expression levels of cells transfected with scrambled siRNAs were normalized to 1.

To analyze whether the regulation of MEOX1 by FOXP3 is reciprocal, we performed MEOX1 siRNA knockdowns in human T_{reg} cells and analyzed FOXP3 and HPGD mRNA levels. While the knockdown efficiency of the MEOX1 siRNAs was not as high as that of the FOXP3 siRNAs, we could still detect a significant decrease in MEOX1 levels of nearly 50% in cells transfected with MEOX1 siRNA compared to cells transfected with scrambled siRNAs as a control (Figure 50 A). However, we could not detect a difference in either FOXP3 (Figure 50 B) or HPGD (Figure 50 C) expression in response to the MEOX1 knockdown. Thus, we conclude that the transcription factor MEOX1, while downstream of the T_{reg} cell lineage defining transcription factor FOXP3, does not play a role in the regulation of either HPGD or FOXP3 expression.

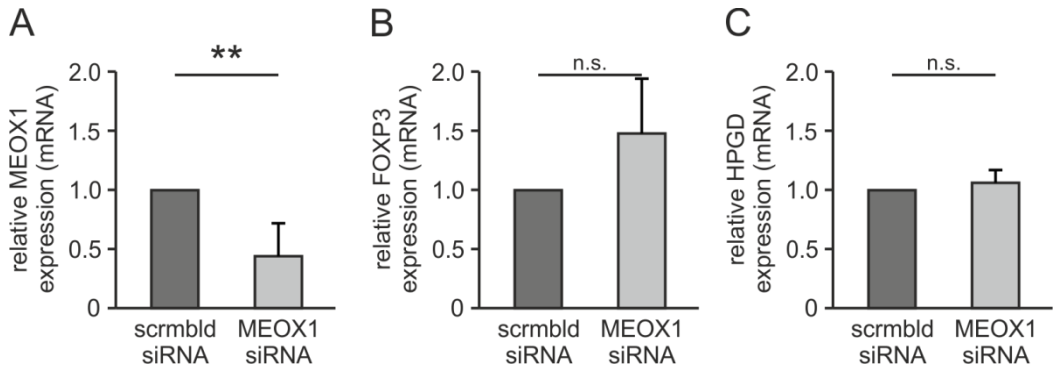

Figure 50: Silencing of MEOX1 in human T_{reg} cells does not affect either FOXP3 or HPGD expression.

Relative **A)** MEOX1 **B)** FOXP3 and **C)** HPGD levels in human T_{reg} cells, 48 hours after transfection with either scrambled or MEOX1 siRNA. Expression levels of cells transfected with scrambled siRNAs were normalized to 1.

All in all, these results indicate that HPGD, through the metabolism of PGE_2 into 15-keto-PGE_2, is an important mediator of T_{reg} cell mediated T_{conv} cell suppression, both in the murine system and in humans, in an, at least partially, Ppar-γ-dependent manner. We could further observe a dysregulation of the metabolism when T_{reg} cells lack Hpgd in aged mice and a downregulation of HPGD in human T2D, indicating that the expression of HPGD plays an important role in the function of T_{reg} cells crucial to maintain metabolic homeostasis.

When analyzing the role of the transcription factor MEOX1 in T_{reg} cell biology, we could show that MEOX1 is highly upregulated in T_{reg} cells, especially after IL-2 stimulation. Furthermore, we could demonstrate that MEOX1 is downstream of FOXP3. However, we could not detect a correlation between HPGD and MEOX1 expression.

5. Discussion

Following immune cell activation, the immune response needs to be modulated to avoid a chronic proinflammatory state and autoimmunity. Here, T_{reg} cells play an important role. However, despite being one of the main mediators of immunoregulation, the exact functionality of T_{reg} cells is poorly understood, especially in a tissue context specific manner.

It has been long accepted that the T_{reg} cell population is diverse and can be classified in a variety of different manners: depending on their tissue of origin either as thymic or peripheral T_{reg} cells or depending on their state of activity as naive or effector T_{reg} cells. More recently, however, T_{reg} cells have been classified based on their tissue of residence (Burzyn et al., 2013; Kolodin et al., 2015). For instance, it has been described that the transcriptional signature of VAT-resident T_{reg} cells varies significantly from that of lymphoid T_{reg} cells, differing in the expression of chemokine receptors, cytokines, metabolic proteins as well as in their TCR repertoire (Feuerer et al., 2009).

We performed a more detailed analysis of human T_{reg} cells and found that the PGE_2 metabolizing enzyme HPGD is upregulated in human T_{reg} cells in general, but also in murine T_{reg} cells. This upregulation is especially prominent in the VAT, a PGE_2-rich environment. Correspondingly, we hypothesized that HPGD might play a role in T_{reg} cell functionality, especially in VAT-resident T_{reg} cells.

Indeed, we could show that the 15-keto-PGE_2, a direct, Hpgd-dependent metabolite of PGE_2, is an important mediator of T_{conv} cell suppression. Furthermore, we could show that T_{reg} cell expression of Hpgd is important for VAT immune-homeostasis and is vital to maintain a healthy metabolism; a finding which we could recapitulate in animals subjected to a HFD, where animals with Hpgd-deficient T_{reg} cells showed reduced insulin sensitivity. Furthermore, we could show that in the PB of human T2D patients HPGD expression is significantly reduced in comparison to healthy age-matched individuals.

Finally, we analyzed whether the transcription factor MEOX1 plays a role in controlling HPGD expression and could show that while MEOX1, like HPGD, is regulated by FOXP3, the T_{reg} cell lineage defining transcription factor, we could not detect an influence of MEOX1 expression on HPGD.

5.1. Suppressive role of the HPGD-mediated PGE_2 metabolite 15-keto-PGE_2 via PPAR-γ-signaling

In a large transcriptome analysis, we could show that HPGD is significantly upregulated across all T_{reg} cell conditions we analyzed. Initially, the upregulation of the PGE_2 metabolizing enzyme HPGD in T_{reg} cells seems counterintuitive since it has been previously published that PGE_2 leads to the upregulation of the lineage defining transcription factor FOXP3 in T_{reg} cells and that the presence of PGE_2 leads to an increase in the suppressive functionality of T_{reg} cells (Baratelli et al., 2005). We could confirm these observations in suppression assays conducted in the presence of PGE_2. However, while it was previously proposed that PGE_2 acts a) directly on T_{conv} cells to exert its suppressive function (Chemnitz et al., 2006) and b) increases T_{reg} cell functionality by augmenting FOXP3 expression and thereby T_{reg} cell identity (Baratelli et al., 2005), we could show that this might not be the main mechanism of action as in the absence of T_{reg} cells, PGE_2 did not affect T_{conv} cell proliferation while the Hpgd-mediated metabolite 15-keto-PGE_2 exhibited suppressive functionality independently of T_{reg} cells. Furthermore, a loss of Hpgd in T_{reg} cells also abrogated that suppressive capacity of PGE_2, both in *in vitro* suppression assays and in *in vivo* colitis experiments. Thus, we were able to confirm the previously published observation that PGE_2 is beneficial for the suppressive capacity of T_{reg} cells and hypothesize that the mechanism in which this suppression occurs is via the HPGD dependent metabolism of PGE_2 into 15-keto-PGE_2.

A 15-keto-PGE_2 mediated suppressive effect has been previously observed, albeit not in the context of T-cell biology. It is particularly well characterized in cancer progression, where 15-keto-PGE_2 has been shown to inhibit the proliferation of pancreatic adenocarcinoma and hepatocellular carcinoma (Chang et al., 2016; Lu et al., 2014). However, the exact mechanism of 15-keto-PGE_2-mediated inhibition of cell proliferation is unclear, even though it has been suggested, at least in hepatocellular carcinoma, that the observed suppressive effect is mediated by Ppar-γ signaling (Lu et al., 2014).

15-keto-PGE_2 has been shown to be a ligand of Ppar-γ (Chou et al., 2007), an observation which we could corroborate as the effect of 15-keto-PGE_2 closely mirrors that of the known Ppar-γ ligand Rosiglitazone. Furthermore, when we analyzed the suppressive effect of 15-keto-PGE_2 on the proliferation of Ppar-γ-deficient T_{conv} cells, we could detect a significant decrease in 15-keto-PGE_2 dependent suppression of proliferation. Thus, Hpgd

seems to induce Ppar-γ signaling through the metabolism of PGE_2 into the Ppar-γ ligand 15-keto-PGE_2.

Ppar-γ signaling has long since been ascribed an immunomodulatory role. For instance, in monocytes an induction of Ppar-γ leads to a downregulation of different proinflammatory cytokines and chemokines (Dasu et al., 2009; Dinarello, 2010). Furthermore, Ppar-γ activation in macrophages leads to inhibition of proliferation and polarization towards an anti-inflammatory phenotype (Bouhlel et al., 2007; Lin et al., 2014) while in B cells, an activation of the Ppar-γ signaling pathway induces cell death (Padilla et al., 2002). In addition, the activation of Ppar-γ signaling leads to an expansion of VAT-resident T_{reg} cells and a decrease in VAT inflammation (Cipolletta et al., 2012). All in all, this shows that Ppar-γ signaling plays an important immunomodulatory role and indicates that activation of Ppar-γ signaling in T_{conv} cells leads to decreased cell proliferation, thus hampering the immune response and leading to a more immunomodulated environment.

Conversely, deleting Ppar-γ leads to the downregulation of Hpgd in lymphatic T_{reg} cells and especially in VAT-resident T_{reg} cells. This indicates that Ppar-γ is not only downstream but also upstream of Hpgd and that the transcription factor is required for the expression of Hpgd. However, how Ppar-γ influences Hpgd is largely unknown. We would hypothesize that the effect is caused by instructional events which determine the T_{reg} cell fate. However, where these signals originate is uncertain, but we believe that these signals are derived from the adipose tissue rather than from T_{conv} cells.

However, HPGD expression is not limited to T_{reg} cells. Rather, a variety of different myeloid cells, such as DCs and macrophages, also express HPGD at relatively high levels. Therefore, it could be argued that these cells may also be involved in the regulation of T_{conv} cell proliferation by affecting the 15-keto-PGE_2 levels in their environment. However, when we analyzed the expression level of PTGR1 and PTGR2, the two major enzymes involved in the further metabolism of 15-keto-PGE_2, we could show that while the enzymes are highly expressed in myeloid cells, the expression is largely absent in T cells. This indicates that in myeloid cells 15-keto-PGE_2 is further metabolized into 13,14-dihydro-15-keto-PGE_2, which is highly unstable under homeostatic conditions and therefore rapidly degraded (Fitzpatrick et al., 1980). Furthermore, it has been previously described that inhibiting PTGR2 and thus the degradation of 15-keto-PGE_2 in pancreatic cancer leads to suppressed cell proliferation and increased apoptosis in the pancreas (Chang et al., 2016), thus indicating that 15-keto-PGE_2,

but not the direct metabolite 13,14-dihydro-15-keto-PGE_2, has a suppressive effect on the proliferation of surrounding cells. Taken together, this indicates that, while it is of course possible that myeloid cells play a role in fine-tuning PGE_2 concentrations, T_{reg} cells seem to be the most important players in controlling local 15-keto-PGE_2 concentrations, thereby influencing T_{conv} cell activation and proliferation.

5.2. Role of Hpgd in VAT T_{reg} cells of aged animals

Subsequently, we analyzed the role of Hpgd in T_{reg} cells of the VAT, as the VAT is an organ rich in PGE_2. We found that Hpgd is significantly upregulated in T_{reg} cells of the VAT, both in comparison to T_{conv} cells and to other tissue resident T_{reg} cells. Thus, it might be interesting to analyze other PGE_2-rich tissues, such as the brain or tumor tissues. However, re-analysis of previously published datasets showed no differences in Hpgd expression either in human or murine tumor tissue T_{reg} cells compared to healthy tissues. When analyzing T_{reg} cells from the brain, we could not isolate a sufficient number to analyze Hpgd expression in T_{reg} cells under homeostatic conditions. Nevertheless, it might be interesting to analyze Hpgd expression in CNS-resident and infiltrating T_{reg} cells after e.g. EAE induction or viral challenges.

T_{reg} cells can be further classified into effector and naïve T_{reg} cells. Recently, effector T_{reg} cells have been implicated in tissue residency and in the maintenance of tissue homeostasis (Sharma and Rudra, 2018). Tissue-resident T_{reg} cells have been shown to further differentiate into effector T_{reg} cells by upregulating critical genes of the T_{reg} cell signature (Dias et al., 2017). Even though we did not analyze the expression level of effector T_{reg} cell markers in Hpgd-expressing VAT-resident T_{reg} cells, we postulate that the upregulation of Hpgd in VAT-resident T_{reg} cells occurs during the differentiation into tissue-resident effector T_{reg} cells. These Hpgd expressing T_{reg} cells make up a specific effector population, which probably originate from the spleen since recent findings show that a subpopulation of splenic T_{reg} cells already expresses Ppar-γ and functions as a precursor for VAT-resident effector T_{reg} cells (Li et al., 2018).

When analyzing the VAT of aged animals with Hpgd-deficient T_{reg} cells, we observed a significant increase in the VAT-resident T_{reg} cell population. We hypothesize that this increase is a compensatory effect to negate the loss of function caused by the deletion of Hpgd in T_{reg} cells. In line with this hypothesis, we could also detect an increase in the proinflammatory macrophage and NK-cell populations, while the corresponding populations

in the spleen remain unaltered. These observations are very similar to what one would expect in an animal subjected to HFD: an increase in inflammation and a deregulation of the immune-cell population in the VAT, such as an increase in NK cells (Lee et al., 2016; Wensveen et al., 2015b). Furthermore, this increase in macrophages has also been described in *ob/ob* mice, which serve as a model for T2D. In *ob/ob* mice, this increase could be reversed by expanding the T_{reg} cell population in the VAT by administering both anti-CD3 and β-glucosylceramide (Ilan et al., 2010). Moreover, increasing the VAT-resident T_{reg} cells also improved different metabolic parameters (Feuerer et al., 2009; Ilan et al., 2010). Conversely, a loss of VAT-resident T_{reg} cells has been previously shown to negatively impact different metabolic parameters, for instance fasting glucose levels and insulin sensitivity (Becker et al., 2017; Eller et al., 2011; Feuerer et al., 2009).

Thus, VAT-resident T_{reg} cells have been implicated in metabolic signaling. Our own findings were able to further validate the metabolic role of T_{reg} cells as a deletion of Hpgd and the consequent accumulation of non-functional T_{reg} cells in the VAT leads to worsened metabolic parameters, decreased insulin and glucose sensitivity as well as decreased insulin signaling and a decrease in the expression of INSR1 in aged animals. This spontaneous development of a metabolic syndrome can be explained by the increased accumulation of PGE_2, an important factor contributing to VAT homeostasis (García-Alonso et al., 2016). Normally, the Hpgd-expressing VAT-resident T_{reg} cell population metabolizes PGE_2 into the suppressive Ppar-γ ligand 15-keto-PGE_2 thus preventing adipose tissue inflammation. However, in the absence of a functional T_{reg} cell population, PGE_2 accumulation leads to increased inflammation and a dysregulation of the metabolism in these animals, thus further confirming the importance of Hpgd for the functionality of VAT-resident T_{reg} cells, as the deletion of the enzyme mirrors the effects of depleting T_{reg} cells from the VAT (Cipolletta et al., 2012).

Interestingly, while we could observe the spontaneous development of a metabolic syndrome in animals with Hpgd-deficient T_{reg} cells, resulting in a reduced insulin and glucose sensitivity, we could observe an increase in pAKT/AKT ratio in the liver and in muscle tissue of these animals in comparison to littermate control animals, indicating increased insulin signaling in these organs. Meanwhile, in the VAT and BAT of these animals we could observe a decrease in pAKT/AKT ratio, in line with the spontaneous development of a metabolic syndrome. These data are slightly incongruous as in the classical development of a

human metabolic syndrome, decreased muscle tissue insulin sensitivity has been shown to be one of the first detectable metabolic pathologies of the disease (Rabøl et al., 2011; Zhang and Liu, 2014). Thus, either the evolution of the metabolic syndrome in these animals differs from the development of T2D or the improved insulin signaling in muscle and liver are indicative of a compensatory mechanism.

5.3. Role of Hpgd in VAT T_{reg} cells in HFD challenged animals

In an attempt to challenge the metabolic state of these animals and to analyze the role of Hpgd in T_{reg} cells under non-homeostatic conditions, we subjected animals with Hpgd-deficient T_{reg} cells and WT littermate control animals to HFD feeding for 15 weeks. There was no difference in the composition of the VAT-resident immune-cell compartment between WT mice and mice with Hpgd-deficient T_{reg} cells after HFD feeding. While we do observe an increase in the T_{reg} cell population per gram of VAT, this difference could be explained by the difference in VAT weight rather than by a difference in the absolute number of T_{reg} cells. Furthermore, no difference in the macrophage population could be observed. This could be explained by the inherently pro-inflammatory state induced by subjecting animals to HFD. Through feeding of a HFD, we elicit a proinflammatory state in both WT and KO animals, thus possibly obfuscating the inherent difference in the inflammatory state of these animals.

Moreover, while we were able to detect a small decrease in insulin sensitivity in the deficient animals after 15 weeks of HFD feeding, this difference was much less pronounced than in the aged animals. This may be explained by the fact that HFD feeding worsens metabolic parameters also in WT animals (Ingvorsen et al., 2017) and thus the difference between KO and WT animals is decreased. Furthermore, while there does seem to be a trend in KO and WT animals after ND feeding, the decrease in insulin sensitivity in the KO animals is not statistically significant. This may be due to the relatively young age of the animals since under steady-state conditions we could only detect a difference in aged animals. It is possible that we would have observed a more pronounced difference in the metabolic state and the VAT-resident immune-cell compartment, had we prolonged the feeding until the animals reach around 40 weeks of age.

5.4. Intrinsic vs. extrinsic functionality of Hpgd

Loss of Hpgd in T_{reg} cells leads to a variety of different effects in aged animals, including a dysregulation of the metabolism and immune-cell homeostasis in the VAT, including an increase in the T_{reg} cell population and an upregulation of the proliferative

marker Ki-67. There are two different explanations for the effects observed: either the changes are intrinsic, i.e. the deletion of Hpgd in T_{reg} cells changes the T_{reg} cell transcriptional profile leading to decreased suppressive capacities and an increase in the proliferation of the cells, or extrinsic in nature and caused by the loss of the enzymatic activity of Hpgd.

However, these two modes of action are not mutually exclusive and have been previously described with other molecules of the T_{reg} cell signature. A deletion of the co-stimulatory molecule CD28 on T_{reg} cells was shown to induce both intrinsic and extrinsic defects in T_{reg} cell functionality. On the one hand, intrinsic CD28 signaling is vital to maintain the peripheral T_{reg} cell pool (Gogishvili et al., 2013) while on the other hand a deletion in CD28 affects the CD25 expression on T_{reg} cells (Tang et al., 2003), thus influencing T_{conv} cell IL-2 deprivation, one of the major methods through which T_{reg} cells confer suppressive capabilities, in an extrinsic manner.

When we analyzed the transcriptome of splenic T_{reg} cells, we could not detect a difference in the T_{reg} cell signature caused by the deletion of Hpgd in T_{reg} cells. Similarly, the VAT-resident T_{reg} cell signature remained unaffected by the loss of Hpgd, with the exception of a downregulation of Entdp1. Entdp1 is also known as CD39 and is the rate-limiting ecto-enzyme which hydrolyses the pro-inflammatory ATP into the anti-inflammatory derivate adenosine (Zhao et al., 2017), which has been described as an important suppressive mechanism in the plethora of T_{reg} cell suppressive mechanisms.. Thus, it is tempting to speculate that a downregulation of Entdp1 in VAT-resident T_{reg} cells caused by a deletion of Hpgd further impairs T_{reg} cell function and contributes to increased inflammation. However, these subtle changes in the VAT-resident T_{reg} cell signature did not affect either metabolic or immunological pathways, as shown by gene ontology enrichment analyses, thus indicating that a loss of Hpgd does not affect the cells intrinsically and that the observed effects are mainly caused by the loss of the enzymatic function of Hpgd.

Furthermore, when we analyzed the effect of a loss of Hpgd on the proliferation of adoptively transferred Hpgd-deficient and sufficient T_{reg} cells, we could not detect a difference in their proliferation, indicating that the increased T_{reg} cell population in the VAT of aged animals is not caused by an altered competitive fitness further indicating that the observed changes caused by the loss of Hpgd are extrinsic in nature.

5.5. Role of HPGD in T_{reg} cells of T2D patients

In human T2D patients, we found a dysregulation of the T_{reg} cell population in peripheral blood. In two microarray datasets, analyzed by linear support vector regression (SVR), the signature from the T_{reg} cell fraction was decreased in whole blood transcriptome data from T2D patients while in flow cytometric data we could observe an increased ratio of T_{reg} cells to T_{conv} cells in T2D patients compared to healthy control patients. However, this apparent incongruity can be explained by the two different analysis approaches: for the microarray datasets, we analyzed the T_{reg} cell fraction in comparison to the entire immune-cell compartment of the patients and could observe that most immune cell types were dysregulated in T2D patients compared to healthy individuals. Thus any changes observed are only relative changes within the immune cell compartment. Meanwhile, when analyzing the T_{reg} cell fraction by flow cytometry, we could observe an increase in the T_{reg} cell fraction, which was also reflected in murine Hpgd-deficient VAT-resident T_{reg} cells isolated from aged animals.

Further, we could show that the HPGD expression in T_{reg} cells isolated from T2D patients is significantly decreased compared to the HPGD level in T_{reg} cells isolated from healthy individuals in two distinct datasets. Considering that we could show that HPGD confers a more suppressive phenotype to T_{reg} cells, this indicates that T_{reg} cells of T2D are less immunosuppressive. This is compatible with the general proinflammatory phenotype of T2D patients (Donath and Shoelson, 2011) and seems to indicate that HPGD expression in T_{reg} cells might play a role in T2D. Moreover, T2D has been historically treated with anti-inflammatory drugs to ameliorate metabolic symptoms of the disease (Williamson, 1901; Yuan et al., 2001), thus showing that the disease progression may be affected by modulating T_{reg} cell functionality, for instance by augmenting HPGD levels. However, whether the downregulation of HPGD in T_{reg} cells of T2D patients is a cause or an effect of T2D remains unclear. It has been described that different signaling pathways are affected by the onset of T2D due to an alteration in, for example, glucose or insulin levels leading to global changes in the transcription profile in different cell types, including T_H cells (Ganeshan and Chawla, 2014; Hall et al., 2018). Furthermore, it has been shown that, in response to environments low in nutrients, Foxp3 can reprogram T_{reg} cells to adapt them to better utilize the available nutrients (Angelin et al., 2017). This indicates that FOXP3 signaling, which is upstream of HPGD, can be affected by a dysregulation of the cellular metabolism and could therefore lead to a decrease in HPGD levels caused by the development of T2D. Conversely, it has also been shown that FOXP3 is vital for metabolic homeostasis, as a FOXP3 mutation which does not

lead to any of the typical IPEX symptoms, caused neo-natal diabetes (Hwang et al., 2018). Thus, it is also credible that a dysregulation of the T_{reg} cell signature leading to a reduction in T_{reg} cell functionality could be one of the factors contributing to the development of T2D.

Another indication that increased HPGD levels may be beneficial in T2D is the observation that the activation of Ppar-γ signaling has been shown to increase insulin sensitization in mice (Cipolletta et al., 2012). Furthermore, treatment with Ppar-γ agonists has been shown to expand the VAT-resident T_{reg} cell population, thereby improving metabolic parameters and decreasing inflammation (Cipolletta et al., 2012). Furthermore, PPAR-γ agonists have been used to treat T2D (Savkur and Miller, 2006). Thus, increased T_{reg} cell HPGD levels, leading to an increased presence of 15-keto-PGE_2 and increased Ppar-γ signaling may be beneficial in combating metabolic dysregulation, such as T2D.

5.6. The role of MEOX1 in T_{reg} cells

In an effort to better understand the underlying transcriptional program of T_{reg} cells, we further analyzed the transcription factor MEOX1, which we could show to be upregulated in all T_{reg} cell conditions we analyzed in a similar manner to HPGD. Furthermore, MEOX1 and HPGD can be found in the same WGCNA module, suggesting a common mechanism of regulation. Indeed, both HPGD and MEOX1 are upregulated in response to IL-2 stimulation and both can be downregulated by an siRNA-mediated knock-down of FOXP3. Due to these commonalities in their regulation, we further attempted to analyze whether the transcription factor MEOX1 can influence HPGD expression. However, knocking down MEOX1 in an siRNA mediated manner did not influence HPGD or FOXP3 expression in human T_{reg} cells.

We therefore conclude that MEOX1 is not directly involved in the regulation of HPGD expression. However, it would be interesting to determine whether MEOX1 influences either T_{reg} cell functionality or the T_{reg} cell signature, since it has been previously published that while the transcription factor FOXP3 is lineage defining for T_{reg} cells and central for both T_{reg} cell functionality and transcription, it is not the sole factor responsible for T_{reg} cell differentiation (Ohkura et al., 2012; Sawant and Vignali, 2014). Furthermore, induction of FOXP3 expression is not sufficient to completely establish the T_{reg} cell signature and vice versa the T_{reg} cell signature can be partially induced even in the absence of FOXP3 (Hill et al., 2007; Lin et al., 2007). This is all indicative that there are other factors, next to FOXP3, which control T_{reg} cell differentiation and the T_{reg} cell signature, such as the genome organizer Satb1 (Beyer et al., 2011) or the transcription factors NFAT and Smad3 (Tone et al., 2008) .

MEOX1, in its role as a transcription factor which is significantly upregulated across most T_{reg} cell conditions, could play a role in this induction of the T_{reg} cell signature.

5.7. Model of HPGD action for the suppressive functionality of T_{reg} cells

All in all, we propose a new role for HPGD for T_{reg} cell dependent suppression of other immune cells in a tissue-specific manner: HPGD metabolizes PGE_2 into the PPAR-γ ligand 15-keto-PGE_2 which leads to the inhibition of T_{conv} cell activation which is at least partially mediated through PPAR-γ signaling. Furthermore, a T_{reg} cell specific deletion of Hpgd leads to increased visceral adipose tissue inflammation in aged animals, most likely caused by the loss of suppressive function in VAT T_{reg} cells. This increased inflammation is characterized by an accumulation of non-functional T_{reg} cells, NK cells and proinflammatory macrophages as well as a decrease in insulin and glucose sensitivity and an increased HOMA-IR (summarized in Figure 51). Thus, we could show that HPGD in T_{reg} cells is not only important for the suppressive function of T_{reg} cells but also for maintaining VAT homeostasis through the regulation of PGE_2 levels.

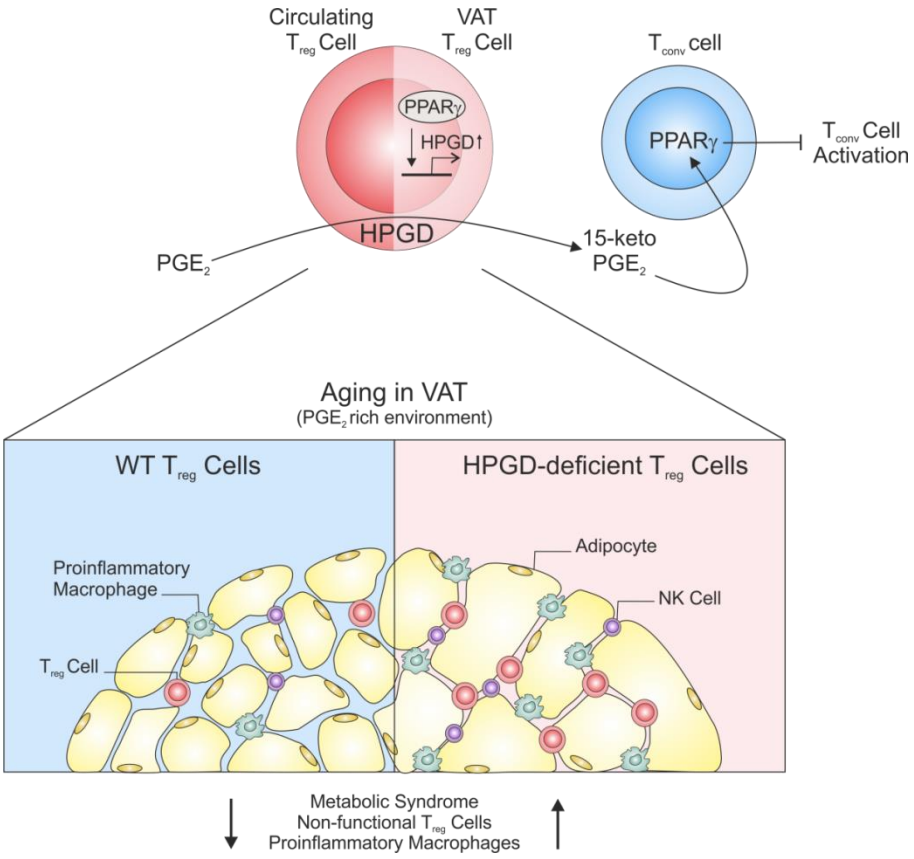

Figure 51: Model for the role of HPGD in T_{reg} cell mediated suppression.
Hpgd metabolizes PGE_2 into the suppressive metabolite 15-keto-PGE_2. A loss of murine Hpgd is implicated in the spontaneous development of a metabolic syndrome, an accumulation of VAT-resident T_{reg} cells and proinflammatory macrophages in aging animals.

6. References

Ahmadian, M., Suh, J.M., Hah, N., Liddle, C., Atkins, A.R., Downes, M., and Evans, R.M. (2013). PPARγ signaling and metabolism: the good, the bad and the future. Nat. Med. *19*, 557–566.

Ahnstedt, H., Roy-O'Reilly, M., Spychala, M.S., Mobley, A.S., Bravo-Alegria, J., Chauhan, A., Aronowski, J., Marrelli, S.P., and McCullough, L.D. (2018). Sex Differences in Adipose Tissue CD8+ T Cells and Regulatory T Cells in Middle-Aged Mice. Front. Immunol. *9*, 659.

Akiyama, T.E., Sakai, S., Lambert, G., Nicol, C.J., Matsusue, K., Pimprale, S., Lee, Y.-H., Ricote, M., Glass, C.K., Brewer, H.B., et al. (2002). Conditional disruption of the peroxisome proliferator-activated receptor gamma gene in mice results in lowered expression of ABCA1, ABCG1, and apoE in macrophages and reduced cholesterol efflux. Mol. Cell. Biol. *22*, 2607–2619.

Ali, N., and Rosenblum, M.D. (2017). Regulatory T cells in skin. Immunology *152*, 372–381.

Alonso, C.R. (2002). Hox proteins: sculpting body parts by activating localized cell death. Curr. Biol. *12*, R776-8.

Andersen, C.J., Murphy, K.E., and Fernandez, M.L. (2016). Impact of Obesity and Metabolic Syndrome on Immunity. Adv. Nutr. *7*, 66–75.

Angelin, A., Gil-de-Gómez, L., Dahiya, S., Jiao, J., Guo, L., Levine, M.H., Wang, Z., Quinn, W.J., Kopinski, P.K., Wang, L., et al. (2017). Foxp3 Reprograms T Cell Metabolism to Function in Low-Glucose, High-Lactate Environments. Cell Metab. *25*, 1282–1293.e7.

Anggård, E. (1966). The biological activities of three metabolites of prostaglandin E 1. Acta Physiol. Scand. *66*, 509–510.

Arima, K., Ohmuraya, M., Miyake, K., Koiwa, M., Uchihara, T., Izumi, D., Gao, F., Yonemura, A., Bu, L., Okabe, H., et al. (2019). Inhibition of 15-PGDH causes Kras-driven tumor expansion through prostaglandin E2-ALDH1 signaling in the pancreas. Oncogene *38*, 1211–1224.

Arosh, J.A., Banu, S.K., Kimmins, S., Chapdelaine, P., MacLaren, L.A., and Fortier, M.A. (2004a). Effect of Interferon-τ on Prostaglandin Biosynthesis, Transport, and Signaling at the Time of Maternal Recognition of Pregnancy in Cattle: Evidence of Polycrine Actions of Prostaglandin E_2. Endocrinology *145*, 5280–5293.

Arosh, J.A., Banu, S.K., Chapdelaine, P., Madore, E., Sirois, J., and Fortier, M.A. (2004b). Prostaglandin Biosynthesis, Transport, and Signaling in Corpus Luteum: A Basis for Autoregulation of Luteal Function. Endocrinology *145*, 2551–2560.

Asano, M., Toda, M., Sakaguchi, N., and Sakaguchi, S. (1996). Autoimmune disease as a consequence of developmental abnormality of a T cell subpopulation. J. Exp. Med. *184*, 387–396.

Asseman, C., Mauze, S., Leach, M.W., Coffman, R.L., and Powrie, F. (1999). An essential role for interleukin 10 in the function of regulatory T cells that inhibit intestinal inflammation. J. Exp. Med. *190*, 995–1004.

Asseman, C., Read, S., and Powrie, F. (2003). Colitogenic Th1 cells are present in the antigen-experienced T cell pool in normal mice: control by CD4+ regulatory T cells and IL-10. J. Immunol. *171*, 971–978.

Baeshen, N.A., Baeshen, M.N., Sheikh, A., Bora, R.S., Ahmed, M.M.M., Ramadan, H.A.I., Saini, K.S., and Redwan, E.M. (2014). Cell factories for insulin production. Microb. Cell Fact. *13*, 141.

Bapat, S.P., Myoung Suh, J., Fang, S., Liu, S., Zhang, Y., Cheng, A., Zhou, C., Liang, Y., LeBlanc, M., Liddle, C., et al. (2015). Depletion of fat-resident Treg cells prevents age-associated insulin resistance. Nature *528*, 137–141.

Baratelli, F., Lin, Y., Zhu, L., Yang, S.-C., Heuzé-Vourc'h, N., Zeng, G., Reckamp, K., Dohadwala, M., Sharma, S., and Dubinett, S.M. (2005). Prostaglandin E2 induces FOXP3 gene expression and T regulatory cell function in human CD4+ T cells. J. Immunol. *175*, 1483–1490.

Barbour, L.A., McCurdy, C.E., Hernandez, T.L., Kirwan, J.P., Catalano, P.M., and Friedman, J.E. (2007). Cellular Mechanisms for Insulin Resistance in Normal Pregnancy and Gestational Diabetes. Diabetes Care *30*, S112–S119.

Bartelt, A., and Heeren, J. (2014). Adipose tissue browning and metabolic health. Nat. Rev. Endocrinol. *10*, 24–36.

Barthlott, T., Moncrieffe, H., Veldhoen, M., Atkins, C.J., Christensen, J., O'Garra, A., and Stockinger, B. (2005). CD25+CD4+ T cells compete with naive CD4+ T cells for IL-2 and exploit it for the induction of IL-10 production. Int. Immunol. *17*, 279–288.

Bayrakli, F., Guclu, B., Yakicier, C., Balaban, H., Kartal, U., Erguner, B., Sagiroglu, M.S., Yuksel, S., Ozturk, A.R., Kazanci, B., et al. (2013). Mutation in MEOX1 gene causes a recessive Klippel-Feil syndrome subtype. BMC Genet. *14*, 95.

Becker, M., Levings, M.K., and Daniel, C. (2017). Adipose-tissue regulatory T cells: Critical players in adipose-immune crosstalk. Eur. J. Immunol. *47*, 1867–1874.

Bell-Parikh, L.C., Ide, T., Lawson, J.A., McNamara, P., Reilly, M., and FitzGerald, G.A. (2003). Biosynthesis of 15-deoxy-Δ(12,14)-PGJ(2) and the ligation of PPARγ. J. Clin. Invest. *112*, 945–955.

Bergholte, J.M., and Okita, R.T. (1986). Isolation and properties of lung 15-hydroxyprostaglandin dehydrogenase from pregnant rabbits. Arch. Biochem. Biophys. *245*, 308–315.

Bergstroem, S., Danielsson, H., and Samuelsson, B. (1964). The Enzymatic formation of prostaglandin E2 from Arachidonic acid prostaglandins and related factors. Biochim. Biophys. Acta *90*, 207–210.

von Bergwelt-Baildon, M.S., Popov, A., Saric, T., Chemnitz, J., Classen, S., Stoffel, M.S., Fiore, F., Roth, U., Beyer, M., Debey, S., et al. (2006). CD25 and indoleamine 2,3-dioxygenase are up-regulated by prostaglandin E2 and expressed by tumor-associated dendritic cells in vivo: additional mechanisms of T-cell inhibition. Blood *108*, 228–237.

Betz, M., and Fox, B.S. (1991). Prostaglandin E2 inhibits production of Th1 lymphokines but not of Th2 lymphokines. J. Immunol. *146*, 108–113.

Beyer, M., Thabet, Y., Muller, R.U., Sadlon, T., Classen, S., Lahl, K., Basu, S., Zhou, X., Bailey-Bucktrout, S.L., Krebs, W., et al. (2011). Repression of the genome organizer SATB1 in regulatory T cells is required for suppressive function and inhibition of effector differentiation. Nat Immunol *12*, 898–907.

Bhattacharya, M., Peri, K.G., Almazan, G., Ribeiro-da-Silva, A., Shichi, H., Durocher, Y., Abramovitz, M., Hou, X., Varma, D.R., and Chemtob, S. (1998). Nuclear localization of prostaglandin E2 receptors. Proc. Natl. Acad. Sci. *95*, 15792–15797.

Boniface, K., Bak-Jensen, K.S., Li, Y., Blumenschein, W.M., McGeachy, M.J., McClanahan, T.K., McKenzie, B.S., Kastelein, R.A., Cua, D.J., and de Waal Malefyt, R. (2009). Prostaglandin E2 regulates Th17 cell differentiation and function through cyclic AMP and EP2/EP4 receptor signaling. J Exp Med *206*, 535–548.

Bonilla, F.A., and Oettgen, H.C. (2010). Adaptive immunity. J. Allergy Clin. Immunol. *125*, S33–S40.

Bonneville, M., O'Brien, R.L., and Born, W.K. (2010). γδ T cell effector functions: a blend of innate programming and acquired plasticity. Nat. Rev. Immunol. *10*, 467–478.

Boord, J.B., Maeda, K., Makowski, L., Babaev, V.R., Fazio, S., Linton, M.F., and Hotamisligil, G.S. (2002). Adipocyte Fatty Acid–Binding Protein, aP2, Alters Late Atherosclerotic Lesion Formation in Severe Hypercholesterolemia. Arterioscler. Thromb. Vasc. Biol. *22*, 1686–1691.

Bopp, T., Becker, C., Klein, M., Klein-Hessling, S., Palmetshofer, A., Serfling, E., Heib, V., Becker, M., Kubach, J., Schmitt, S., et al. (2007). Cyclic adenosine monophosphate is a key component of regulatory T cell-mediated suppression. J Exp Med *204*, 1303–1310.

Boucher, J., Kleinridders, A., and Kahn, C.R. (2014). Insulin receptor signaling in normal and insulin-resistant states. Cold Spring Harb. Perspect. Biol. *6*.

Bouhlel, M.A., Derudas, B., Rigamonti, E., Dièvart, R., Brozek, J., Haulon, S., Zawadzki, C., Jude, B., Torpier, G., Marx, N., et al. (2007). PPARγ Activation Primes Human Monocytes into Alternative M2 Macrophages with Anti-inflammatory Properties. Cell Metab. *6*, 137–143.

Braithwaite, S.S., and Jarabak, J. (1975). Studies on a 15-hydroxyprostaglandin dehydrogenase from human placenta. Purification and partial characterization. J. Biol. Chem. *250*, 2315–2318.

Broere, F., Apasov, S.G., Sitkovsky, M. V., and van Eden, W. (2011). T cell subsets and T cell-mediated immunity. In Principles of Immunopharmacology, (Basel: Birkhäuser Basel), pp. 15–27.

Brubaker, S.W., Bonham, K.S., Zanoni, I., and Kagan, J.C. (2015). Innate Immune Pattern Recognition: A Cell Biological Perspective. Annu. Rev. Immunol. *33*, 257–290.

Brunkow, M.E., Jeffery, E.W., Hjerrild, K.A., Paeper, B., Clark, L.B., Yasayko, S.-A., Wilkinson, J.E., Galas, D., Ziegler, S.F., and Ramsdell, F. (2001). Disruption of a new forkhead/winged-helix protein, scurfin, results in the fatal lymphoproliferative disorder of the scurfy mouse. Nat. Genet. *27*, 68–73.

Bruun, J.M., Verdich, C., Toubro, S., Astrup, A., and Richelsen, B. (2003). Association between measures of insulin sensitivity and circulating levels of interleukin-8, interleukin-6 and tumor necrosis factor-alpha. Effect of weight loss in obese men. Eur. J. Endocrinol. *148*, 535–542.

Bryn, T., Yaqub, S., Mahic, M., Henjum, K., Aandahl, E.M., and Tasken, K. (2008). LPS-activated monocytes suppress T-cell immune responses and induce FOXP3+ T cells through a COX-2-PGE2-dependent mechanism. Int. Immunol. *20*, 235–245.

Buchanan, F.G., Gorden, D.L., Matta, P., Shi, Q., Matrisian, L.M., and DuBois, R.N. (2006). Role of β-arrestin 1 in the metastatic progression of colorectal cancer. Proc. Natl. Acad. Sci. *103*, 1492 LP-1497.

Burzyn, D., Kuswanto, W., Kolodin, D., Shadrach, J.L., Cerletti, M., Jang, Y., Sefik, E., Tan, T.G., Wagers, A.J., Benoist, C., et al. (2013). A Special Population of Regulatory T Cells Potentiates Muscle Repair. Cell *155*, 1282–1295.

Byun, S.-H., Lee, J.-H., Jung, N.-C., Choi, H.-J., Song, J.-Y., Seo, H.G., Choi, J., Jung, S.Y., Kang, S., Choi, Y.-S., et al. (2016). Rosiglitazone-mediated dendritic cells ameliorate collagen-induced arthritis in mice. Biochem. Pharmacol. *115*, 85–93.

Cao, X., Cai, S.F., Fehniger, T.A., Song, J., Collins, L.I., Piwnica-Worms, D.R., and Ley, T.J. (2007). Granzyme B and perforin are important for regulatory T cell-mediated suppression of tumor clearance. Immunity *27*, 635–646.

Castellino, F., and Germain, R.N. (2006). Cooperation between CD4 + and CD8 + T cells: When, Where, and How. Annu. Rev. Immunol. *24*, 519–540.

Challis, J.R.G., Patel, F.A., and Pomini, F. (1999). Prostaglandin dehydrogenase and the initiation of labor. J. Perinat. Med. *27*, 26–34.

Chang, E.Y.-C., Chang, Y.-C., Shun, C.-T., Tien, Y.-W., Tsai, S.-H., Hee, S.-W., Chen, I.-J., and Chuang, L.-M. (2016). Inhibition of Prostaglandin Reductase 2, a Putative Oncogene Overexpressed in Human Pancreatic Adenocarcinoma, Induces Oxidative Stress-Mediated Cell Death Involving xCT and CTH Gene Expressions through 15-Keto-PGE2. PLoS One *11*, e0147390.

Chang, W.C., Wu, H.L., Hsu, S.Y., and Chen, F.S. (1990). Isolation of rat renal NAD(+)-dependent 15-hydroxyprostaglandin dehydrogenase. Prostaglandins. Leukot. Essent. Fatty Acids *41*, 19–25.

Chassaing, B., Aitken, J.D., Malleshappa, M., and Vijay-Kumar, M. (2014). Dextran sulfate sodium (DSS)-induced colitis in mice. Curr. Protoc. Immunol. *104*, Unit 15.25.

Chemnitz, J.M., Driesen, J., Classen, S., Riley, J.L., Debey, S., Beyer, M., Popov, A., Zander, T., and Schultze, J.L. (2006). Prostaglandin E2 impairs CD4+ T cell activation by inhibition of lck: implications in Hodgkin's lymphoma. Cancer Res. *66*, 1114–1122.

Chou, W.-L.L., Chuang, L.-M.M., Chou ţ, C.-C., H-J Wang ţ, A., Lawson, J.A., FitzGerald, G.A., Chang, Z.-F.F., Chou, C.-C.C., Wang, A.H.-J.J., Lawson, J.A., et al. (2007). Identification of a novel prostaglandin reductase reveals the involvement of prostaglandin E2 catabolism in regulation of peroxisome proliferator-activated receptor gamma activation. J Biol Chem *282*, 18162–18172.

Cipolletta, D., Kolodin, D., Benoist, C., and Mathis, D. (2011). Tissular Tregs: A unique population of adipose-tissue-resident Foxp3+CD4+ T cells that impacts organismal metabolism. Semin. Immunol. *23*, 431–437.

Cipolletta, D., Feuerer, M., Li, A., Kamei, N., Lee, J., Shoelson, S.E., Benoist, C., and Mathis, D. (2012). PPAR-γ is a major driver of the accumulation and phenotype of adipose tissue Treg cells. Nature *486*, 549–553.

Cipolletta, D., Cohen, P., Spiegelman, B.M., Benoist, C., and Mathis, D. (2015). Appearance and disappearance of the mRNA signature characteristic of Treg cells in visceral adipose tissue: age, diet, and PPARγ effects. Proc. Natl. Acad. Sci. U. S. A. *112*, 482–487.

Coggins, K.G., Latour, A., Nguyen, M.S., Audoly, L., Coffman, T.M., and Koller, B.H. (2002). Metabolism of PGE2 by prostaglandin dehydrogenase is essential for remodeling the ductus arteriosus. Nat. Med. *8*, 91–92.

Collison, L.W., Workman, C.J., Kuo, T.T., Boyd, K., Wang, Y., Vignali, K.M., Cross, R., Sehy, D., Blumberg, R.S., and Vignali, D.A.A. (2007). The inhibitory cytokine IL-35 contributes to regulatory T-cell function. Nature *450*, 566–569.

Coombes, J.L., Robinson, N.J., Maloy, K.J., Uhlig, H.H., and Powrie, F. (2005). Regulatory T cells and intestinal homeostasis. Immunol. Rev. *204*, 184–194.

Dasu, M.R., Park, S., Devaraj, S., and Jialal, I. (2009). Pioglitazone Inhibits Toll-Like Receptor Expression and Activity in Human Monocytes and db/db Mice. Endocrinology *150*, 3457–3464.

Deaglio, S., Dwyer, K.M., Gao, W., Friedman, D., Usheva, A., Erat, A., Chen, J.-F.F., Enjyoji, K., Linden, J., Oukka, M., et al. (2007). Adenosine generation catalyzed by CD39 and CD73 expressed on regulatory T cells mediates immune suppression. J Exp Med *204*, 1257–1265.

DeFronzo, R.A., Ferrannini, E., Groop, L., Henry, R.R., Herman, W.H., Holst, J.J., Hu, F.B., Kahn, C.R., Raz, I., Shulman, G.I., et al. (2015). Type 2 diabetes mellitus. Nat. Rev. Dis. Prim. *1*, 15019.

Dias, S., D'Amico, A., Cretney, E., Liao, Y., Tellier, J., Bruggeman, C., Almeida, F.F., Leahy, J., Belz, G.T., Smyth, G.K., et al. (2017). Effector Regulatory T Cell Differentiation and Immune Homeostasis Depend on the Transcription Factor Myb. Immunity *46*, 78–91.

Dinarello, C.A. (2010). Anti-inflammatory Agents: Present and Future. Cell *140*, 935–950.

Donath, M.Y., and Shoelson, S.E. (2011). Type 2 diabetes as an inflammatory disease. Nat. Rev. Immunol.

Van Dorp, D., Beerthuis, R.K., Nugeteren, D.H., and Vonkeman, H. (1964). Enzymatic conversion of all cis-polyunsaturated fatty acids into prostaglandins. Nature *203*, 839–841.

Dustin, M.L., Tseng, S.-Y., Varma, R., and Campi, G. (2006). T cell–dendritic cell immunological synapses. Curr. Opin. Immunol. *18*, 512–516.

Eller, K., Kirsch, A., Wolf, A.M., Sopper, S., Tagwerker, A., Stanzl, U., Wolf, D., Patsch, W., Rosenkranz, A.R., and Eller, P. (2011). Potential Role of Regulatory T Cells in Reversing Obesity-Linked Insulin Resistance and Diabetic Nephropathy. Diabetes *60*, 2954–2962.

Eming, S.A., Werner, S., Bugnon, P., Wickenhauser, C., Siewe, L., Utermöhlen, O., Davidson, J.M., Krieg, T., and Roers, A. (2007). Accelerated wound closure in mice deficient for interleukin-10. Am. J. Pathol. *170*, 188–202.

Eruslanov, E., Kaliberov, S., Daurkin, I., Kaliberova, L., Buchsbaum, D., Vieweg, J., and Kusmartsev, S. (2009). Altered expression of 15-hydroxyprostaglandin dehydrogenase in tumor-infiltrated CD11b myeloid cells: a mechanism for immune evasion in cancer. J. Immunol. *182*, 7548–7557.

Fahlén, L., Read, S., Gorelik, L., Hurst, S.D., Coffman, R.L., Flavell, R.A., and Powrie, F. (2005). T cells that cannot respond to TGF-β escape control by $CD4^+$ $CD25^+$ regulatory T cells. J. Exp. Med. *201*, 737–746.

Fessler, J., Ficjan, A., Duftner, C., and Dejaco, C. (2013). The impact of aging on regulatory T-cells. Front. Immunol. *4*, 231.

Feuerer, M., Herrero, L., Cipolletta, D., Naaz, A., Wong, J., Nayer, A., Lee, J., Goldfine, A.B., Benoist, C., Shoelson, S., et al. (2009). Lean, but not obese, fat is enriched for a unique population of regulatory T cells that affect metabolic parameters. Nat Med *15*, 930–939.

Filion, F., Bouchard, N., Goff, A.K., Lussier, J.G., and Sirois, J. (2001). Molecular cloning and induction of bovine prostaglandin E synthase by gonadotropins in ovarian follicles prior to ovulation in vivo. J. Biol. Chem. *276*, 34323–34330.

Fitzpatrick, F.A., Aguirre, R., Pike, J.E., and Lincoln, F.H. (1980). The stability of 13,14-dihydro-15 keto-PGE2. Prostaglandins *19*, 917–931.

Fontenot, J.D., Gavin, M.A., and Rudensky, A.Y. (2003). Foxp3 programs the development and function of CD4+CD25+ regulatory T cells. Nat. Immunol. *4*, 330–336.

Forman, B.M., Tontonoz, P., Chen, J., Brun, R.P., Spiegelman, B.M., and Evans, R.M. (1995). 15-Deoxy-delta 12, 14-prostaglandin J2 is a ligand for the adipocyte determination factor PPAR gamma. Cell *83*, 803–812.

Franckaert, D., Dooley, J., Roos, E., Floess, S., Huehn, J., Luche, H., Fehling, H.J., Liston, A., Linterman, M.A., and Schlenner, S.M. (2015). Promiscuous Foxp3-cre activity reveals a differential requirement for CD28 in Foxp3+ and Foxp3- T cells. Immunol Cell Biol *93*, 417–423.

Franks, D.J., MacManus, J.P., and Whitfield, J.F. (1971). The effect of prostaglandins on cyclic AMP production and cell proliferation in thymic lymphocytes. Biochem. Biophys. Res. Commun. *44*, 1177–1183.

Frayn, K.N., Khan, K., Coppack, S.W., and Elia, M. (1991). Amino acid metabolism in human subcutaneous adipose tissue in vivo. Clin. Sci. (Lond). *80*, 471–474.

Fujino, H., Xu, W., and Regan, J.W. (2003). Prostaglandin E2 induced functional expression of early growth response factor-1 by EP4, but not EP2, prostanoid receptors via the phosphatidylinositol 3-kinase and extracellular signal-regulated kinases. J. Biol. Chem. *278*, 12151–12156.

Funk, C.D. (2001). Prostaglandins and leukotrienes: advances in eicosanoid biology. Science *294*, 1871–1875.

Furuhashi, M., Tuncman, G., Görgün, C.Z., Makowski, L., Atsumi, G., Vaillancourt, E., Kono, K., Babaev, V.R., Fazio, S., Linton, M.F., et al. (2007). Treatment of diabetes and atherosclerosis by inhibiting fatty-acid-binding protein aP2. Nature *447*, 959–965.

Futreal, P.A., Cochran, C., Rosenthal ', J., Mlkj, Y., Swenson, J., Hobbs ', M., Bennett, L.M., Haugen-Strano, A., Marks, J., Barrett, J.C., et al. (1994). Isolation of a diverged homeobox gene, M0X1, from the BRCA1 region on 17q21 by solution hybrid capture. Hum. Mol. Genet. *3*, 1359–1364.

Ganeshan, K., and Chawla, A. (2014). Metabolic regulation of immune responses. Annu. Rev. Immunol. *32*, 609–634.

García-Alonso, V., Titos, E., Alcaraz-Quiles, J., Rius, B., Lopategi, A., López-Vicario, C., Jakobsson, P.-J., Delgado, S., Lozano, J., and Clària, J. (2016). Prostaglandin E2 Exerts Multiple Regulatory Actions on Human Obese Adipose Tissue Remodeling, Inflammation, Adaptive Thermogenesis and Lipolysis. PLoS One *11*, e0153751.

Ge, Q., Bai, A., Jones, B., Eisen, H.N., and Chen, J. (2004). Competition for self-peptide-MHC complexes and cytokines between naive and memory CD8+ T cells expressing the same or different T cell receptors. Proc. Natl. Acad. Sci. U. S. A. *101*, 3041–3046.

Godfrey, D.I., MacDonald, H.R., Kronenberg, M., Smyth, M.J., and Kaer, L. Van (2004). NKT cells: what's in a name? Nat. Rev. Immunol. *4*, 231–237.

Godfrey, D.I., Stankovic, S., and Baxter, A.G. (2010). Raising the NKT cell family. Nat. Immunol. *11*, 197–206.

Godfrey, V.L., Wilkinson, J.E., Rinchik, E.M., and Russell, L.B. (1991). Fatal lymphoreticular disease in the scurfy (sf) mouse requires T cells that mature in a sf thymic environment: potential model for thymic education. Proc. Natl. Acad. Sci. U. S. A. *88*, 5528–5532.

Gogishvili, T., Lühder, F., Goebbels, S., Beer-Hammer, S., Pfeffer, K., and Hünig, T. (2013). Cell-intrinsic and -extrinsic control of Treg-cell homeostasis and function revealed by induced *CD28* deletion. Eur. J. Immunol. *43*, 188–193.

Hall, E., Dekker Nitert, M., Volkov, P., Malmgren, S., Mulder, H., Bacos, K., and Ling, C. (2018). The effects of high glucose exposure on global gene expression and DNA methylation in human pancreatic islets. Mol. Cell. Endocrinol. *472*, 57–67.

Heng, T.S.P., Painter, M.W., Elpek, K., Lukacs-Kornek, V., Mauermann, N., Turley, S.J., Koller, D., Kim, F.S., Wagers, A.J., Asinovski, N., et al. (2008). The Immunological Genome Project: networks of gene expression in immune cells. Nat. Immunol. *9*, 1091–1094.

Hétu, P.-O., Riendeau, D., Hetu, P.O., and Riendeau, D. (2007). Down-regulation of microsomal prostaglandin E2 synthase-1 in adipose tissue by high-fat feeding. Obes. (Silver Spring) *15*, 60–68.

Hill, J.A., Feuerer, M., Tash, K., Haxhinasto, S., Perez, J., Melamed, R., Mathis, D., and Benoist, C. (2007). Foxp3 transcription-factor-dependent and -independent regulation of the regulatory T cell transcriptional signature. Immunity *27*, 786–800.

Hoffman, W., Lakkis, F.G., and Chalasani, G. (2016). B Cells, Antibodies, and More. Clin. J. Am. Soc. Nephrol. *11*, 137–154.

Honda, T., Segi-Nishida, E., Miyachi, Y., and Narumiya, S. (2006). Prostacyclin-IP signaling and prostaglandin E2-EP2/EP4 signaling both mediate joint inflammation in mouse collagen-induced arthritis. J. Exp. Med. *203*, 325–335.

Hori, S., Nomura, T., and Sakaguchi, S. (2003). Control of Regulatory T Cell Development by the Transcription Factor Foxp3. Science (80-.). *299*, 1057–1061.

Hotamisligil, G.S., Johnson, R.S., Distel, R.J., Ellis, R., Papaioannou, V.E., and Spiegelman, B.M. (1996). Uncoupling of obesity from insulin resistance through a targeted mutation in aP2, the adipocyte fatty acid binding protein. Science *274*, 1377–1379.

Hu, F.B., Manson, J.E., Stampfer, M.J., Colditz, G., Liu, S., Solomon, C.G., and Willett, W.C. (2001). Diet, Lifestyle, and the Risk of Type 2 Diabetes Mellitus in Women. N. Engl. J. Med. *345*, 790–797.

Huang, C.-T.T., Workman, C.J., Flies, D., Pan, X., Marson, A.L., Zhou, G., Hipkiss, E.L., Ravi, S., Kowalski, J., Levitsky, H.I., et al. (2004). Role of LAG-3 in regulatory T cells. Immunity *21*, 503–513.

Huh, J.Y., Park, Y.J., Ham, M., and Kim, J.B. (2014). Crosstalk between adipocytes and immune cells in adipose tissue inflammation and metabolic dysregulation in obesity. Mol. Cells *37*, 365–371.

Huynh, A., DuPage, M., Priyadharshini, B., Sage, P.T., Quiros, J., Borges, C.M., Townamchai, N., Gerriets, V.A., Rathmell, J.C., Sharpe, A.H., et al. (2015). Control of PI(3) kinase in Treg cells maintains homeostasis and lineage stability. Nat Immunol *16*, 188–196.

Hwang, J.L., Park, S.-Y., Ye, H., Sanyoura, M., Pastore, A.N., Carmody, D., del Gaudio, D., Wilson, J.F., Hanis, C.L., Liu, X., et al. (2018). *FOXP3* mutations causing early-onset insulin-requiring diabetes but without other features of immune dysregulation, polyendocrinopathy, enteropathy, X-linked syndrome. Pediatr. Diabetes *19*, 388–392.

Ilan, Y., Maron, R., Tukpah, A.-M., Maioli, T.U., Murugaiyan, G., Yang, K., Wu, H.Y., and Weiner, H.L. (2010). Induction of regulatory T cells decreases adipose inflammation and alleviates insulin resistance in ob/ob mice. Proc. Natl. Acad. Sci. U. S. A. *107*, 9765–9770.

Ingvorsen, C., Karp, N.A., and Lelliott, C.J. (2017). The role of sex and body weight on the metabolic effects of high-fat diet in C57BL/6N mice. Nutr. Diabetes *7*, e261.

Izcue, A., Coombes, J.L., and Powrie, F. (2006). Regulatory T cells suppress systemic and mucosal immune activation to control intestinal inflammation. Immunol. Rev. *212*, 256–271.

Janssens, W., Carlier, V., Wu, B., VanderElst, L., Jacquemin, M.G., and Saint-Remy, J.-M.R. (2003). CD4+CD25+ T cells lyse antigen-presenting B cells by Fas-Fas ligand interaction in an epitope-specific manner. J. Immunol. *171*, 4604–4612.

Jiang, C., Ting, A.T., and Seed, B. (1998). PPAR-γ agonists inhibit production of monocyte inflammatory cytokines. Nature *391*, 82–86.

Kahn, C.R. (1994). Banting Lecture. Insulin action, diabetogenes, and the cause of type II diabetes. Diabetes *43*, 1066–1084.

Kampmann, U., Madsen, L.R., Skajaa, G.O., Iversen, D.S., Moeller, N., and Ovesen, P. (2015). Gestational diabetes: A clinical update. World J. Diabetes *6*, 1065–1072.

Kang, J., Chapdelaine, P., Parent, J., Madore, E., Laberge, P.Y., and Fortier, M.A. (2005). Expression of Human Prostaglandin Transporter in the Human Endometrium across the Menstrual Cycle. J. Clin. Endocrinol. Metab. *90*, 2308–2313.

Kasuga, M., Zick, Y., Blithe, D.L., Crettaz, M., and Kahn, C.R. (1982). Insulin stimulates tyrosine phosphorylation of the insulin receptor in a cell-free system. Nature *298*, 667–669.

Katsarou, A., Gudbjörnsdottir, S., Rawshani, A., Dabelea, D., Bonifacio, E., Anderson, B.J., Jacobsen, L.M., Schatz, D.A., and Lernmark, Å. (2017). Type 1 diabetes mellitus. Nat. Rev. Dis. Prim. *3*, 17016.

Kawahara, K., Hohjoh, H., Inazumi, T., Tsuchiya, S., and Sugimoto, Y. (2015). Prostaglandin E2-induced inflammation: Relevance of prostaglandin E receptors. Biochim. Biophys. Acta - Mol. Cell Biol. Lipids *1851*, 414–421.

Kishore, A.H., Liang, H., Kanchwala, M., Xing, C., Ganesh, T., Akgul, Y., Posner, B., Ready, J.M., Markowitz, S.D., and Word, R.A. (2017). Prostaglandin dehydrogenase is a target for successful induction of cervical ripening. Proc. Natl. Acad. Sci. *114*, E6427–E6436.

Kolodin, D., van Panhuys, N., Li, C., Magnuson, A.M., Cipolletta, D., Miller, C.M., Wagers, A., Germain, R.N., Benoist, C., and Mathis, D. (2015). Antigen- and cytokine-driven accumulation of regulatory T cells in visceral adipose tissue of lean mice. Cell Metab *21*, 543–557.

Kornete, M., Mason, E.S., and Piccirillo, C.A. (2013). Immune Regulation in T1D and T2D: Prospective Role of Foxp3+ Treg Cells in Disease Pathogenesis and Treatment. Front. Endocrinol. (Lausanne). *4*, 76.

Krook, M., Ghosht, D., Strdmbergt, R., Carlquist, M., J4, H., and Rnvall,) (1993). Carboxyethyllysine in a protein: Native carbonyl reductase/NADP+- dependent prostaglandin dehydrogenase (multiplicity reductive alkylation/pyruvate/short-chan debydrogenase). *90*, 502–506.

Kullberg, M.C., Hay, V., Cheever, A.W., Mamura, M., Sher, A., Letterio, J.J., Shevach, E.M., and Piccirillo, C.A. (2005). TGF-β1 production by CD4+CD25+ regulatory T cells is not essential for suppression of intestinal inflammation. Eur. J. Immunol. *35*, 2886–2895.

de la Rosa, M., Rutz, S., Dorninger, H., and Scheffold, A. (2004). Interleukin-2 is essential for CD4+CD25+ regulatory T cell function. Eur. J. Immunol. *34*, 2480–2488.

Lacroix, A., Toussay, X., Anenberg, E., Lecrux, C., Ferreirós, N., Karagiannis, A., Plaisier, F., Chausson, P., Jarlier, F., Burgess, S.A., et al. (2015). COX-2-Derived Prostaglandin E2 Produced by Pyramidal Neurons Contributes to Neurovascular Coupling in the Rodent Cerebral Cortex. J. Neurosci. *35*, 11791–11810.

Lages, C.S., Suffia, I., Velilla, P.A., Huang, B., Warshaw, G., Hildeman, D.A., Belkaid, Y., and Chougnet, C. (2008). Functional regulatory T cells accumulate in aged hosts and promote chronic infectious disease reactivation. J. Immunol. *181*, 1835–1848.

Lalier, L., Cartron, P.-F., Olivier, C., Logé, C., Bougras, G., Robert, J.-M., Oliver, L., and Vallette, F.M. (2011). Prostaglandins antagonistically control Bax activation during apoptosis. Cell Death Differ. *18*, 528–537.

Lawand, M., Déchanet-Merville, J., and Dieu-Nosjean, M.-C. (2017). Key Features of Gamma-Delta T-Cell Subsets in Human Diseases and Their Immunotherapeutic Implications. Front. Immunol. *8*, 761.

Lee, S.C., and Levine, L. (1975). Prostaglandin metabolism. II. Identification of two 15-hydroxyprostaglandin dehydrogenase types. J. Biol. Chem. *250*, 548–552.

Lee, B.-C., Kim, M.-S., Pae, M., Yamamoto, Y., Eberlé, D., Shimada, T., Kamei, N., Park, H.-S., Sasorith, S., Woo, J.R., et al. (2016). Adipose Natural Killer Cells Regulate Adipose Tissue Macrophages to Promote Insulin Resistance in Obesity. Cell Metab. 685–698.

Lee, P.P., Fitzpatrick, D.R., Beard, C., Jessup, H.K., Lehar, S., Makar, K.W., Pérez-Melgosa, M., Sweetser, M.T., Schlissel, M.S., Nguyen, S., et al. (2001). A Critical Role for Dnmt1 and DNA Methylation in T Cell Development, Function, and Survival. Immunity *15*, 763–774.

Legler, D.F., Bruckner, M., Uetz-von Allmen, E., and Krause, P. (2010). Prostaglandin E2 at new glance: Novel insights in functional diversity offer therapeutic chances. Int. J. Biochem. Cell Biol. *42*, 198–201.

Lehmann, J.M., Moore, L.B., Smith-Oliver, T.A., Wilkison, W.O., Willson, T.M., and Kliewer, S.A. (1995). An antidiabetic thiazolidinedione is a high affinity ligand for peroxisome proliferator-activated receptor gamma (PPAR gamma). J. Biol. Chem. *270*, 12953–12956.

Li, C., DiSpirito, J.R., Zemmour, D., Spallanzani, R.G., Kuswanto, W., Benoist, C., and Mathis, D. (2018). TCR Transgenic Mice Reveal Stepwise, Multi-site Acquisition of the Distinctive Fat-Treg Phenotype. Cell *174*, 285–299.e12.

Li, H., Chen, H.-Y., Liu, W.-X., Jia, X.-X., Zhang, J.-G., Ma, C.-L., Zhang, X.-J., Yu, F., and Cong, B. (2017). Prostaglandin E 2 restrains human Treg cell differentiation via E prostanoid receptor 2-protein kinase A signaling. Immunol. Lett. *191*, 63–72.

Li, M.O., Wan, Y.Y., Sanjabi, S., Robertson, A.-K.L., and Flavell, R.A. (2005). Transforming Growth Factor-B Regulation of Immune Responses. Annu. Rev. Immunol. *24*, 99–146.

Lin, C.-F., Young, K.-C., Bai, C.-H., Yu, B.-C., Ma, C.-T., Chien, Y.-C., Chiang, C.-L., Liao, C.-S., Lai, H.-W., and Tsao, C.-W. (2014). Rosiglitazone Regulates Anti-Inflammation and Growth Inhibition via PTEN. Biomed Res. Int. *2014*, 1–14.

Lin, W., Haribhai, D., Relland, L.M., Truong, N., Carlson, M.R., Williams, C.B., and Chatila, T.A. (2007). Regulatory T cell development in the absence of functional Foxp3. Nat. Immunol. *8*, 359–368.

Lombardi, A., Cantini, G., Piscitelli, E., Gelmini, S., Francalanci, M., Mello, T., Ceni, E., Varano, G., Forti, G., Rotondi, M., et al. (2008). A New Mechanism Involving ERK Contributes to Rosiglitazone Inhibition of Tumor Necrosis Factor- and Interferon- Inflammatory Effects in Human Endothelial Cells. Arterioscler. Thromb. Vasc. Biol. *28*, 718–724.

Lu, D., Han, C., and Wu, T. (2014). 15-PGDH inhibits hepatocellular carcinoma growth through 15-keto-PGE2/PPARγ-mediated activation of p21WAF1/Cip1. Oncogene *33*, 1101–1112.

Luckheeram, R.V., Zhou, R., Verma, A.D., and Xia, B. (2012). $CD4^+$T cells: differentiation and functions. Clin. Dev. Immunol. *2012*, 925135.

Luo, Y., Yin, W., Signore, A.P., Zhang, F., Hong, Z., Wang, S., Graham, S.H., and Chen, J. (2006). Neuroprotection against focal ischemic brain injury by the peroxisome proliferator-activated receptor-γ agonist rosiglitazone. J. Neurochem. *97*, 435–448.

Luu, M., Steinhoff, U., and Visekruna, A. (2017). Functional heterogeneity of gut-resident regulatory T cells. Clin. Transl. Immunol. *6*, e156.

Maddox, J.F., and Serhan, C.N. (1996). Lipoxin A4 and B4 are potent stimuli for human monocyte migration and adhesion: selective inactivation by dehydrogenation and reduction. J. Exp. Med. *183*, 137–146.

Maeda, K., Cao, H., Kono, K., Gorgun, C.Z., Furuhashi, M., Uysal, K.T., Cao, Q., Atsumi, G., Malone, H., Krishnan, B., et al. (2005). Adipocyte/macrophage fatty acid binding proteins control integrated metabolic responses in obesity and diabetes. Cell Metab. *1*, 107–119.

Makowski, L., Boord, J.B., Maeda, K., Babaev, V.R., Uysal, K.T., Morgan, M.A., Parker, R.A., Suttles, J., Fazio, S., Hotamisligil, G.S., et al. (2001). Lack of macrophage fatty-acid-binding protein aP2 protects mice deficient in apolipoprotein E against atherosclerosis. Nat. Med. *7*, 699–705.

Mannie, M.D., Prevost, K.D., and Marinakis, C.A. (1995). Prostaglandin E2 promotes the induction of anergy during T helper cell recognition of myelin basic protein. Cell. Immunol. *160*, 132–138.

Miceli, M.C., and Parnes, J.R. (1991). The roles of CD4 and CD8 in T cell activation. Semin. Immunol. *3*, 133–141.

Michalek, R.D., Gerriets, V.A., Jacobs, S.R., Macintyre, A.N., MacIver, N.J., Mason, E.F., Sullivan, S.A., Nichols, A.G., and Rathmell, J.C. (2011). Cutting edge: distinct glycolytic and lipid oxidative metabolic programs are essential for effector and regulatory CD4+ T cell subsets. J. Immunol. *186*, 3299–3303.

Mills, D.M., and Cambier, J.C. (2003). B lymphocyte activation during cognate interactions with CD4+ T lymphocytes: molecular dynamics and immunologic consequences. Semin. Immunol. *15*, 325–329.

Mohamed, J.Y., Faqeih, E., Alsiddiky, A., Alshammari, M.J., Ibrahim, N.A., and Alkuraya, F.S. (2013). Mutations in MEOX1, encoding mesenchyme homeobox 1, cause Klippel-Feil anomaly. Am. J. Hum. Genet. *92*, 157–161.

Myung, S.-J., Rerko, R.M., Yan, M., Platzer, P., Guda, K., Dotson, A., Lawrence, E., Dannenberg, A.J., Lovgren, A.K., Luo, G., et al. (2006). 15-Hydroxyprostaglandin dehydrogenase is an in vivo suppressor of colon tumorigenesis. Proc. Natl. Acad. Sci. U. S. A. *103*, 12098–12102.

Nakamura, K., Kitani, A., and Strober, W. (2001). Cell contact-dependent immunosuppression by CD4(+)CD25(+) regulatory T cells is mediated by cell surface-bound transforming growth factor beta. J Exp Med *194*, 629–644.

Narumiya, S. (1994). Prostanoid Receptors: Structure, Function and Distribution. Ann. N. Y. Acad. Sci. *744*, 126–138.

NCD Risk Factor Collaboration (NCD-RisC), N.R.F.C. (2016). Worldwide trends in diabetes since 1980: a pooled analysis of 751 population-based studies with 4.4 million participants. Lancet (London, England) *387*, 1513–1530.

Newman, A.M., Liu, C.L., Green, M.R., Gentles, A.J., Feng, W., Xu, Y., Hoang, C.D., Diehn, M., and Alizadeh, A.A. (2015). Robust enumeration of cell subsets from tissue expression profiles. Nat Methods *12*, 453–457.

NIH (2011). Guide for the Care and Use of Laboratory Animals (National Academies Press (US)).

Nolte, R.T., Wisely, G.B., Westin, S., Cobb, J.E., Lambert, M.H., Kurokawa, R., Rosenfeld, M.G., Willson, T.M., Glass, C.K., and Milburn, M. V. (1998). Ligand binding and co-activator assembly of the peroxisome proliferator-activated receptor-γ. Nature *395*, 137–143.

Ohkura, N., Hamaguchi, M., Morikawa, H., Sugimura, K., Tanaka, A., Ito, Y., Osaki, M., Tanaka, Y., Yamashita, R., Nakano, N., et al. (2012). T Cell Receptor Stimulation-Induced Epigenetic Changes and Foxp3 Expression Are Independent and Complementary Events Required for Treg Cell Development. Immunity *37*, 785–799.

Olokoba, A.B., Obateru, O.A., and Olokoba, L.B. (2012). Type 2 diabetes mellitus: a review of current trends. Oman Med. J. *27*, 269–273.

Omori, K., Kida, T., Hori, M., Ozaki, H., and Murata, T. (2014). Multiple roles of the PGE2 -EP receptor signal in vascular permeability. Br. J. Pharmacol. *171*, 4879–4889.

Ostanin, D. V, Bao, J., Koboziev, I., Gray, L., Robinson-Jackson, S.A., Kosloski-Davidson, M., Price, V.H., and Grisham, M.B. (2009). T cell transfer model of chronic colitis: concepts, considerations, and tricks of the trade. Am. J. Physiol. Gastrointest. Liver Physiol. *296*, G135-46.

Padilla, J., Leung, E., and Phipps, R.P. (2002). Human B Lymphocytes and B Lymphomas Express PPAR-γ and Are Killed by PPAR-γ Agonists. Clin. Immunol. *103*, 22–33.

Pandiyan, P., Zheng, L., Ishihara, S., Reed, J., and Lenardo, M.J. (2007). CD4+CD25+Foxp3+ regulatory T cells induce cytokine deprivation-mediated apoptosis of effector CD4+ T cells. Nat Immunol *8*, 1353–1362.

Papiernik, M., do Carmo Leite-de-MoraesM, T., Pontoux, C., Joret, A.M., Rocha, B., Penit, C., and Dy, M. (1997). T cell deletion induced by chronic infection with mouse mammary tumor virus spares a CD25-positive, IL-10-producing T cell population with infectious capacity. J. Immunol. *158*, 4642–4653.

Parent, M., Madore, E., MacLaren, L.A., and Fortier, M.A. (2006). 15-Hydroxyprostaglandin dehydrogenase in the bovine endometrium during the oestrous cycle and early pregnancy. *131*, 573–582.

Parkin, J., and Cohen, B. (2001). An overview of the immune system. Lancet *357*, 1777–1789.

Pettersson, U.S., Waldén, T.B., Carlsson, P.-O., Jansson, L., and Phillipson, M. (2012). Female Mice are Protected against High-Fat Diet Induced Metabolic Syndrome and Increase the Regulatory T Cell Population in Adipose Tissue. PLoS One *7*, e46057.

Phipps, R.P., Stein, S.H., and Roper, R.L. (1991). A new view of prostaglandin E regulation of the immune response. Immunol. Today *12*, 349–352.

Picelli, S., Björklund, Å.K., Faridani, O.R., Sagasser, S., Winberg, G., and Sandberg, R. (2013). Smart-seq2 for sensitive full-length transcriptome profiling in single cells. Nat. Methods *10*, 1096–1098.

Powrie, F., Carlino, J., Leach, M.W., Mauze, S., and Coffman, R.L. (1996). A critical role for transforming growth factor-beta but not interleukin 4 in the suppression of T helper type 1-mediated colitis by CD45RB(low) CD4+ T cells. J. Exp. Med. *183*, 2669–2674.

Rabøl, R., Petersen, K.F., Dufour, S., Flannery, C., and Shulman, G.I. (2011). Reversal of muscle insulin resistance with exercise reduces postprandial hepatic de novo lipogenesis in insulin resistant individuals. Proc. Natl. Acad. Sci. U. S. A. *108*, 13705–13709.

Raynor, J., Lages, C.S., Shehata, H., Hildeman, D.A., and Chougnet, C.A. (2012). Homeostasis and function of regulatory T cells in aging. Curr. Opin. Immunol. *24*, 482–487.

Regan, J.W. (2003). EP2 and EP4 prostanoid receptor signaling. Life Sci. *74*, 143–153.

Reinhardt, R.L., Kang, S.-J., Liang, H.-E., and Locksley, R.M. (2006). T helper cell effector fates — who, how and where? Curr. Opin. Immunol. *18*, 271–277.

Ricciotti, E., and FitzGerald, G.A. (2011). Prostaglandins and inflammation. Arterioscler. Thromb. Vasc. Biol. *31*, 986–1000.

Roizen, J.D., Asada, M., Tong, M., Tai, H.-H.H., and Muglia, L.J. (2008). Preterm birth without progesterone withdrawal in 15-hydroxyprostaglandin dehydrogenase hypomorphic mice. Mol Endocrinol *22*, 105–112.

Rubtsov, Y.P., Rasmussen, J.P., Chi, E.Y., Fontenot, J., Castelli, L., Ye, X., Treuting, P., Siewe, L., Roers, A., Henderson, W.R., et al. (2008). Regulatory T Cell-Derived Interleukin-10 Limits Inflammation at Environmental Interfaces. Immunity *28*, 546–558.

Sakaguchi, S., Sakaguchi, N., Asano, M., Itoh, M., and Toda, M. (1995). Immunologic self-tolerance maintained by activated T cells expressing IL-2 receptor alpha-chains (CD25). Breakdown of a single mechanism of self-tolerance causes various autoimmune diseases. J. Immunol. *155*, 1151–1164.

Saltiel, A.R., and Kahn, C.R. (2001). Insulin signalling and the regulation of glucose and lipid metabolism. Nature *414*, 799–806.

Samuelsson, B. (1964). Prostaglandin and related factors. 28. Metabolism of Prostaglandin E1 in Guinea Pig Lung: The structures of two metabolites. J. Biol. Chem. *239*, 4097–4102.

Sather, B.D., Treuting, P., Perdue, N., Miazgowicz, M., Fontenot, J.D., Rudensky, A.Y., and Campbell, D.J. (2007). Altering the distribution of Foxp3 $^{+}$ regulatory T cells results in tissue-specific inflammatory disease. J. Exp. Med. *204*, 1335–1347.

Savkur, R.S., and Miller, A.R. (2006). Investigational PPAR-γ agonists for the treatment of Type 2 diabetes. Expert Opin. Investig. Drugs *15*, 763–778.

Sawant, D. V, and Vignali, D.A.A. (2014). Once a Treg, always a Treg? Immunol. Rev. *259*, 173–191.

Schindelin, J., Arganda-Carreras, I., Frise, E., Kaynig, V., Longair, M., Pietzsch, T., Preibisch, S., Rueden, C., Saalfeld, S., Schmid, B., et al. (2012). Fiji: an open-source platform for biological-image analysis. Nat. Methods *9*, 676–682.

Schmidt, S., Moric, E., Schmidt, M., Sastre, M., Feinstein, D.L., and Heneka, M.T. (2004). Anti-inflammatory and antiproliferative actions of PPAR-γ agonists on T lymphocytes derived from MS patients. J. Leukoc. Biol. *75*, 478–485.

Schmitz, K., de Bruin, N., Bishay, P., Männich, J., Häussler, A., Altmann, C., Ferreirós, N., Lötsch, J., Ultsch, A., Parnham, M.J., et al. (2014). R-flurbiprofen attenuates experimental autoimmune encephalomyelitis in mice. EMBO Mol Med *6*, 1398–1422.

Schönfeld, E.A. (2011). Characterization of the role of Hydroxyprostaglandin dehydrogenase 15- (NAD) in human regulatory T cells. Rheinische Friedrich-Wilhelms-Universität Bonn.

Schubert, M., Brazil, D.P., Burks, D.J., Kushner, J.A., Ye, J., Flint, C.L., Farhang-Fallah, J., Dikkes, P., Warot, X.M., Rio, C., et al. (2003). Insulin receptor substrate-2 deficiency impairs brain growth and promotes tau phosphorylation. J. Neurosci. *23*, 7084–7092.

Schupp, M., and Lazar, M. a (2010). Endogenous ligands for nuclear receptors: digging deeper. J. Biol. Chem. *285*, 40409–40415.

Sharma, A., and Rudra, D. (2018). Emerging Functions of Regulatory T Cells in Tissue Homeostasis. Front. Immunol. *9*, 883.

Sharma, R., Sung, S.J., Fu, S.M., and Ju, S.-T. (2009). Regulation of multi-organ inflammation in the regulatory T cell-deficient scurfy mice. J. Biomed. Sci. *16*, 20.

Sharma, S., Yang, S.C., Zhu, L., Reckamp, K., Gardner, B., Baratelli, F., Huang, M., Batra, R.K., and Dubinett, S.M. (2005). Tumor cyclooxygenase-2/prostaglandin E2-dependent promotion of FOXP3 expression and CD4+CD25+ T regulatory cell activities in lung cancer. Cancer Res. *65*, 5211–5220.

Sheng, M.H.C., Lau, K.H.W., and Baylink, D.J. (2014). Role of Osteocyte-derived Insulin-Like Growth Factor I in Developmental Growth, Modeling, Remodeling, and Regeneration of the Bone. J. Bone Metab. *21*, 41–54.

Shinkai, Y., Rathbun, 0Gary, Lam, K.-P., Oltz, E.M., Stewart, V., Mendelsohn, M., Charron, J., Datta, M., Young, F., Stall, A.M., et al. (1992). RAG-2-deficient mice lack mature lymphocytes owing to inability to initiate V(D)J rearrangement. Cell *68*, 855–867.

Shrestha, S., Yang, K., Guy, C., Vogel, P., Neale, G., and Chi, H. (2015). Treg cells require the phosphatase PTEN to restrain TH1 and TFH cell responses. Nat Immunol *16*, 178–187.

Simmons, D.L., Botting, R.M., and Hla, T. (2004). Cyclooxygenase isozymes: the biology of prostaglandin synthesis and inhibition. Pharmacol. Rev. *56*, 387–437.

Singh, U., and Owen, J.J. (1975). Studies on the effect of various agents on the maturation of thymus stem cells. Eur. J. Immunol. *5*, 286–288.

Sojka, D.K., Hughson, A., Sukiennicki, T.L., and Fowell, D.J. (2005). Early kinetic window of target T cell susceptibility to CD25+ regulatory T cell activity. J. Immunol. *175*, 7274–7280.

Sojka, D.K., Huang, Y.-H., and Fowell, D.J. (2008). Mechanisms of regulatory T-cell suppression - a diverse arsenal for a moving target. Immunology *124*, 13–22.

Sreeramkumar, V., Fresno, M., and Cuesta, N. (2012). Prostaglandin E_2 and T cells: friends or foes? Immunol. Cell Biol. *90*, 579–586.

Staels, B., and Fruchart, J.-C. (2005). Therapeutic roles of peroxisome proliferator-activated receptor agonists. Diabetes *54*, 2460–2470.

Steinman, R.M. (2006). Linking innate to adaptive immunity through dendritic cells. Novartis Found. Symp. *279*, 101-9; discussion 109-13, 216–219.

Sugii, S., Olson, P., Sears, D.D., Saberi, M., Atkins, A.R., Barish, G.D., Hong, S.-H., Castro, G.L., Yin, Y.-Q., Nelson, M.C., et al. (2009). PPARγ activation in adipocytes is sufficient for systemic insulin sensitization. Proc. Natl. Acad. Sci. *106*, 22504–22509.

Sukiennicki, T.L., and Fowell, D.J. (2006). Distinct molecular program imposed on CD4+ T cell targets by CD4+CD25+ regulatory T cells. J. Immunol. *177*, 6952–6961.

Summers, L.K. (2006). Adipose tissue metabolism, diabetes and vascular disease — lessons from *in vivo* studies. Diabetes Vasc. Dis. Res. *3*, 12–21.

Sun, L., Burnett, J., Gasparyan, M., Xu, F., Jiang, H., Lin, C.-C., Myers, I., Korkaya, H., Liu, Y., Connarn, J., et al. (2016). Novel cancer stem cell targets during epithelial to mesenchymal transition in PTEN-deficient trastuzumab-resistant breast cancer. Oncotarget *7*, 51408–51422.

Suri-Payer, E., Amar, A.Z., Thornton, A.M., and Shevach, E.M. (1998). CD4+CD25+ T Cells Inhibit Both the Induction and Effector Function of Autoreactive T Cells and Represent a Unique Lineage of Immunoregulatory Cells. J. Immunol. *160*, 1212 LP-1218.

Tai, H.-H., Ensor, C.M., Tong, M., Zhou, H., and Yan, F. (2002). Prostaglandin catabolizing enzymes. Prostaglandins Other Lipid Mediat. *68–69*, 483–493.

Tai, H.-H., Cho, H., Tong, M., and Ding, Y. (2006). NAD+-linked 15-hydroxyprostaglandin dehydrogenase: structure and biological functions. Curr. Pharm. Des. *12*, 955–962.

Tai, X., Van Laethem, F., Pobezinsky, L., Guinter, T., Sharrow, S.O., Adams, A., Granger, L., Kruhlak, M., Lindsten, T., Thompson, C.B., et al. (2012). Basis of CTLA-4 function in regulatory and conventional CD4(+) T cells. Blood *119*, 5155–5163.

Takayama, K., García-Cardeña, G., Sukhova, G.K., Comander, J., Gimbrone, M.A., and Libby, P. (2002). Prostaglandin E_2 Suppresses Chemokine Production in Human Macrophages through the EP4 Receptor. J. Biol. Chem. *277*, 44147–44154.

Talukdar, S., Oh, D.Y., Bandyopadhyay, G., Li, D., Xu, J., McNelis, J., Lu, M., Li, P., Yan, Q., Zhu, Y., et al. (2012). Neutrophils mediate insulin resistance in mice fed a high-fat diet through secreted elastase. Nat. Med. *18*, 1407–1412.

Tang, Q., Henriksen, K.J., Boden, E.K., Tooley, A.J., Ye, J., Subudhi, S.K., Zheng, X.X., Strom, T.B., and Bluestone, J.A. (2003). Cutting edge: CD28 controls peripheral homeostasis of CD4+CD25+ regulatory T cells. J. Immunol. *171*, 3348–3352.

Tone, Y., Furuuchi, K., Kojima, Y., Tykocinski, M.L., Greene, M.I., and Tone, M. (2008). Smad3 and NFAT cooperate to induce Foxp3 expression through its enhancer. Nat. Immunol. *9*, 194–202.

Tong, M., Ding, Y., and Tai, H.-H. (2006). Reciprocal regulation of cyclooxygenase-2 and 15-hydroxyprostaglandin dehydrogenase expression in A549 human lung adenocarcinoma cells. Carcinogenesis *27*, 2170–2179.

Tontonoz, P., Nagy, L., Alvarez, J.G., Thomazy, V.A., and Evans, R.M. (1998). PPARgamma promotes monocyte/macrophage differentiation and uptake of oxidized LDL. Cell *93*, 241–252.

Uppal, S., Diggle, C.P., Carr, I.M., Fishwick, C.W.G., Ahmed, M., Ibrahim, G.H., Helliwell, P.S., Latos-Bieleńska, A., Phillips, S.E. V, Markham, A.F., et al. (2008). Mutations in 15-hydroxyprostaglandin dehydrogenase cause primary hypertrophic osteoarthropathy. Nat. Genet. *40*, 789–793.

Uysal, K.T., Scheja, L., Wiesbrock, S.M., Bonner-Weir, S., and Hotamisligil, G.S. (2000). Improved Glucose and Lipid Metabolism in Genetically Obese Mice Lacking aP2. Endocrinology *141*, 3388–3396.

Vignali, D.A.A., Collison, L.W., and Workman, C.J. (2008). How regulatory T cells work. Nat. Rev. Immunol. *8*, 523–532.

Watanabe, M., Inukai, K., Katagiri, H., Awata, T., Oka, Y., and Katayama, S. (2003). Regulation of PPARγ transcriptional activity in 3T3-L1 adipocytes. Biochem. Biophys. Res. Commun. *300*, 429–436.

Wensveen, F.M., Valentić, S., Šestan, M., Turk Wensveen, T., and Polić, B. (2015a). Interactions between adipose tissue and the immune system in health and malnutrition. Semin. Immunol. *27*, 322–333.

Wensveen, F.M., Jelenčić, V., Valentić, S., Šestan, M., Wensveen, T.T., Theurich, S., Glasner, A., Mendrila, D., Štimac, D., Wunderlich, F.T., et al. (2015b). NK cells link obesity-induced adipose stress to inflammation and insulin resistance. Nat Immunol *16*, 376–385.

Wermuth, B. (1992). NADP-dependent 15-hydroxyprostaglandin dehydrogenase is homologous to NAD-dependent 15-hydroxyprostaglandin dehydrogenase and other short-chain alcohol dehydrogenases. Prostaglandins *44*, 5–9.

Wermuth, B., Platts, K.L., Seidel, A., and Oesch, F. (1986). Carbonyl reductase provides the enzymatic basis of quinone detoxication in man. Biochem. Pharmacol. *35*, 1277–1282.

White, M.F. (2003). Insulin signaling in health and disease. Science *302*, 1710–1711.

White, N.H. (2015). Long-term Outcomes in Youths with Diabetes Mellitus. Pediatr. Clin. North Am. *62*, 889–909.

Williamson, R.T. (1901). On the Treatment of Glycosuria and Diabetes Mellitus with Sodium Salicylate. Br. Med. J. *1*, 760–762.

Wolf, I., O'Kelly, J., Rubinek, T., Tong, M., Nguyen, A., Lin, B.T., Tai, H.-H., Karlan, B.Y., and Koeffler, H.P. (2006). 15-Hydroxyprostaglandin Dehydrogenase Is a Tumor Suppressor of Human Breast Cancer. Cancer Res. *66*, 7818–7823.

World Health Organization (WHO) (2010). Diabetes - Data and statistics.

Xue, J., Schmidt, S.V. V, Sander, J., Draffehn, A., Krebs, W., Quester, I., De Nardo, D., Gohel, T.D.D., Emde, M., Schmidleithner, L., et al. (2014). Transcriptome-Based Network Analysis Reveals a Spectrum Model of Human Macrophage Activation. Immunity *40*, 274–288.

Yan, M., Rerko, R.M., Platzer, P., Dawson, D., Willis, J., Tong, M., Lawrence, E., Lutterbaugh, J., Lu, S., Willson, J.K. V., et al. (2004). 15-Hydroxyprostaglandin dehydrogenase, a COX-2 oncogene antagonist, is a TGF- -induced suppressor of human gastrointestinal cancers. Proc. Natl. Acad. Sci. *101*, 17468–17473.

Yu, M.-K., Lee, J.-C., Kim, J.-H., Lee, Y.-H., Jeon, J.-G., Jhee, E.-C., and Yi, H.-K. (2009). Anti-inflammatory Effect of Peroxisome Proliferator Activated Receptor Gamma on Human Dental Pulp Cells. J. Endod. *35*, 524–528.

Yuan, M., Konstantopoulos, N., Lee, J., Hansen, L., Li, Z.W., Karin, M., and Shoelson, S.E. (2001). Reversal of obesity- and diet-induced insulin resistance with salicylates or targeted disruption of Ikkbeta. Science *293*, 1673–1677.

Zarek, P.E., Huang, C.-T.T., Lutz, E.R., Kowalski, J., Horton, M.R., Linden, J., Drake, C.G., and Powell, J.D. (2008). A2A receptor signaling promotes peripheral tolerance by inducing T-cell anergy and the generation of adaptive regulatory T cells. Blood *111*, 251–259.

Zhang, J., and Liu, F. (2014). Tissue-specific insulin signaling in the regulation of metabolism and aging. IUBMB Life *66*, 485–495.

Zhang, Y., Desai, A., Yang, S.Y., Bae, K.B., Antczak, M.I., Fink, S.P., Tiwari, S., Willis, J.E., Williams, N.S., Dawson, D.M., et al. (2015). Inhibition of the prostaglandin-degrading enzyme 15-PGDH potentiates tissue regeneration. Science *348*, aaa2340.

Zhao, H., Bo, C., Kang, Y., and Li, H. (2017). What Else Can CD39 Tell Us? Front. Immunol. *8*, 727.

Zhou, X., Tang, J., Cao, H., Fan, H., and Li, B. (2015). Tissue resident regulatory T cells: novel therapeutic targets for human disease. Cell. Mol. Immunol. *12*, 543–552.

7. Appendix

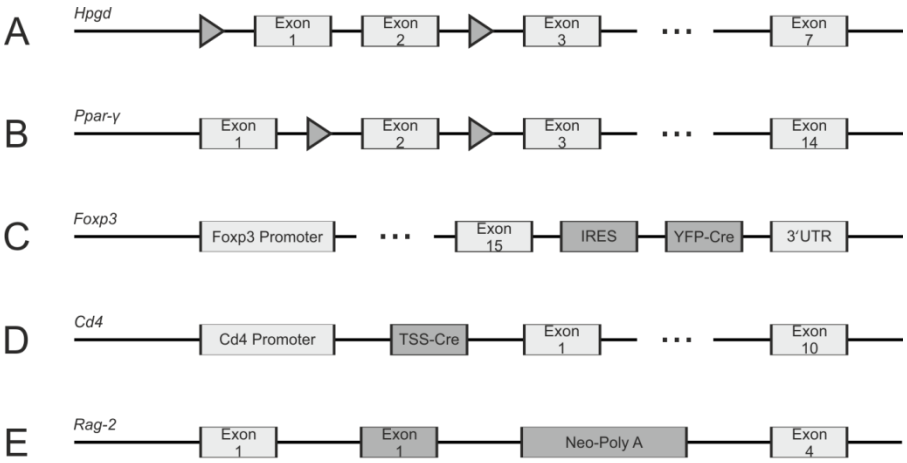

Figure 52: Schematic representation of mouse constructs.
A) *Hpgd* locus: Exon 1 of the *Hpgd* locus is flanked by two loxP sites to allow for the selective deletion of Hpgd by crossing of the line to a line expressing a Cre-recombinase (Roizen et al., 2008) **B)** *Ppar-γ* locus: Exon 2, containing the DNA binding domain, is flanked by two loxP sites, allowing for the deletion of Ppar-γ upon crossing with animals expressing a Cre-recombinase (Akiyama et al., 2002) **C)** *Foxp3* locus: A YFP-Cre construct is inserted into the 3' UTR of the Foxp3 locus under the control of an IRES site. (Rubtsov et al., 2008) **D)** CD4 locus: a construct containing an independent TSS followed by a Cre-recombinase is inserted proximal to the CD4 promoter (Lee et al., 2001) **E)** *Rag-2* locus: the Rag-2 coding region was replaced with a Neo-Poly A cassette (Shinkai et al., 1992). UTR, untranslated region; IRES, internal ribosomal entry site; YFP, yellow fluorescent protein; TSS, transcriptional start site.

8. Zusammenfassung

Regulatorische T-Zellen (T_{reg}-Zellen) sind essentiell für die Aufrechterhaltung der Immunhomöostase. Wie T_{reg}-Zellen ihre Funktion in unterschiedlichen Geweben ausüben, ist jedoch oft unbekannt. Wir haben festgestellt, dass Hydroxyprostaglandin Dehydrogenase (Hpgd), ein Enzym welches Prostaglandin E_2 (PGE_2) metabolisiert, in T_{reg}-Zellen im Vergleich zu konventionellen T-Zellen signifikant hochreguliert ist, sowohl beim Menschen als auch in der Maus. In der Maus ist dies besonders im viszeralen Fettgewebe, einem Prostaglandin-reichen Organ der Fall.

Darüber hinaus konnten wir zeigen, dass Hpgd durch den Metabolismus von PGE_2 zu 15-keto-PGE_2 die suppressiven Fähigkeiten von T_{reg}-Zellen, in einer zumindest teilweise Pparγ-abhängigen Art, verstärkt. *In vivo* konnten wir zeigen, dass Hpgd-defiziente T_{reg} Zellen das Auftreten induzierter Colitis weniger effizient hemmen als Hpgd-kompetente T_{reg} Zellen. Dies weist darauf hin, dass Hpgd eine Rolle in der Suppressionsfähigkeit von T_{reg} Zellen spielt. Transkriptionell unterscheiden sich Hpgd-defiziente T_{reg} Zellen und wildtypische T_{reg} Zellen jedoch kaum. Dies deutet darauf hin, dass die beobachteten Unterschiede auf den extrinsischen Effekt zurückzuführen sind, welcher durch den Verlust der enzymatischen Funktion von Hpgd hervorgerufen wird.

Bei der Analyse des viszeralen Fettgewebes alter Tiere mit Hpgd-defizienten T_{reg} Zellen konnten wir eine Anreicherung von nicht-funktionellen T_{reg} Zellen sowie eine Ansammlung aktivierter Makrophagen und eine signifikante Vergrößerung der Adipozyten nachweisen. Obwohl wir keine Veränderung im Körpergewicht oder im Spontanverhalten, d.h. in der Motilität, in der Nahrungs- und Wasseraufnahme oder in der Atmung, dieser Tiere feststellten, konnten wir eine Fehlregulation des Metabolismus beobachten: Alte Mäuse mit Hpgd-defizienten T_{reg}-Zellen reagieren weniger auf Insulin- und Glukose. Des Weiteren scheint in den Tieren die Insulinsignalkaskade teilweise inhibiert zu sein.

Werden Tiere mit Hpgd-defizienten T_{reg}-Zellen einer Fütterung mit hochkalorischem Futter unterzogen, kommt es zu einer verminderten Reaktion auf Insulin im Vergleich zu wildtypischen Tieren auf gleicher Diät. Ansonsten haben wir jedoch keinen Unterschied in der Gewichtszunahme, in anderen metabolischen Parametern oder in den im viszeralen Fettgewebe ansässigen Immunzellen beobachten können.

Des Weiteren konnten wir im Blut von Patienten mit Typ-II-Diabetes (T2D) eine Fehlregulation der T_{reg}-Zellpopulation sowie eine verminderte HPGD-Expression in diesen Zellen identifizieren. Zusammengefasst zeigen diese Daten, dass sowohl beim Menschen als auch in der Maus die HPGD-Expression in T_{reg}-Zellen an der metabolischen Regulation beteiligt sein könnte.

Schließlich analysierten wir die Rolle des T_{reg}-Zell-spezifischen Transkriptionsfaktors Mesenchym Homeobox 1 (MEOX1) in der Expression von HPGD und konnten nachweisen, dass MEOX1 in humanen T_{reg}-Zellen hochreguliert ist, besonders nach Stimulation mit Interleukin (IL) 2. Darüber hinaus konnten wir zeigen, dass die MEOX1-Expression in humanen T_{reg} Zellen zwar wie die Expression von HPGD durch FOXP3 reguliert wird, der Verlust von MEOX1 jedoch die HPGD-Expression nicht beeinflusst. Dadurch widerlegten wir unsere Hypothese, dass HPGD von MEOX-1 reguliert wird.

Zusammenfassend konnten wir zeigen, dass die Expression von HPGD in T_{reg} Zellen sowohl im murinen System als auch beim Menschen ein wichtiger Mediator der Suppressionsfähigkeit ist, unabhängig von MEOX1. Des Weiteren konnten wir nachweisen, dass eine T_{reg}-Zell-spezifische Deletion von Hpgd in der Maus zu einer Fehlregulation des Metabolismus führt. Dieses Phänomen spiegelt sich im Menschen in T2D-Patienten wieder, da hier die HPGD-Level in T_{reg}-Zellen aus dem peripheren Blut signifikant reduziert sind.

9. Publication List

Schmidleithner, L., Thabet, Y., Schönfeld, E., Köhne, M., . . . Schultze, J.L., Beyer, M. Enzymatic Activity of HPGD in Treg Cells Suppresses Tconv Cells to maintain Adipose Tissue Homeostasis and Prevent Metabolic Dysfunction. *Immunity;* doi:10.1016/j.immuni.2019.03.014

Beyer, M., Abdullah, Z., Chemnitz, J. M., . . . **Schmidleithner, L**., . . . Schultze, J. L. (2016). Tumor-necrosis factor impairs CD4 T cell–mediated immunological control in chronic viral infection. *Nat Immunol*, *17*(5), 593-603. doi:10.1038/ni.3399

Xue, J., Schmidt, S., Sander, J., . . . **Schmidleithner, L**., . . . Schultze, J.L. (2014). Transcriptome-Based Network Analysis Reveals a Spectrum Model of Human Macrophage Activation. *Immunity*, *40*(2), 274-288. doi:10.1016/j.immuni.2014.01.006